BRE Attenuates Apoptosis through Maintaining the Cellular Level of an Apoptotic Inhibitor XIAP

LI, Wei

A Thesis Submitted in Partial Fulfilment
of the Requirements for the Degree of
Master of Philosophy
in
Chemical Pathology

The Chinese University of Hong Kong
August 2012

Abstract

BRE is a broad-spectrum anti-apoptotic protein, which attenuates both extrinsic and intrinsic apoptosis. However, the molecular and biochemical mechanisms by which BRE inhibits apoptosis remain completely unknown. Here I provide evidence that BRE attenuates apoptosis through maintaining the cellular level of XIAP, which is a potent endogenous inhibitor of caspases functioning in intrinsic and extrinsic pathways.

Using a mouse Lewis lung carcinoma cell line D122, we found that shRNA-mediated stable depletion of BRE rendered the cells susceptible to TNF-α-induced apoptosis even in the absence of cycloheximide (CHX). CHX plays a critical pro-apoptotic role by inhibiting synthesis of anti-apoptotic proteins, which TNF-α also up-regulates through activation of NF-κB pathway. Western blot analysis of the NF-κB-driven and CHX-sensitive anti-apoptotic proteins revealed only XIAP, but not cIAP-1, cIAP-2, or cFLIP, was down-regulated in BRE-depleted cells. Reconstitution of the BRE-depleted mouse cells with highly homologous human BRE restored the XIAP protein level, confirming a positive regulatory role of BRE on XIAP protein expression. Furthermore, reconstitution of the BRE-depleted cells with human BRE or XIAP rendered the cells less sensitive to TNF-α-induced apoptosis.

Addition of NEM (N-Ethylmaleimide), which binds irreversibly to cysteine residues of proteins, to cell lysates, was found to abrogate, the recognition of BRE by our anti-BRE antibody (Mab489-7) in Western blot analysis. Correspondingly, XIAP level was also found reduced in cell lysates. This correlation provides in vitro evidence that BRE has a protective role for XIAP, and that this role is related to cysteine residues of BRE.

I have shown that that XIAP is not only cleaved by caspases during apoptosis, but also subjected to proteaosomal degradation, indicating that ubiquitination of XIAP is an important regulatory mechanism for the stability of this protein. As BRE is known to contain polyubiquitin-binding domains and forms complexes with deubiquitination activity, the issue of whether BRE could remove the ubiquitination of XIAP was investigated. I found that over-expressed XIAP underwent K48-linked, K63-linked, and K0-linked polyubiquitination, respectively. Overexpression of BRE led to the removal of or inhibited K0- but not K48- or K63-linked ubiquitination of XIAP.

Taken together, I have provided evidence that BRE exerts its anti-apoptotic function through maintaining the cellular level of XIAP, a potent endogenous inhibitor of apoptosis. Promoting removal of linear ubiquitin chain of XIAP, or inhibition of the chain formation to prevent linear polyubiquitin-mediated proteasomal degradation of XIAP may be the mechanism by

which BRE stabilizes this protein. Whether such interaction between BRE and XIAP is direct or indirect needs further investigation.

中文摘要

以前的研究表明，BRE 是一種能在內源和外源凋亡路徑中均發揮作用的抗凋亡蛋白。然而，我們卻完全不知道它發揮抗凋亡功能的分子機制和生物化學機制是怎樣的。在本論文中，我們報導了 BRE 通過保護細胞內的 XIAP 水準來發揮抗凋亡功能。XIAP 是一種強大的內源性的半胱氨酸天冬氨酸蛋白酶的抑制劑，與 BRE 一樣，XIAP 也在內源和外源凋亡路徑中均發揮作用。

我們使用鼠 Lewis 細胞系為母細胞系，產生了 shRNA 介導的 BRE 基因敲除穩定細胞系。我們發現這種 BRE 敲除細胞系使得細胞對於在即使沒有放線菌酮作用下的腫瘤壞死因數 α 介導的凋亡也異常敏感。放線菌酮通過抑制抗凋亡蛋白的合成以發揮重要的促凋亡作用，相反地，腫瘤壞死因數-α 通過 NF-κB 通路可以上調上述抗凋亡蛋白。蛋白質印跡結果顯示，上述通過 NF-κB 通路被上調且對放線菌酮敏感的抗凋亡蛋白中，只有 XIAP 的水準，而不是 cIAP-1, cIAP-2 或者 cFLIP 的水準, 在 BRE 敲除細胞中明顯被降低。用具有高度同源性的人 BRE 在上述鼠 BRE 敲除細胞中恢復 BRE 的水準，XIAP 水準也隨之上升。該實驗也證實了 BRE 正向調節 XIAP 的作用。並且當在上述 BRE 敲除細胞中恢復人 BRE 或者 XIAP 時，這些細胞對腫瘤壞死因數-α 介導的凋亡的敏感性也都得以降低。

當具有使蛋白中半胱氨酸殘基改變作用的 N-乙基馬來醯亞胺被加入細胞裂解液中時，抗 BRE 抗體 Mab489-7 對於 BRE 的識別作用會因為 BRE 蛋白中半胱氨酸殘基的改變而受到影響。與之對應地，裂解液中的 XIAP 水準也同時降低。該結果提示在細胞裂解液中，BRE 保護 XIAP 的基團可能與半胱氨酸殘基有關。

我們發現在凋亡過程中 XIAP 不僅被半胱氨酸天冬氨酸蛋白酶分解，它也會被蛋白體所降解。這提示我們 XIAP 的泛素化對於保持其穩定性有重要作用。我們已經知道 BRE 具有泛素鏈結合域，也可以形成具有降泛素作用的複合物。因此我們想通過實驗，瞭解 BRE 是否能降解掉鏈結在 XIAP 上的泛素鏈。實驗表明 XIAP 至少可以鏈結三種類型的泛素鏈，分別為 K48 型，K63 型和 K0 型。然而 BRE 卻只特異性地降解鏈結在 XIAP 上的 K0 型泛素鏈或抑制 XIAP 上的 K0 型泛素鏈的形成。

綜上所述，BRE 特異性地降解鏈結在 XIAP 上的線型泛素鏈或者抑制該種泛素鏈的形成，並通過它影響 XIAP 的穩定性，從而在外源和內源凋亡通路中發揮抗凋亡的作用。BRE 和 XIAP 之間的相互作用是間接的還是直接的仍有待進一步證實。

Acknowledgements

I would like to give my thanks to my supervisor Dr. Yiu-Loon Chui firstly for his continuous encouragement and excellent guidance.

I would also like to give my thanks to Chun Hung MA for technical assistance and discussion. Special thanks are due to Dr. CK Wong for allowing us to use the flow cytometry. I wish to give my thanks to Professor Ka Ho Lee, Professor Wing Tai Cheung, and Mr. Jesse Pang for material sharing and discussion.

I would like to thank all the other colleagues in our clinical immunology laboratory: Dr. Danny Leung, Ms Janet Tang for their kindness and practical support from time to time, as well as Ms Fonda Chan and Yuk, for the preparation of lab wares, and in particular to Ms Peggy Fung for her great help in clerical works and warm care.

Last but not least, my thanks would go to my parents for their endless love and constant support. I also would like to thank all my friends in CUHK for their helps and sharing.

List of Figures

List of Tables

Abbreviations

aa	Amino acid
ABR	Active BCR-related gene
Abraxas/Abra1/CCDC98	Coiled-coil domain-containing 98
ABRO1/KIAA0157	Family with sequence similarity 175, member B
AIF	Apoptosis-inducing factors
AIR	Abraxas-interacting region
ALS	Amyotrophic lateral sclerosis
AMP	Adenosine monophosphate
AOS1/RHC31	Ad31 homologue in S. cerevisiae
Apaf-1	Apoptotic protease-activating factor
Apo-1	Apoptosis antigen 1
Apo-2	Apoptosis antigen 2
Apo-3	Apoptosis antigen 3
APP-BP-1	Beta-amyloid precursor-binding protein 1
ARF	ADP-ribosylation factor
ARTS	Tumor necrosis factor receptor shedding amino peptidase regulator
ATG	Autophagy-related protein
BAK	Bcl-2 homologous antagonist killer
BARD1	BRCA1-associated RING domain protein 1
BAX	Bcl-2-associated X protein
Bcl-2	B-cell lymphoma 2
Bcl-3	B-cell lymphoma 3
Bcl-XL	B-cell lymphoma-extra large
BID	BH3 interacting-domain death agonist
BIR	Baculovirus Inhibitor of apoptosis protein repeat
BMP	Bone morphogenetic protein
BMP-RI/II	Bone morphogenic protein receptor, type I/II
BRCA1	Breast cancer type 1 susceptibility protein
BRCC36/BRCC3	BRCA1/BRCA2-containing complex, subunit 3
BRCT	BRCA1 C-terminus
BRE/BRCC4/BRCC45	Brain and reproductive organ-expressed
BRISC	BRCC36 isopeptidase complex
CARD	Caspase recruitment domain
CaM	Calcium/calmodulin-binding motif
CC	Coiled-coil
c-Cbl	Casitas B-lineage lymphoma
CD120a	Cluster of differentiation 120a
CD95	Cluster of differentiation 95
CEU	Europe
CHB	China
CHIP	CG5203 gene product from transcript CG5203-RA
CHX	Cyclohexamide
cIAP-1	Baculoviral IAP repeat-containing protein 2
cIAP-2	Baculoviral IAP repeat-containing protein 3
CLPX	Caseinolytic peptidase X homolog
CNP	Copy number polymorphism
COMMD1	Copper metabolism (MURR1) domain-containing 1
COX-2	Prostaglandin-endoperoxide synthase 2, also known as cyclooxygenase-2
CSN	The CO9 signalosome
CYLD	Cylindromatosis tumor-suppressor gene

Cys	Cysteine
Cyt c	Cytochrome c
dATP	Deoxyadenosine triphosphate
DD	Death domain
DED	Death effector domains
DEN	Diethylnitrosamine
DIABLO	IAP-binding mitochondrial protein
DIAP1	Drosophila melanogaster IAP1
DIAP2	Drosophila melanogaster IAP2
DISC	Death-inducing signaling complex
DR1	Down-regulator of transcription 1
DR2	Down-regulator of transcription 2
DR3	Down-regulator of transcription 3
DR4	Down-regulator of transcription 4
DR5	Down-regulator of transcription 5
DR6	Down-regulator of transcription 6
DSB	Double strand break
DUB	Deubiquitinating enzymes
E1	Ubiquitin-activating enzyme
E2	Ubiquitin-conjugating enzyme
E3	Ubiquitin-protein ligases
E6-AP/UBE3A	Ubiquitin protein ligase E3A
E6-AP1	E6-associated protein 1
EDD	Glycyl-tRNA synthetase 2
EGFR	Epidermal growth factor receptor
EndoG	Endonuclease G
Eps15	Epidermal growth factor receptor pathway substrate 15
ER	Endoplasmatic reticulum
FADD	Fas-associated protein with death domain
FAT10	Human leukocyte antigen F-associated transcript 10
FKBD	FK506-binding domain
cFLIP	FLICE-inhibitory protein
$cFLIP_L$	The long isoform of FLICE-inhibitory protein
$cFLIP_S$	The short isoform of FLICE-inhibitory protein
GdH	Glutamate dehydrogenase
GFP	Green fluorescent protein
GTP	Guanosine triphosphate
H2A	Histone H2A
H2AX	Gamma histone variant H2AX
H2B	Histone H2B
H3	Histone H3
H4	Histone H4
HCC	Hepatocellular carcinoma
HECT	Homologous to E6-associated protein C-terminus
Hgs	HGF-regulated tyrosine kinase substrate
hHR6A/UBE2A	Ubiquitin-conjugating enzyme E2A
HIF-1α	HIF1A hypoxia inducible factor 1, alpha subunit (basic helix-loop-helix transcription factor)
HIF-2α/ EPAS1	Endothelial PAS domain protein 1
His	Histidine
HPV	Human papillomavirus
HtrA2	HtrA serine peptidase 2
Huwe1	HECT, UBA, and WWE domain-containing 1
IAP	Inhibitor of apoptosis
IBMs	IAP-binding motifs

IκB	Nuclear factor of kappa light polypeptide gene enhancer in B-cells inhibitor
IκBα	Nuclear factor of kappa light polypeptide gene enhancer in B-cells inhibitor, alpha
IκBe	Nuclear factor of kappa light polypeptide gene enhancer in B-cells inhibitor, e
IκBg	Nuclear factor of kappa light polypeptide gene enhancer in B-cells inhibitor, g
IκBSR	IκB-super repressor
IκBβ	Nuclear factor of kappa light polypeptide gene enhancer in B-cells inhibitor, beta
IKK	IκB kinase
IL-1	Interleukin 1 family
ILP2	IAP-like protein 2
IP	Immunoprecipitation
IRES	Internal ribosome entry site
ISG15	Interferon-stimulated gene 15
IsoT/USP5	Ubiquitin specific peptidase 5
ITAFs	IRES trans-acting factors
Itch	Itchy E3 ubiquitin protein ligase homolog
JAMM	Jab1/Mov34/Mpr1 Pad1 N-terminal+
JPT	Japan
KLF	Kruppel-like factor
LRPPR	Leucine-rich pentatricopeptide repeat motif-containing protein
LUBAC	Linear ubiquitin chain assembly complex
MAFbX	F-box protein 32
MAP2K4/MKK4	Dual specificity mitogen-activated protein kinase kinase 4
MAP3K2/MEKK2	Mitogen-activated protein kinase kinase kinase 2
MAP3K7P1/TAB1	Transforming growth factor β activated kinase (TAK1)-binding protein 1
MAP3K7P2/TAB2	TAK1-binding protein 2
MAP3K8	Mitogen-activated protein kinase 8
MAPK8/JNK	c-Jun N-terminal kinase
MDM2	Murine double minute clone 2 oncoprotein
MDMX/Mdm4	Transformed mouse 3T3 cell double minute 4
MERIT40/NBA1/BABAM1	Mediator of Rap80 interactions and targeting 40 kDa/BRISC and BRCA1 A complex member 1
MJD	Machado-Joseph disease protease
MnSOD	Superoxide dismutase 2
MOMP	Mitochondrial outer membrane permeabilization
MPN-	Mpr1/Pad1 N-terminal region lacking catalytic activity
MPN+	Mpr1/Pad1 N-terminal region with an intact protease catalytic site
MuRF1/TRIM63	Tripartite motif-containing 63
NAIP	Baculoviral IAP repeat-containing protein 1
NCBI	National center for biotechnology information
NO	Nitric oxide
Nedd4	Neural precursor cell expressed, developmentally down-regulated 4
NEDD-8	Neuronal precursor cell-expressed developmentally down-regulated Protein 8
NF-κB	Nuclear factor kappa-light-chain-enhancer of activated B cells

Notch1	Notch homolog 1, translocation-associated (Drosophila)
Nsp4	Nipsnap 4
Numb	CG3779 gene product from transcript CG3779-RB
OTU	Otubain protease
PCR	Polymerase chain reaction
Poh1	The pad one homolog-1
PTEN	Phosphatase and tensin homolog
RAP80/UIMC1	Ubiquitin interaction motif-containing 1
RBKS	Ribokinase
RE	Response elements
RelA	V-rel reticuloendotheliosis viral oncogene homolog A
RelB	V-rel reticuloendotheliosis viral oncogene homolog B
RHD	Rel homology domain
RING	Really interesting new gene
RIP/RIPK1/RIP	Receptor (TNFRSF)-interacting serine-threonine kinase 1
RIPK1/RIP1	Receptor-interacting serine/threonine-protein kinase 1
RNS	Reactive nitrogen species
ROS	Reactive oxygen species
RPL23AP34	Ribosomal protein L 23a, pseudogene 34
Rpn	Regulatory proteasome non-atpase subunit
Rpt	Proteasome regulatory particle, ATPase-like
Rsp5	The saccharomyces cerevisae orthologue of NEDD4
Sam68	The 68-kDa Src-associated protein in mitosis
SCF	Skp1-Cullin-F-box
Siah-1	Seven in absentia homolog 1
siRNAs	Small interfering RNAs
Smac	Second mitochondria-derived activator of caspases
Smurf1	SMAD specific E3 ubiquitin protein ligase 1
Smurf2	SMAD specific E3 ubiquitin protein ligase 2
SNP	Single-nucleotide polymorphism
SOD1	Superoxide dismutase 1, soluble
SUMO	Small ubiquitin-like modifier
TADs	Transcriptional activation domains
TAK1	TGF-β-activated kinase 1
tBID	Truncated BH3 interacting-domain death agonist
TM	Transmembrane motif
TNF	Tumor necrosis factors
TNF-R1	Tumor necrosis factor-receptor 1
TNFRSF1A	Tumor necrosis factor receptor superfamily member 1A
TopBP1	Topoisomerase (DNA) II-binding protein 1
TPR	Tripartite tetra-tricopeptide repeat
TRABID	TRAF-binding domain-containing protein
TRADD	Tumor necrosis factor receptor type 1-associated death domain protein
TRAF-1	TNF receptor-associated factor 1
TRAF-2	TNF receptor-associated factor 2
TRAF5	TNF receptor-associated factor 5
TRAF6	TNF receptor-associated factor 6
TRAIL-R1	TNF-related apoptosis-inducing ligand-receptor 1
TRAIL-R2	TNF-related apoptosis-inducing ligand-receptor 2
TβR-I/II	TGF-β receptors-I/II
Ub	Ubiquitin
UBA	Ubiquitin-binding domain
UBA1	Ubiquitin-like modifier activating enzyme 1

UBA2	Ubiquitin-like modifier activating enzyme 2
UBA3	Ubiquitin-like modifier activating enzyme 3
UBA4	Ubiquitin-like modifier activating enzyme 4
UBA5	Ubiquitin-like modifier activating enzyme 5
UBA6/ Ube1L2	Ubiquitin-like modifier activating enzyme 6
UBC	Ubiquitin-conjugating catalytic
UBC12	NEDD8-conjugating enzyme 12
Ubc12/UBE2M	Ubiquitin-conjugating enzyme E2M
UBC9/UBE2I	Ubiquitin-conjugating enzyme E2I
UbcH5B/UBE2D2	Ubiquitin-conjugating enzyme E2D 2
UbcH6/UBE2E2	Ubiquitin-conjugating enzyme E2E 2
UbcH8/UBE2L6	Ubiquitin-conjugating enzyme E2L 6
UBE1L2	Ubiquitin-activating enzyme E1-like protein 2
UBE3C	Ubiquitin protein ligase E3C
U-box	A modified RING motif without the full complement of Zn2-binding ligands
Ubp2	Ubiquitin C-terminal hydrolase 2
UCH	Ubiquitin C-terminal hydrolase
UEV	Ubiquitin E2 variant
Ufc1	E2-like ubiquitin-fold modifier conjugating enzyme 1
UFM-1	Ubiquitin-fold modifier 1
UIM	Ubiquitin-interacting motif domain
ULPs	Ubiquitin-like proteins
URM-1	Ubiquitin related modifier 1
USE1	Uba6-specific E2
USP	Ubiquitin-specific protease
UsP2	Ubiquitin C-terminal hydrolase 2
USPV	Ubiquitin-specific protease variant
UTR	Untranslated region
VCB	VHL (Von Hippel-Lindau) E3 or VHL elongin C-elongin B
VWA	Von Willebrand factor type A
WWP1	WW domain-containing E3 ubiquitin protein ligase 1
XAF1	XIAP associated factor
XIAP	X-linked inhibitor of apoptosis protein
YRI	Yoruba
γGCS	γ-Glutamylcysteine Synthetase

CONTENTS

CHAPTER 1: Introduction

1.1 Apoptosis

1.1.1 Overview of apoptosis

The original meaning of apoptosis is the falling of leaves from a tree. This ancient Greek word was used to describe the morphological characters of the energy used process of formation of 'apoptotic bodies' from a cell by John Kerr first (1). The morphological changes of apoptosis comprise cellular shrinkage, membrane blebbing, nuclear condensation, chromatin condensation, DNA fragmentation, and permeabilization of mitochondria (2). Abnormality of apoptosis generates pathological consequences, such as cancer, neurodegenerative and autoimmune diseases (3).

Apoptosis can be divided into three main stages: induction, effector, and degradation. The induction stage involves the initiation and activation of procaspase cascades. Alteration of mitochondrial membrane permeability, and release of proteins and proteases from mitochondria into cytosol form the effector stage (4). Degradation stage involves cleavage of cellular proteins and disintegration of internucleosomal DNA.

1.1.2 Caspases

Caspases, which are the well-conserved and efficient cysteinyl aspartate-specific proteases, play a central role in the execution of apoptosis (5). Caspases are produced by cells as catalytically inactive zymogens which undergo proteolytic processing during activation (6). To date, 14 caspases have been found, which can be sub-grouped into proinflammatory (caspases 1, 4, 5, 11, 12, 13, 14) and pro-apoptotic caspases. The latter can be subdivided further into initiator caspases (2, 8, 9, and 10) and effector caspases (3, 6, and 7). When cells are exposed to pro-apoptotic stimulus, the initiator caspases are activated first, which in turn activate the effector caspases to cleave cellular substrates, resulting in cell death. Many endogenous cellular factors regulate caspases. The IAP family proteins are the most potent ones among them. The characteristic domain of IAP family proteins is BIR domain. Members of this family contain one or more BIR domains. For example, XIAP, NAIP, cIAP-1, and cIAP-2 have three BIR domains each. XIAP is the most potent one in inhibiting caspases among all members of the IAP family. The BIR2 domain together with a short N-terminal flanking sequence of XIAP binds and inhibits caspase 3 and 7. The BIR3 domain of XIAP binds and inhibits caspase 9 (7). The activities of IAP family members can be regulated by some endogenous cell factors, which are released, form mitochondria. For example, the mitochondrial proteins Smac/DIABLO and Omi/HtrA2 can bind to XIAP and antagonize its inhibitory activity on caspases. Another example of the endogenous inhibitors of caspases is cFLIP. It has a pro-domain similar to that of procaspase-8, but lacks a caspase active site. It

can inhibit procaspases 8 and 10.

1.1.3 Extrinsic and intrinsic apoptotic pathways

In mammalian cells, apoptosis has been subdivided into two major pathways: extrinsic pathway and intrinsic pathway. The extrinsic pathway is initiated by pro-apoptotic receptor signals on the cellular surface. The intrinsic pathway is activated by the signals inside the cell itself, which involve the destruction of mitochondrial membrane integrity. The molecular signal transduction of these two pathways is showed in Figure 1-1 (8).

The initial step of the extrinsic pathway is the binding of death receptors with their specific ligands. The transmembrane death receptors belong to TNF family. These receptors contain two important domains. One is cysteine-rich extracellular domain, which enables them to recognize their ligands specifically. The other is intra-cellular death domain (DD). The 80 amino-acids-containing DD domain is crucial due to its role in transferring the death signal from cellular surface to the intercellular pathways.

Currently, six types of death receptors have been identified. They are TNF-R1 (also called DR1, p55, p60, or CD120a), Fas (also called DR2, CD95, or APO-1), DR3 (also known as APO-3, LARD, TRAMP, or WSL1), TRAIL-R1 (also known as DR4 or APO-2), TRAIL-R2 (DR5, KILLER, or TRICK2), and DR6 (9). After binding of transmembrane death receptors with their specific ligands (FasR/FasL, TNFR1/TNF-α, DR-4/TRAIL, DR-5/TRAIL, DR3/Apo-3L/TWEAK), the intra-cellular death domain of the death receptors binds to FADD or TRADD to form DISC complex with the recruitment of pro-caspase 8. Then, pro-caspase 8 is further activated to become active caspase 8, which serves as an initiator caspase to activate downstream effector caspases, such as caspase 3 and 7, which in turn cleave vital substrates and lead to apoptosis.

The intrinsic pathway, also named mitochondrial pathway, is usually activated by stimuli from inside the cell such as DNA damage, oxidants, ceramide, and other factors, which via a complex chain of events leads to mitochondrial outer membrane permeabilization (MOMP) and release of cytochrome c from the mitochondria. The intermembrane space of mitochondria contains many proteins important to cell death induction and regulation, such as cytochrome c (cyt c), apoptosis-inducing factors (AIF), EndoG, Omi/HtrA2, and Smac/DIABLO. Cytochrome c stimulates apoptosome formation after being released into cytoplasm. Apaf-1, dATP, cytochrome c, and caspase 9 constitute apoptosome complex. The caspase 9, which belongs to initiator caspases, then activates downstream effector caspases, such as caspases 3, 6, 7, which in turn cleave vital substrates and lead to cellular death. The release of cytochrome c is mainly regulated by interactions between anti-apoptotic and pro-apoptotic members of Bcl-2 family (10, 11). Under normal conditions, cytochrome c is

sequestered in the inter-membrane space of mitochondria. However, upon apoptotic stimulation, BAX and BAK are activated to form homo-oligomers at the outer mitochondrial membrane, resulting in pore formation and MOMP, during which cytochrome c exits and enters into the cytosol (12). Anti-apoptotic Bcl-2 family member, such as Bcl-2 prevents the release of cytochrome c. Bcl-2 interacts directly with BAK and BAX and inhibits their oligomerization (13). The pro-apoptotic member of Bcl-2 family, BID is the primary activators of BAX and BAK (14). Active BID, also known as truncated BID (tBID), induces the oligomerization of BAX and BAK (15, 16). Furthermore, tBID induces mitochondrial cristae remodelling that can promote the mobilization of cytochrome c (17).

These two pathways do not act separately. They interact with one another, allowing components from one pathway to affect those of the other. For example, active caspase 8 from extrinsic pathway cleaves BID protein into tBID, which can then bind to the pro-apoptotic BAX and BAK to activate intrinsic pathway via causing to MOMP and cytochrome c release (18).

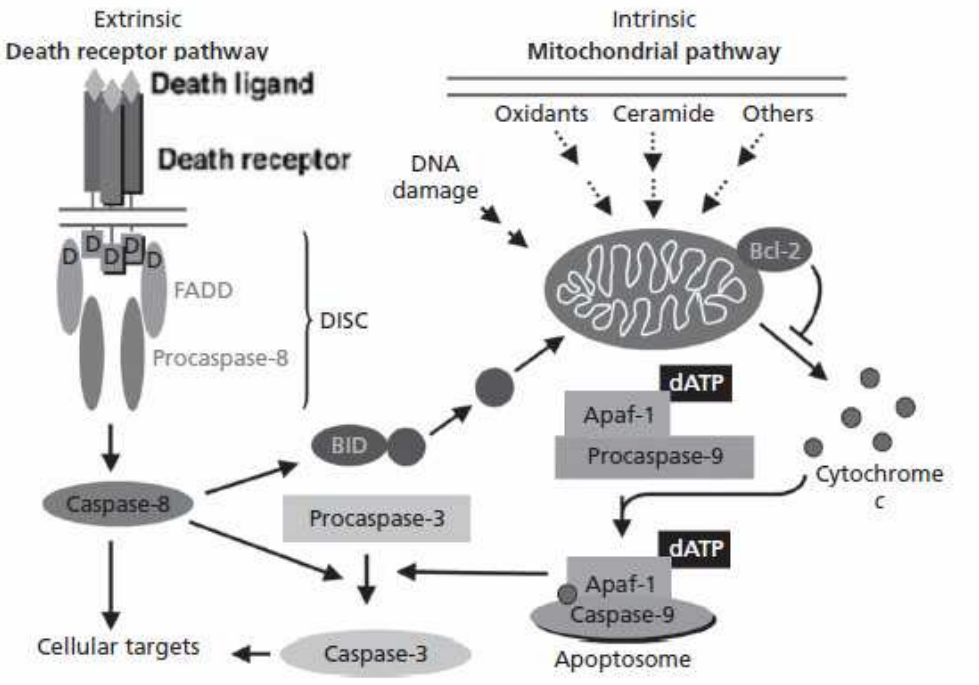

Figure 1-1. **Extrinsic and intrinsic apoptosis** (reproduced from reference (8))

1.2 NF-κB

1.2.1 Overview of NF-κB

NF-κB, a protein complex which regulates the transcription of DNA, was first discovered in the immunoglobulin light-chain enhancer in B cells via its interaction with an 11-base-pairs

sequence (19). NF-κB can be activated by many bacterial products and stimulation of a wide variety of cell-surface receptors. Once activated, it can change gene expression very quickly. It regulates the expression of many targets, which are involved in many tissues and systems. Its major function is involved in the immune system. Apart from that, NF-κB is closely related to apoptosis and cancer (20). It can promote cell survival by either up-regulating the activity of anti-apoptotic genes or down-regulating the activity of apoptotic genes. The anti-apoptotic target genes of NF-κB include Survivin, MnSOD, CyclinD1, γGCS, cIAP-1, cIAP-2, XIAP, A20, COX-2, IEX-IL, c-Myc, Bcl-2, Bcl-XL, TRAF-1, and TRAF-2 etc.

NF-κB family comprises five members, which are RelA, RelB, c-Rel, p50 and p52 (21). These members form homodimers or heterodimers to bind to DNA. This binding is between the Rel homology domain (RHD) in the NF-κB and the κB sites in DNA. The latter is located in the promoters and enhancer regions of genes, which in turn regulates gene expression.
RelA, RelB, c-Rel contain transcriptional activation domains (TADs) in their C-terminus and can activate target gene expression directly due to the TADs. p50 and p52 are derived from their large precursors, p105 and p100, respectively. p50 and p52 do not contain TADs; thus, they have to bind to a TAD-containing protein, such as RelA, c-Rel, or RelB, to execute their functions. The classic NF-κB dimer contains RelA and p50, while many other Rel-containing dimers also exist. In inactivated state, NF-κB is inhibited by inhibitory IκB proteins present in cytoplasm. Currently, seven IκB family members, IκBa, IκB, Bcl-3, IκBe, IκBg, and precursor proteins p100 and p105, have been identified. They all have the characteristic ankyrin repeats.

As shown in Figure 1-2 (22), in an inactivated state, NF-κB, bound with the inhibitory protein IκB, is located in cytosol. A variety of extracellular signals can activate the enzyme IκB kinase (IKK), which in turn phosphorylates the IκB. This causes ubiquitination of IκB and its dissociation from NF-κB, and degradation by proteosome. The activated NF-κB is then translocated into the nucleus where it binds to specific DNA sites in target genes. This DNA/NF-κB complex recruits many other proteins such as co-activators and RNA polymerase to activate transcription of downstream DNA, resulting in a change of cell function (20, 23, 24).

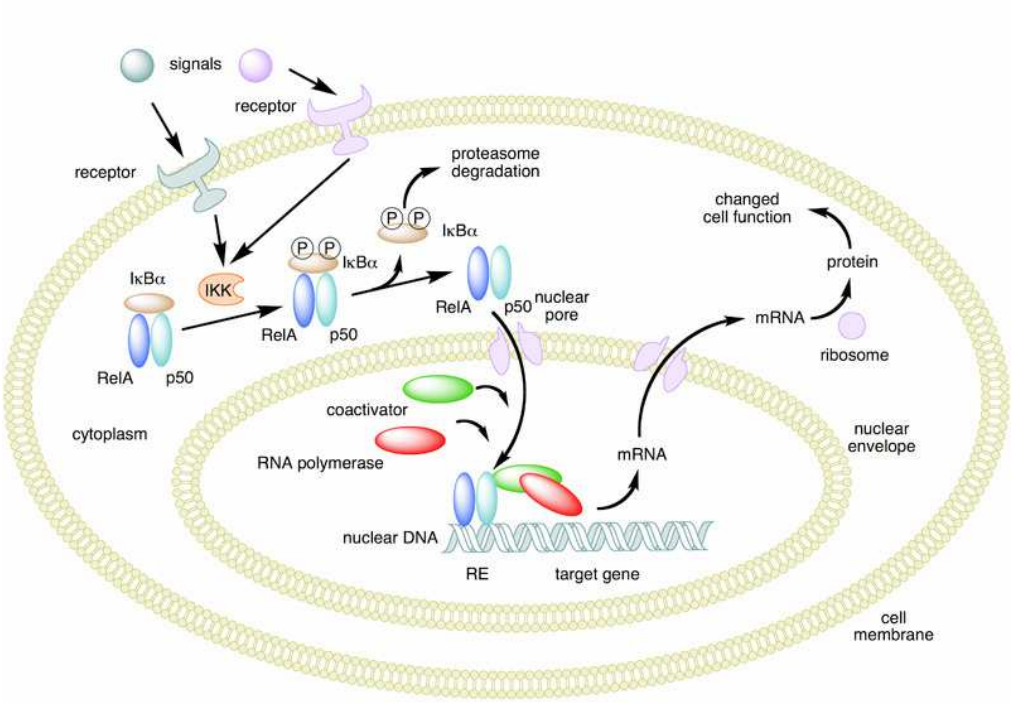

Figure 1-2. **NF-κB mechanism of action** (reproduced from reference (22))

1.2.2 NF-κB and two signaling complexes

Signaling by tumour necrosis factor receptor (TNF-R1) can stimulate a plethora of seemingly opposing biological processes, ranging from inflammatory cytokine production, cell survival, cell proliferation, and cell death (25). TNF mediates most of its effects through activating a set of transcription factors that are collectively referred to as NF-κB (26). Binding of TNF-α to TNFR1 results in sequential formation of two signaling complexes (Figure 1-3). The rapidly forming complex-I is constituted on the receptor's cytoplasmic tail and consists of TRADD, Sam68, RIPK1 (also named RIP1), TRAF2, TRAF5, and cIAP-1/2 (27). The TRADD is an adaptor. The RIPK1 is a protein kinase. Of note, TRAF5 can also be part of this complex; however, its clear function in complex-I is not known. The function of the signal transducer TRAF2 in this complex is to recruit the E3 ligases cIAP-1 and cIAP-2, which subsequently ubiquitylate several components of this complex, required for to recruiting LUBAC (the E3 ligase linear ubiquitin chain assembly complex), which in turn strengthens this complex by promoting further ubiquitylation. This above process not only stabilizes complex-I, but also activates TAK1 and IKK, which in turn phosphorylates IκB leading to its degradation and the release of NF-κB to regulate expression of its target genes important to cell survival. Thus, this complex signals cell survival through activation NF-κB.

On the other hand, TNF can also induce cell death. Micheau and Tschopp (27) were the first to identify the cytoplasmic death-facilitating complex that is derived from the complex-I after TNF stimulation. It is usually called complex-II. After the dissociation of complex-I from the

receptor, TRAF2 and TRADD together with RIP1 associate with an adaptor protein FADD and pro-caspase-8 to form complex-II. Unlike the rapid formation of complex-I, complex-II is formed 2 hours later after ligation of TNF to TNF-R1. Complex-II signals apoptosis through activation of caspase 8.

Remarkably, the apoptotic function of complex-II is manifested only under some special conditions where expression of NF-κB target genes is blocked, such as upon genetic deletion of NF-κB, expression of the IκB-super repressor (IκBSR), or in the presence of cycloheximide (27, 28). Thus, in normal condition, if TNF successfully stimulates NF-κB-regulated expression of target genes, formation of complex-II cannot lead to apoptosis. This is because NF-κB activation results in up-regulation of anti-apoptotic proteins, such as cFLIP, cIAP-1, cIAP-2, XIAP, which in turn suppresses cell death induced by complex-II (27, 28). Thus, in order to induce TNF-α-activated apoptosis to cell lines, cycloheximide (CHX) is usually included. Cycloheximide is a protein synthesis inhibitor that can shut down synthesis of anti-apoptotic proteins, such as cFLIP, cIAP-1, cIAP-2, XIAP, induced by NF-κB.

cFLIP, which suppresses caspase-8 in complex-II, contains 11 known isoforms. The two predominant isoforms are the long ($cFLIP_L$) and the short ($cFLIP_S$) (29). Unlike caspase-8, $cFLIP_L$ lacks a catalytic cysteine necessary for enzymatic activity, so despite its resemblance to caspase-8 in domain architecture; $cFLIP_L$ is just an inactive pseudo-caspase. $cFLIP_L$ and caspase-8 can form heterodimer. Through dimerisation-induced conformational changes of this heterodimer, $cFLIP_L$ mediates activation of caspase-8. Hetero-dimerization rotates the catalytic pocket of caspase-8 into position for catalysis, allowing $cFLIP_L$-caspase-8 heterodimers to be functionally active (30, 31). However, the weak catalytic activity formed by such process is not enough to trigger cell death, because $cFLIP_L$ prevents cleavage of the prodomain of caspase-8, and the active caspase-8 cannot be released from FADD. Moreover, heterodimers formed by $cFLIP_L$ and caspase 8 show less proteolytic activity than caspase-8 homodimers on apoptotic substrates such as Bid and caspase-3 (31, 32). Unlike $cFLIP_L$, $cFLIP_S$ only encodes the prodomain, which contains the death effector domain (DED) necessary for FADD binding. Unlike $cFLIP_L$, which promotes localized activation of caspase-8, $cFLIP_S$ can completely inhibit caspase-8 activation (31, 33, 34).

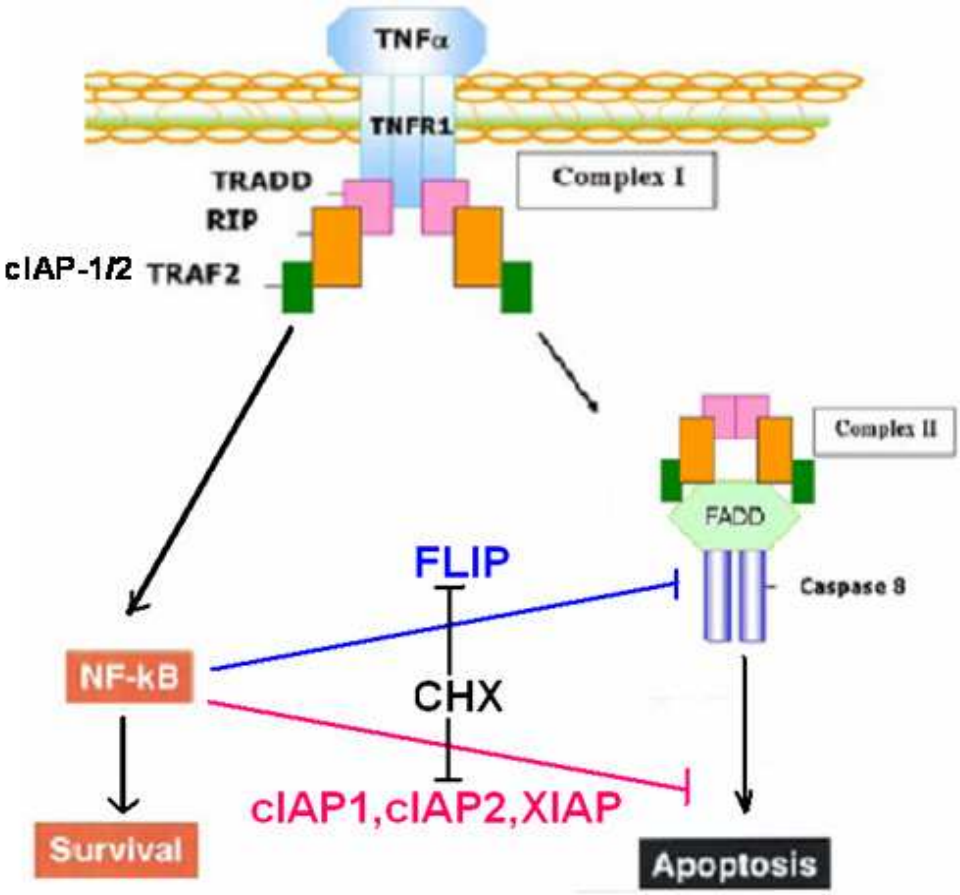

Figure 1-3. **TNF-R1 mediates apoptosis via two signaling complexes** (modified from reference (35))

1.3 IAP

1.3.1 Structure

IAP, which serves as endogenous inhibitors of apoptosis, is a family of structurally and functionally related proteins. The eight human members include Apollon, ILP2, Livin, Survivin, NAIP, cIAP-1, cIAP-2, and XIAP (Figure 1-4) (36). The defining feature of an IAP family protein is the BIR repeat, a zinc-binding fold of about 70 amino-acids residues that mediates protein and protein interactions, and is essential for the anti-apoptotic potential of most IAPs (37-39). IAPs carry one to three copies of this domain. BIR domains can be divided into type I and type II domains according to the presence of a deep peptide-binding groove. Type I BIR domains only have a shallow pocket instead of a peptide-binding groove, whereas type II BIRs carry a distinctive peptide-binding groove which enable them to bind to N-terminal tetrapeptides known as IAP-binding motifs (IBMs) (40-42). Apoptosis regulatory IAPs such as XIAP, cIAP-1, cIAP-2, DIAP1, and DIAP2 (DIAP1 and DIAP2 are homologs in Drosophila) possess two type II BIR domains. All of these IAPs, except DIAP1, also carry one type I BIR domain (40). It is important to note that type I and II BIR domains possess different binding features. Type II domains interact with caspases or IAP antagonists. Type I

BIR domains interact with other complete different set of proteins, such as TRAF1, TRAF2, and TAB1 (43, 44, 45).

These IAPs also harbor some other domains such as the carboxy terminal RING finger domain which enables them with ubiquitin ligase (E3) activity (46). Besides, they comprise a ubiquitin associated (UBA) domain through which they interact with ubiquitinated proteins (47, 48). Furthermore, cIAP-1 and cIAP-2 contain a caspase recruitment domain (CARD), whose function is currently not clear.

1.3.2 Function

Apart from the primary function of IAPs as regulating caspases, IAPs also influence many other cellular processes. For example, these proteins can affect ubiquitin-dependent signaling events that regulate activation of NF-κB transcription factors. Besides, IAPs can regulate signaling events which are included in activation of cell metastasis (49, 50). Further, they modulate mitosis and proliferation. Many of these cellular processes are related to disease initiation directly or indirectly (51, 52).

Furthermore, IAPs have important roles in tumour maintenance and resistance to chemotherapy treatments, although IAP expression on its own is clearly not the only determinant that increases apoptotic threshold and enables tumour growth (51-54). Cancer cells can propagate under unfavourable circumstances such as chromosomal aberrations, oncogene deregulation, hypoxia, DNA damage, and nutrient limitation. These adverse conditions while normally trigger caspase activation leading to apoptosis may fail to do so in cancer cells because of disordered expression and activity of IAPs.

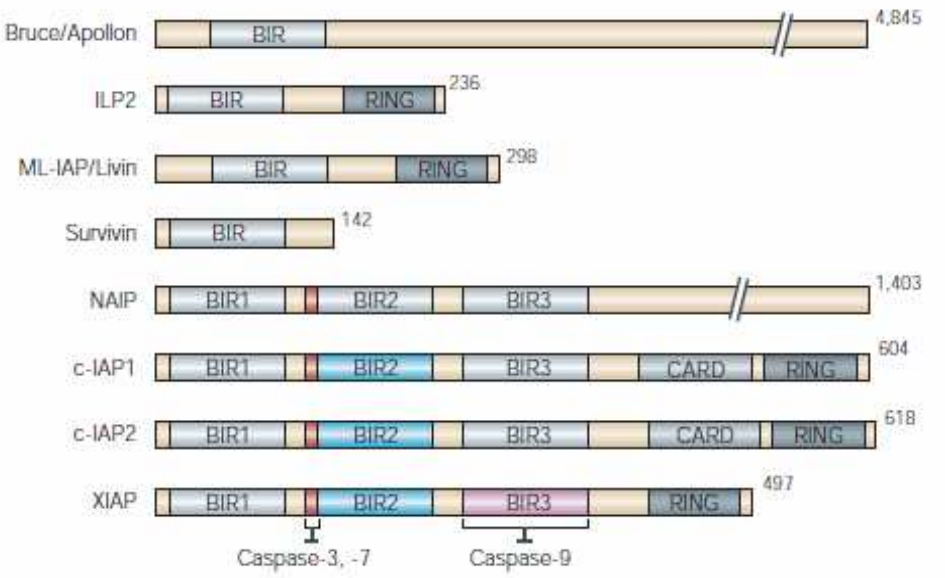

Figure 1-4. **IAP family proteins** (reproduced from reference (36))

1.4 XIAP

1.4.1 Discovery and function

The first identified homolog of IAP family in humans is NAIP (55). NAIP has three BIR domains at N-terminus but no RING finger motif. It is mainly expressed in neurons where its role is to protect cells against apoptosis (56) and it plays a crucial role for survival of neurons in pathological condition (57, 58). Later, a RING finger- and three BIR domains-containing IAP family member was found, which was named as X-linked inhibitor of apoptosis protein, XIAP. The transcript size of XIAP is 9.0 kb. It has a 1.8 kb long open reading frame (55). The mRNA of XIAP has been found in all of human adult and fetal tissues except peripheral blood leukocytes (55). Other members of the IAP family proteins were identified in succession based on their homology to XIAP sequence.

In vitro kinetic studies showed that XIAP had Ki values of 0.2 to 0.8 nM when compared with a 1-20 nM range for the other members of the IAP family proteins for inhibition of apoptosis (59). XIAP is known to be the most potent caspase inhibitor in the IAP family. XIAP inhibits both the initiator caspase 9 and the effector caspases 3 and caspases 7. Overexpression of XIAP efficiently inhibits caspase activation and apoptosis stimulated by the intrinsic apoptosis pathways and extrinsic apoptosis pathways (60-65). Conversely, cells that lack XIAP are sensitized to apoptosis (66-69).

1.4.2 BIR domain of XIAP and its function as direct caspase inhibitor

Among all of the members of IAPs, mammalian XIAP is the only one which can directly bind and inhibit caspase 3, caspase 7, and caspase 9, functioning as a direct caspase inhibitor (70). The potent ability of XIAP in inhibiting caspases owes to its BIR domains, which have distinct functions. Thus, XIAP inhibit initiator and effector caspases using different kinds of ways.

The second BIR domain (BIR2) binds and inhibits the active site pocket of caspase 3 and caspase 7 by completely filling the active site to prevent entry of substrates (39, 71-75). It has been found that Gly144, Val146, Val147, and Asp148 of XIAP form either hydrogen bonds or Van der Waals interactions with caspase 7 substrate-binding sites S1, S2, S3, and S4, respectively (74). Of these interactions, the one between Asp148 and S4 is the most important for docking interaction (72). The structural arrangement between XIAP and caspase 3 is similar to that between XIAP and caspase 7 (75). Since caspase 3 and caspase 7 have almost the same backbone structures and share 54% sequence identity (74), binding of XIAP to caspase 3 is mediated by the same four pairs of residues as caspase 7 in a similar way (75). The four caspase-interacting residues, Gly144, Val146, Val147, and Asp148, are conserved

among XIAP and two other IAP family proteins, cIAP-2 and cIAP-1 (72). All of these three IAPs have a function in inhibiting the effector caspases 3 and 7 (76).

There are two binding interactions between XIAP and caspase 3 and 7. Residues in the linker region between the BIR1 and BIR2 domain of XIAP bind to the active site pocket of caspase 3 and caspase 7, occluding the substrate entry and resulting in the inhibition of the catalytic activity of these two effector caspases (39, 71-75). Besides, BIR2 domain of XIAP makes additional contact with an IBM motif present at the neo-amino-terminus of the activated caspase 3 and caspase 7 (75, 77). In non-active caspases, the IBM motif is hidden. It is only exposed in the active caspase 3 and 7 after a cleavage-mediated activation process. These two binding interactions strengthen the interaction with one another, which is essential for XIAP to dock effectively onto effector caspases for inhibition.

It was shown recently that the isolated BIR3 domain is enough to inhibit caspase-9 potently (39). However, the mechanism by which XIAP inhibits the initiator caspase 9 is very different from its inhibition of the effector caspases 3 and 7. XIAP binds only to processed caspase 9, not to the inactive procaspase 9 (42). After recruitment of procaspase 9 to oligomerized Apaf-1 within apoptosome, small subunits, named p12, and a large subunit of caspase 9 can be released at Asp315 of procaspase 9 in an autocatalytic procedure. In normal condition, these two subunits join together to form dimer. In order to carry out its apoptotic function, caspase 9 requires a dimerization induced conformational change to generate a productive catalytic pocket. However, the XIAP BIR3 domain can bind directly with the new free amino terminus of p12, which is important for the dimerization (42, 78). This binding of XIAP to caspase 9 prevents the joining of large and small caspase subunits, and interferes with caspase 9 dimerization. This kind of interference inactivates caspase 9 and blocks the caspase cascade.

The function of the BIR1 domain of XIAP is still unknown. No data indicates that BIR1 of XIAP can inhibit caspases. Indeed, a truncated XIAP with only BIR1 domain, loses its interaction ability with caspase 3 or caspase 7, and cannot inhibit apoptosis (64).

1.4.3 RING domain of XIAP and its function as E3 in ubiquitination

Apart from BIRs, XIAP harbors a C_3HC_4 RING finger motif, which is a zinc-binding and carboxy terminal domain. The function of the motif was unknown when first discovered, but is now widely accepted as critically important to the ubiquitin ligase activity of RING-containing E3 ligases (79), by serving as the dimerization interface and docking site for ubiquitin conjugating enzymes (E2s). The change of a single zinc-chelating residue in this region can eliminate E3 activity (46). This RING finger enables XIAP to catalyze ubiquitination of self, XIAP interacting proteins involved in apoptosis, and other targets

whose physiologic roles likely extend beyond cell death (80). Furthermore, XIAP harbors a UBV domain, which allows XIAP to bind polyubiquitin (81). XIAP is capable of auto-ubiquitination in a manner dependent on the E3 activity, which counts on the RING domain itself. The general assumption has been that the auto-ubiquitination of XIAP is a K48 ubiquitin conjugation process, which leads to proteasomal degradation (82).

Two types of proteins can trigger or promote the ubiquitination of XIAP:

(1) IBM-bearing antagonists of XIAP

XIAP has two types of antagonists. One is of IBM-bearing antagonists, such as mitochondrial interaction proteins Smac/DIABLO, Omi/HtrA2, CLPX, LRPPR, GdH, Nsp4, or ER associated protein GstPT/eRF3, which have been described to bind and antagonize XIAP via their IAP-binding motifs (IBMs) potentially (83). The other type is of the antagonists that do not have IBMs, such as AIF and ARTS, which are thought to bind IAPs through distinct mechanisms independent of IBMs (84, 85). Only the IBM-bearing antagonists can trigger the degradation of XIAP in auto-ubiquitination degradation manner under some circumstances (86-89). The essential reason is that the binding of these IBM-containing XIAP-interacting proteins can induce a structural change to XIAP, which favours auto-ubiquitination.

(2) Other RING-bearing IAPs

Some other RING-bearing IAPs, such as cIAP-1, can cause the ubiquitination of XIAP. RING motif of cIAP-1 binds directly to the RING motif of XIAP. Via the E3 ligase activity of the RING from cIAP-1, XIAP is ubiquitinated and degraded by proteasome (90, 91).

Apart from XIAP itself, the RING finger also modulates the level of other substrates in a similar manner. Some of them are involved in apoptosis, while some are related to other signaling pathways apart from death. These substrates are as follows:

(1) Caspases

Through the Ub ligase E3 activity of RING motif, XIAP is capable of caspase 3, 7, and 9 ubiquitination in vitro and caspase 3 ubiquitination in vivo (73, 92). This type of ubiquitination has been linked to degradation and non-degradation inactivation of caspases (73, 81, 92).

(2) AIF, Smac

AIF, a positive intrinsic regulator of apoptosis, can cause DNA fragmentation and chromatin condensation, initiating a caspase-independent pathway of apoptosis. It also acts as an NADH oxidase. SMAC is a mitochondrial protein, which promotes cytochrome c-dependent apoptosis activation by eliminating XIAP . These two XIAP associated proteins, Smac and AIF, have been demonstrated to be the targets for ubiquitination through interaction with XIAP, which requires the RING finger (84, .

(3) Survivin

Another IAP family member, Survivin, has also been reported to be down-regulated by XIAP

via its RING motif (95). This process requires the synergism of another protein, XAF1. Survivin is also a member of the IAP family, which antagonizes the anti-caspase activity of XIAP and may be important in mediating apoptosis resistance in cancer cells.

(4) TAK1

TAK1 belongs to the serine/threonine protein kinase family. This kinase controls a variety of cell functions including transcription regulation and apoptosis and mediates signaling transduction induced by TGF β and BMP. This protein forms a kinase complex, which is required for activation of NF-κB in response to IL-1. The components of this complex also include TRAF6, MAP3K7P1/TAB1, and MAP3K7P2/TAB2. Furthermore, TAK1 plays an important role in cell response to environmental stresses by activating MAP2K4/MKK4 and MAPK8/JNK. XIAP can activate the NF-κB activity (96-98). The target of XIAP in this process is the serine threonine kinase, TAK1 (99, . This mechanism also requires an association with TAB, which is mediated by the BIR1 domain of XIAP (101, 102). XIAP can shut down the JNK activity also by promoting the ubiquitin-mediated degradation of TAK1 via the RING finger. Once JNK is inhibited, the JNK-induced cell death is prevented .

(5) MEKK2

XIAP also directs the ubiquitination of the NF-κB-activating kinase MEKK2, which activates IκB kinases by phosphorylation directly. The non-K48 conjugated ubiquitin chains of MEKK2 are catalyzed by XIAP. Non-K48 ubiquitination has diverse non-degradative functions, which include altering protein structure, localization, interaction, or activity (103).

(6) COMMD1

XIAP is also a negative regulator of COMMD1, by promoting degradation of COMMD1 via the E3 ubiquitin ligase activity. COMMD1 is a NF-κB suppressor. COMMD1 binds to multimeric ubiquitin ligases containing Elongins B/C, Cul2, and SOCS1 (ECSSOCS1) to form a complex. In this complex, COMMD1 facilitates the binding of NF-κB to the ligase, thereby promoting ubiquitination and degradation of NF-κB (104). Apart from the function as a NF-κB suppressor, COMMD1 is also involved in a variety of other cellular functions, including hypoxia (105) and copper homeostasis (106). Whether XIAP also involved in the latter two activations needs further evidence to support (107, 108).

1.4.4 XIAP associates with apoptosome

Subsequent to the release of cytochrome c from the mitochondria to cytosol during apoptosis, the adaptor molecule Apaf-1 is oligomerized and procaspase-9 is recruited into apoptosome, a holoenzyme multi-protein ‘death’ complex. Caspase 9 is activated by the oligomerization of procaspase 9 in this complex. At the same time, caspase 3 is recruited and activated by either active caspase 9 or the procaspase 9. After that, the active caspase 3 is released from apoptosome to execute its function. Evidence shows that XIAP is associated with apoptosome where it interacts with either caspase 9 or caspase 3. It can prevent not only the release of caspase 3 from apoptosome but also the activation of caspase 3 by caspase 9 (109).

1.4.5 Antagonists of XIAP

Smac/DIABLO is the best understood antagonists of XIAP, which promotes apoptosis. In normal condition, Smac/DIABLO is a catalytically inactive precursor protein located in mitochondria. Under activation of the mitochondrial apoptotic pathway, the 55 amino-acids amino-terminal targeting sequence of Smac/DIABLO is removed, resulting in exposure of the IBM domain for the binding to IAPs. Subsequent cytosolic release of the N-terminally cleaved Smac/DIABLO can promote apoptosis by binding to XIAP and inhibit its anti-apoptotic activity. Besides, Smac/DIABLO can likewise interact with other members of the IAP family proteins including cIAP-1, cIAP-2, and Survivin (110, 111).

Another important inhibitor of XIAP is the XIAP-interacting protein (XAF1). In contrast to Smac/DIABLO which requires pre-processing for activation, this seven zinc fingers-containing protein can readily interact and inhibit XIAP directly (112). Of note, XIAP levels are relatively high in most cancers while the XAF1 levels are very low or even undetectable in various cancer cell lines (112). This phenomenon indicates that XAF1 may play an important role as a tumour suppressor (113).

1.4.6 Clinical significance of XIAP

Deregulation of XIAP can result in cancer, neurodegenerative disorders, and autoimmunity related disease (55, 65). XIAP is found overexpressed in cancer cells. XIAP mRNA, assayed by reverse transcription polymerase chain reaction, is a useful tumor marker for discriminating cancer tissue from normal tissue. It can be applied to lung cancer (114), prostatic epithelium cancer (115), and colorectal cancer (116) etc. Furthermore, combination of XIAP with other tumor makers, such as Survivin and CEA (carcinoembryonic antigen) can increase diagnostic performance (117). In addition to its function in cancer, deregulation of XIAP can result in abnormal autoimmunity related disease (65), such as the inflammatory bowel disease (118). Furthermore, XIAP is involved in neurodegenerative disorders (65). Defects in XIAP gene can also result in an extremely rare condition called X-linked lymphoproliferative disease (118).

1.5 Ubiquitin and ubiquitination

1.5.1 Overview of ubiquitin

Ubiquitin, a small protein, has been found in almost all of tissues of eukaryotic organisms universally. It is named because of its ubiquitous expression. It is highly conserved among eukaryotic species: human and yeast ubiquitin has 96% sequence similarity. This small protein consists of 76 amino acids and has a molecular mass of about 8.5 kDa. The human ubiquitin sequence in one letter code is MQIFVKTLTGKTITLEVEPSDTIENVKAKIQDKE

GIPPDQQRLIFAGKQLEDGRTLSDYNIQKESTLHLVLRLRGG. Its C-terminal tail and 7 lysine residues are important for its structure and function. These 7 lysine residues are K6, K11, K27, K29, K33, K48, and K63.

Ubiquitin can conjugate together to form isopeptide-linked polymers known as polyubiquitin chains. Most of the ubiquitin chains are built by formation of an isopeptide bond between Gly76 of one ubiquitin to the ε-NH_2 group of one of the seven potential lysines (K6, K11, K27, K29, K33, K48, and K63) of the preceding ubiquitin. Specific E2 enzymes and E2/E3 combinations result in the formation of linkage-specific ubiquitin chains. Mono-ubiquitin or different kinds of polyubiquitin chains have different conformations. They all can be attached to a large range of target proteins while mono-ubiquitin or different types of polyubiquitin chains play different roles on their targets.

Residue K48 is a major site of chain initiation. K48-linked ubiquitin chain is constituted through isopeptide bond formation between the carboxy-terminal Gly76 of one ubiquitin and K48 residue of another ubiquitin. K48-linked ubiquitin chains can be attached to proteins and label them for degradation by proteasome. These chains display a rather twist conformation.

The other principle and relatively abundant polyubiquitin chains have K63-linkages, which do not seem to play a role in protein turnover. Instead, K63-linked ubiquitin chains perform a more diverse set of functions, such as altering protein structure, localization (protein docking), interaction, or activity. The K63-linked polyubiquitin chains labeled proteins are related to receptor endocytosis and sorting, DNA damage repair, translation and stress response, etc. These chains, linked via the Gly76 of one ubiquitin and K63 of another ubiquitin, display an open conformation.

Importantly, different from all of the chains linked by lysines, the head-to-tail linear ubiquitin chains are those linked via the C- and N-terminus of ubiquitins without involving any lysine residue of the ubiquitin. Linear ubiquitin chains can also alter protein localization (protein docking). They display an equivalent conformation to K63-linked chains.

Protein mono-ubiquitination has been shown to play key functional roles that are apparently independent of degradation. It plays an important role as a signal in protein trafficking and extra-cellular receptor internalization (119). The mono-ubiquitin labeled proteins are related to enzymatic activity, endocytosis, DNA-repair, and transcription etc. (120).

1.5.2 Ubiquitination process

Ubiquitination is a process of marking a protein with ubiquitin, also named ubiquitylation or ubiquitination. The amide bond is formed between the epsilon amine of the lysine in the

modified protein and the carboxylic acid of the terminal glycine, located in the di-glycine motif, in the activated ubiquitin. As shown in Figure 1-5 (121), this enzymatic, protein post-translational modification process consists of a three main steps. The first step is the activation of ubiquitin in a two-step reaction by an E1 (ubiquitin-activating enzyme) requiring ATP as an energy source. Initially, an ubiquitin-adenylate intermediate is produced. Next, ubiquitin is transferred to E1 active site cysteine residue, releasing AMP at the same time. After that, a thioester linkage between the E1 cysteine sulfhydryl group and the C-terminal carboxyl group of ubiquitin is created. The second step of this cascade is transferring of ubiquitin from the cysteine of E1 to the active site cysteine of an E2 (ubiquitin-conjugating enzyme). This process is a trans (thio) esterification reaction. The third step is conjugating the C-terminal glycine of ubiquitin from the cysteine of E2 to a lysine of the target protein via an isopeptide with the help of E3 (ubiquitin-protein ligase), which is capable of interaction with both E2 and substrate. The substrate recognition responsibility owes to E3. That is why there are hundreds of E3s in the cell. In the ubiquitination cascade, the number constitution of E1, E2, and E3 is like a pyramid. A few E1s can bind with dozens of E2s, which can work with hundreds of E3s in a hierarchical way. Besides, other ubiquitin-like proteins (ULPs) are also modified via the E1-E2-E3 cascade analogously.

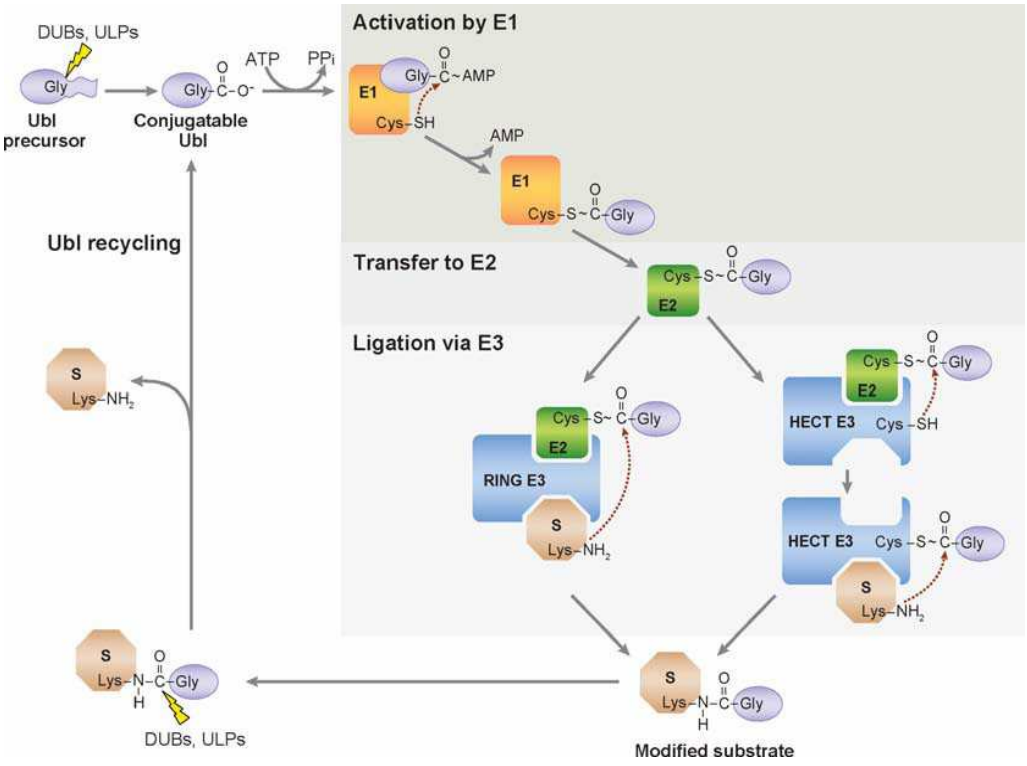

Figure 1-5. **Ubiquitination cascade** (reproduced from reference (121))

1.5.3 Ubiquitin-activating enzymes, E1s

Using ATP as energy source, the adenylation active site of E1 catalyzes an adenylylation at

the C-terminal of ubiquitin. This intermediate is usually called ubiquitin adenylation intermediate (122-124). After that, this intermediate is attacked by the catalytic cysteine of E1, producing a covalent thioester linkage between the cysteine sulfhydryl of E1 and the C-terminus carboxyl of ubiquitin, with the release of AMP at the same time (122, 123, 125, 126). Thus, E1 binds two ubiquitin molecules at the same time at different active sites asymmetrically. One ubiquitin is linked to the cysteine of E1 via its C-terminal carboxy, forming a covalent thioester bond. The other ubiquitin is bound to the adenylation active site of E1 via its C-terminus non-covalently. Each step of the E1 reaction is reversible. Progression of the cascade is driven by releasing of the small molecule products PPi and AMP at different steps, respectively (122-124, 127, 128).

For more than twenty years, it was accepted that there is only one ubiquitin activating enzyme, which can work with all of the E2s in ubiquitin system. This E1 is called UBA1. This 118-kDa enzyme contains an adenylation domain. However, this central dogma has been challenged recently. A second E1 enzyme for ubiquitin was identified, which was called UBA6 or Ube1L2 (129, 130). UBA6 is charged by ubiquitin in vitro and in cells. Having the same molecular weight as UBA1, UBA6 shares around 40% identity with UBA1. UBA6 also contains an adenylation domain, which is responsible for ubiquitin recognition and acyl-adenylation. Different from UBA1, which charges most of the E2s, UBA6 is uniquely responsible for transferring ubiquitin to its selective E2, which is named USE1 (Uba6-specific E2) (129). UBA6 and USE1 are expressed broadly. They have been found in organisms from humans to zebra fishes, and even in sea urchins, but not in flies, worms, or yeasts. This expression pattern indicates a selective role of UBA6 and USE1 in a specific phylogenetic branch of metazoa that leads to humans.

Apart from the above-mentioned two E1s for ubiquitin, other E1s have been found for ubiquitin-like proteins, which are also modified via the E1-E2-E3 cascade similarity. These E1s together with their selective E2s and ubiquitin-like proteins are: UBE1L, which shares 46% identity with UBA1, is specific for ISG 15, working together with the E2, UbcH8 (131). ISG15 is a ubiquitin-like protein that becomes conjugated to many cellular proteins upon activation by interferon-α and -β (132). Both APP-BP-1 and UBA3 can activate NEDD-8 using UBC12 as their unique E2 (133). The ubiquitin-like proteins SUMO 1, 2, 3 can be activated by either AOS1 or UBA2 with the help of their unique E2 UBC9 (134, 135). The 50 kDa E1 UBA4 is specific for URM-1, while their E2 is unknown (136). E1 UFM-1 and E2 Ufc1 are unique for the ubiquitin-like protein UBA5 (137). E1 for ATG12 and ATG8 is ATG7. ATG means autophagy-related. ATG7 shows homology to the ATP-binding and catalytic sites of UBA1. ATG12 and ATG8 are ubiquitin-like proteins. ATG12, ATG8, and ATG7 are indispensable for formation of the autophagosome (138). Their E2s are ATG10 or ATG3 (139). Of note, the UBA6 which is the E1 for ubiquitin, can also activate the ubiquitin-like protein

FAT10 (129, 130, 140).

1.5.4 Ubiquitin-conjugating enzymes, E2s

With the active cysteine of E2, ubiquitin is transferred from the cysteine of E1 to a cognate E2. This a trans (thio) esterification reaction which creates a high-energetic conjugation between the C-terminus of ubiquitin and the cysteine of E2 (123, 127, 128). The characteristic of E2s is their ubiquitin-conjugating catalytic (UBC) fold. This 150-200 amino acids, 14-16 kDa domain is highly conserved among different family members , 142). This domain provides a platform for the interactions between ubiquitin (or ubiquitin-like proteins), E1s and E3s (142). The key residue of this domain is the embedded catalytic cysteine, which conjugates the ubiquitin or ubiquitin-like protein via thioester bond first. Then it interacts with E3 prior to the subsequent substrate conjugation.

Each ubiquitin-conjugating catalytic fold can be divided into three shells of amino acids. The cysteine and conserved residues surrounding it are embedded in the first shell. The cysteine has direct catalytic activity while the residues surrounding it regulate the ubiquitin conjugation directly. These residues are solvent approachable and regulate the activated ubiquitin. The second shell contains the inner core structures and overlaps with the first shell partially. The actual surface residues constitute the third shell, which are important for the interactions of E2 with other proteins, like E1 and E3.

Up till now, around a dozen ubiquitin-like proteins have been found, such as ISG15, SUMO-1, 2, 3, NEDD-8, URM-1, UFM-1, FAT10, ATG12, ATG8, etc. Almost each of those has its own particular E2 specificity. Thus, the conjugation between ubiquitin and ubiquitin-like proteins with E2s is parallel . However, some comprehensive crosstalks between different pathways may happen. For example, crosstalks between ubiquitin and ISG15 conjugation pathways (143) and between ubiquitin and SUMO (small ubiquitin-like modifier) (144) have been identified. E2 enzymes have been found in all of eukaryotes, emphasizing the significance of ubiquitin systems in biology (145, 146). The family protein is expanded during evolution. The higher the eukaryotes are, the more E2s they possess (145). Thirty-five E2s have been identified in humans to date. Other eukaryotic genomes have sixteen to thirty-five E2 family members.

Depending on the presence of additional extensions to the catalytic core, E2s have been grouped into four types. Class-I only harbors the catalytic domain. Class-II and III have additional N- and C-terminal extension, respectively; whereas Class-IV has both extensions , 146). Because of these extensions, different E2 enzymes have marked differences in size. For example, class-I E2s, like UbcH5B (UBE2D2) and hHR6A (UBE2A) are small molecular. The size of other E2s is larger. For example, Ubc12 (UBE2M) and UbcH6 (UBE2E2) of

class-II and class-III UBE2U, containing non-conserved extensions, can reach 200-400 amino acids in size. The functions of E2 are also different because of these extensions. These functional differences include modulation of the activity of E3, stabilization of interaction with E1 and subcellular localization.

1.5.5 Ubiquitin-protein ligases, E3s

E3s are a large, diverse group of proteins. They can be divided into three main types depend on different defining motifs. The first group is HECT, which can catalyze ubiquitin directly. The other two types are RING and U-box, which promote protein ubiquitination indirectly. RING and U-box work like an adaptor, which performs as a platform to bring together the E2 and substrate ubiquitination of the latter.

As mentioned above, proteasomal degradation of proteins is not always the primary function of ubiquitination. E3s together with their substrates are identified to have diverse and wide functions. For example, RING type E3 TRAF6 and its substrate NEMO are necessary in NF-κB processing and NF-κB activation (147). Interestingly, the levels of E3s themselves can also be regulated by proteasome-mediated degradation via self-regulation by auto-ubiquitination (148-151).

1.5.5.1 HECT domain E3s

After the identification of the first E3, E6-AP1, a total of 28 human HECT type E3s, which contain a similar 350 amino-acids catalytic cysteine domain have been characterized by database searches (152). Similar to the E2, a thioester bond is conjugated between the central cysteine residue within the HECT domain and the carboxy group of the C-terminal glycine ubiquitin. E2 accepts ubiquitin before transferring it to the substrate. Whereas the C-terminal HECT domain contains E3 activity of ubiquitin conjugation, the N-terminal domain, many of which are larger than 100 kDa, is responsible for substrate binding. The members of HECT E3s together with their targets have been demonstrated to have a role in disease processes, in particular in cancer. These cancer related E3s and their targets are shown in Table 1-1 (153). HECT E3s use multiple ways to form polyubiquitin chains. For example, the E6AP builds K48-linked chains. The UBE3C constitutes K48- and K29-linked chains to the targets , 155). Besides, the Rsp5 prefers to build up K63-linked chains (156).

Table 1-1. **HECT E3s, their substrates and their involvement in cancer**

E3	Substrate	Outcome of substrate ubiquitylation	Adaptors/regulators	Biological function	Alterations in cancer
E6-AP	p53	Proteasomal degradation	E6	Apoptosis	Infection by high-risk HPV

E3	Substrate	Outcome of substrate ubiquitylation	Adaptors/regulators	Biological function	Alterations in cancer
					in cervical carcinomas
Huwe1	p53	Proteasomal degradation	ARF	Apoptosis, growth arrest	Overexpression in breast, lung, and colorectal carcinomas
EDD	TopBP1	Proteasomal degradation	Unknown	DNA damage	Amplification and overexpression in breast and ovarian cancers
Nedd4-1	PTEN, Hgs, Eps15	Proteasomal degradation, cytoplasmic/nuclear shuffling	Unknown	Apoptosis, Genome integrity, endocytosis	Overexpression in bladder and prostate carcinomas
Nedd4-2	Smad2, Smad4, TβR-I/II	Proteasomal degradation	Smad6, Smad7	Apoptosis, growth arrest	Unknown
Itch	p73, p63, Notch1, c-Jun	Proteasomal degradation	Numb	Apoptosis, differentiation	Unknown
WWP1	p53, Notch1, KLF2, KLF5, Smad2, Smad4, TβR-I/II	Proteasomal degradation, nuclear export	Smad2, Smad6, Smad7	Apoptosis, growth arrest	Amplification and overexpression in prostate and breast cancers
Smurf1	Smad1, Smad4, Smad5, TβR-I/II, BMP-RI/II	Proteasomal/lysosomal degradation	Smad6, Smad7	Apoptosis, growth arrest	Amplification and overexpression in pancreatic cancers
Smurf2	Smad1, Smad2, Smad4, Smad5, TβR-I/II	Proteasomal/lysosomal degradation	Smad2, Smad7	Apoptosis, growth arrest	Overexpression in esophageal squamous cell carcinomas

1.5.5.2 RING finger E3s

This RING type E3 contains many more members than other types of E3. To date, hundreds of proteins containing a RING finger domain have been identified in mammalian genomic databases (157, 158). Of note, although their structures suggesting an E3 function, not all of the proteins containing this finger motif have the activity in vivo. The function of RING is not direct. It acts as scaffolding partners, facilitating the interaction between an E2 and a substrate (157, 158). The RING finger domain is defined as Cys1-Xaa2-Cys2-Xaa9-39-Cys3-Xaa1-3-

His4-Xaa2-3-Cys/His5-Xaa2-Cys6-Xaa4-48-Cys7-Xaa2-Cys8 (where Xaa can be any amino-acid residue) (157). The two important factors of the domain are the cysteine/histidine and zinc atoms, which are important in promoting both of protein-protein and protein-DNA interactions. Depending on whether a cysteine or histidine residue is found at Cys/His5 within the motif, RING finger motifs are further subdivided. The RING-HC type RING contains a Cys5 while the RING-H2 type RING contains His5. Both of the Cys5 and His5 are important for E2 recognition. Two zinc atoms in the RING are complexed by the cysteine/histidine residues in a 'cross-brace' manner, which is structural important for correct folding and biological activity of the RING domain. See Figure 1-6 (159).

RING E3s come in four molecular architectures: single chain, homo-dimeric, hetero-dimeric, and multi-component. In large RING-containing complex, the other components in the complex facilitate the functional specificity and potency of the RING type E3. The best-known complex of this kind is the anaphase-promoting complex. Since there are hundreds of pairs of RING E3s and their substrates, the functions of them are wide and diverse in cell. These functions are related to apoptosis and cancer, neurological disorders, as well as a host of other conditions. See Table 1-2 (159).

Table 1-2. **RING type E3s and their target(s)**

Disease		**E3**	**Target(s)**
Cancer	Breast/ovarian	BRCA1, BARD1	H2A, H2B, H3, H4
	Colonic, gastric	SCF Multi-complex	β-catenin, NF-κB
	Renal cell carcinoma and others	VCB Multi-complex	HIF-1α, HIF-2α
	Sarcoma, leukaemia	MDM2, MDMX	p53
	Ewings sarcoma, acute leukaemia	c-Cbl	EGFR
	Lung cancer, prostate cancer	XIAP	XIAP, caspases 3 and 7 Smac, AIF Survivin
Neurological disorders	Parkinson's disease	Parkin, Dorfin, Siah-1,	Multiple
	ALS	Dorfin	Mutant SOD1
	Lafora disease	Malin	Unknown
Miscellaneous conditions	Muscle cachexia	E3α, MuRF1, MAFbX multi-complex	Multiple

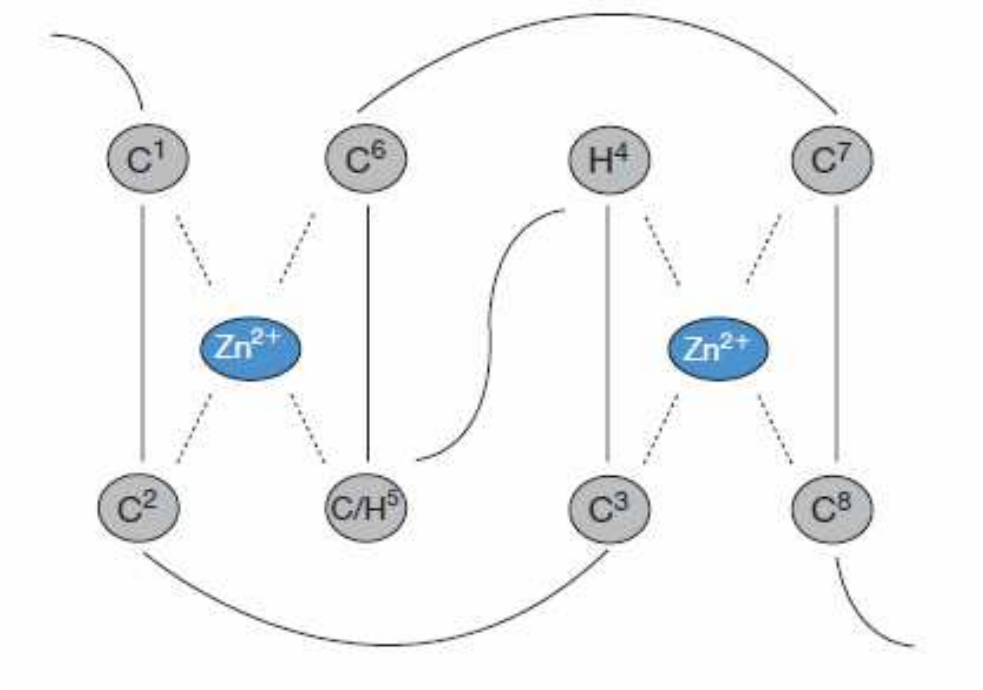

Figure 1-6. **Structure of RING finger** (reproduced from reference (159))

1.5.5.3 U-box E3s

U-box, 74 amino-acids domain, shares similar structure with the RING finger domain (160, 161). The difference is that the U-box does not contain the important Zn required for metal chelation. Thus, it utilizes a salt bridge instead of zinc chelation to maintain correct folding. Similar to the RING, some of the U-box E3s can work independently while some others have to associate with other multi-proteins to exert the E3 function. Famous well studied U-box E3 is CHIP, which has multiple substrates. CHIP and its substrates are related to neurological disorders, such as Parkinson's disease, ALS, and Alzheimer's disease.

1.5.6 Proteasomes

1.5.6.1 Overview of proteasomes

The major enzyme system catalyzing the degradation of intracellular proteins is the ubiquitin proteasomes system. This catalytic system carries out its function hierarchically. Firstly, unwanted protein is tagged by K48-linked polyubiquitin chains via the E1-E2-E3 cascade. Then this protein is degraded in the proteasomes with the ubiquitins released and recycled. The proteasomes consist of two components, the key 20S proteasome containing the active site to fulfill the degradation and the 19S regulatory particles, which is important to pre-treat folded substrates. Depending on the number of the attached regulatory 19S, the proteasomes appear in various forms. One 19S regulatory particles binding to one end of the 20S constitute the 26S proteasome, which is the most common type of proteasomes. The 20S attached by double 19S composes 30S proteasome. Besides, hybrid proteasomes are also been identified. The three-dimensional shape of the 20S proteasome looks like a cylinder. Proteins are

degraded down into small peptides of 3 to 25 amino acids by 20S.

Although 20S proteasome is pivotal for protein degradation, it is extremely inefficient in degrading folded substrate. The polyubiquitin conjugated and folded substrates need to be pre-processed by the multi-subunit 19S regulatory particles. This regulatory 19S, attaching to one or two ends of 20S, contains multiple functions. It recognizes and captures its substrates. It initiates substrates unfolding and facilitates their translocation from 19S to the central 20S. Besides, this complex has deubiquitinating activity, which can remove polyubiquitin chains from substrates. After that, the ubiquitin is released and can be re-used by cell (162-165).

1.5.6.2 19S regulator complex

The 19S regulator, also named cap, is a multi-protein complex composed of two sub-complexes, base and lid. Eight different non-ATPase subunits, Rpn3, Rpn5-Rpn9, Rpn11, and Rpn12, constitute this upper sub-complex, lid. The base is constituted by eight subunits. Six of them, named Rpt1-Rpt6, harbor ATP-hydrolysing activity, while the other two, name Rpn1 and Rpn2, are non-ATPase. The Rpn1 and Rpn2 are the largest subunits of 19S. Base and lid are conjugated by Rpn10.

The 19S pre-treats its substrates prior to the final destruction in the following way:

(1) A subunit in the lid recognizes substrates. The 19S has the ability to bind ubiquitinated as well as several non-ubiquitinated substrates.

(2) An unstructured initiation site of base anchors the substrates via polyubiquitin chains. After that, the substrates begin unfolding by the same site.

(3) In non-activated state, entrance pore of 20S is closed partially. This is done by the N-terminus of the α subunits of 20S, which form a mesh to separate the 20S. Upon completing the unfolding of the substrate, docking of the 19S will displace this N-terminus to open the entrance pore.

(4) With the help of 19S, the unfolded protein can be translocated from 19S into the chambers of 20S through the entrance pore formed by the α ring.

(5) Rpn11 in lid contains deubiquitinating function, which removes the polyubiquitin chains from substrates (166).

1.5.6.3 20S, 26S, and 30S proteasomes

The 20S is the pivotal complex, which catalyzes substrates degradation. The 20S is a high molecular-mass complex. The shape is like a cylinder or barrel. The size is 11 nm × 15 nm. This complex is built up by four stacked rings. The internal two stacked rings each consists of seven β subunits. The two outer rings, composed of seven α subunits, are attached to the two ends of β rings, respectively. Thus, the overall architecture of 20S is α1-α7/β1-β7/β1-β7/α1-α7. Based on the function of 20S, it can be divided into several segments. The entrance and exit

pores are built up by α rings. Between the rings of α and β subunits, the pores enlarge into antechambers. The antechambers enlarge further into proteolytic chamber, which is built up by the inner walls of β rings.

With the help of 19S, the entrance pore opens to allow the substrate entering. The unfolded protein accesses to the proteolytic chamber through the antechamber. The volume of this proteolytic chamber is around 84 nm^3. It is the site for catalysis of peptide bond hydrolysis. The N-terminal threonine residues, located in the inner wall of β rings, contain the active site. The degraded products, small peptides of 3 to 25 amino acids, leave 20S through the other α ring pore. After that, the amino acids are released and can be re-used by cell. The complete function of proteasomes is based on the cooperation of 19S and 20S. The conjugation between them requires the binding of ATP to the 19S ATPase subunits (167).

1.5.7 Deubiquitinating enzymes

1.5.7.1 Overview of deubiquitinating enzymes

These deubiquitinating enzymes (DUBs) play several roles related to ubiquitin pathway:

(1) DUBs have the function to activate ubiquitin proproteins. This procedure is likely to be cotranslational.

(2) In ubiquitination process, some ubiquitins may be captured by small cellular nucleophiles accidentally. DUBs have the function to remove these wrongly connected ubiquitins and release them for re-use.

(3) The ubiquitination of target proteins can be controlled by DUBs negatively. DUBs release the ubiquitin from target substrate.

(4) Not all of the polyubiquitin chains synthesized by cell are useful. These include the free polyubiquitin or unanchored polyubiquitin. Some of these are produced de novo by conjugating system, while some are released from target proteins. DUBs have the additional function to unpack free polyubiquitin chains to regenerate mono ubiquitin.

(5) DUBs can also reverse the ubiquitin-like modification of target proteins.

DUBs are members of proteases. Proteases form a superfamily, which contains 561 members in human genome (168). According to their catalytic mechanism, they are further grouped into five classes, which are aspartic, metallo, serine, threonine, and cysteine proteases. They can be divided further depending on phylogeny. However, only two types of proteases cysteine and metallo have DUBs.

Most DUBs are cysteine proteases. Three residues, cysteine, aspartate, and histidine consist of the catalytic triad. In this triad, the aspartate residue polarizes the histidine. While the histidine in turn de-protonates the adjacent cysteine. The thiol group of the cysteine contains the active site. During catalysis, the carbonyl of the scissile peptide bond between target and

ubiquitin is attacked by the catalytic active site of cysteine. After this nucleophilic attack, two components are released. One is the target protein. The other is a covalent intermediate formed by DUB and ubiquitin. The intermediate, which contains an oxyanion, has to be stabilized in oxyanion hole, which is composed of the main chain of the catalytic cysteine, a glutamine, glutamate, or asparagine residue. Then the intermediate reacts with a water to generate free DUB and ubiquitin.

In the metalloprotease, Zn^{2+} atom is stabilized by an aspartate and two histidine residues. The stabilized Zn^{2+} bond in turn polarizes water molecule to generate an intermediate formed by DUB and ubiquitin. Different from the cysteine proteases, the conjugation of the intermediate is non-covalent. By proton transfer from a water molecule, the intermediate is broken down, releasing free DUB and ubiquitin (169).

Depending on ubiquitin protease domains, the cysteine protease DUBs can be divided into four subclasses. They are ubiquitin-specific protease (USP), ubiquitin C-terminal hydrolase (UCH), Otubain protease (OTU), and Machado-Joseph disease protease (MJD). Since the metallo-DUBs have catalytic domains called JAMM (Jab1/Mov34/Mpr1 Pad1 N-terminal+), these metalloproteases are also named as JAMM. Human genome encodes around 95 DUBs. They are 58 USP, 4 UCH, 5 MJD, 14 OTU, and 14 JAMM domain-containing genes (170).

The activity of cysteine type DUBs can be inhibited by N-Ethylmaleimide (NEM). NEM is an organic compound that is derived from maleic acid. It contains the imide functional group, but more importantly it is an alkene that is commonly used to inhibit and modify all of cysteine residues in proteins and peptides, with alkylation occurring at the active site thiol group of cysteine residues (171, 172). The resulting thioether features a strong C-S bond and the reaction is virtually irreversible. Please see Figure 1-7 (173).

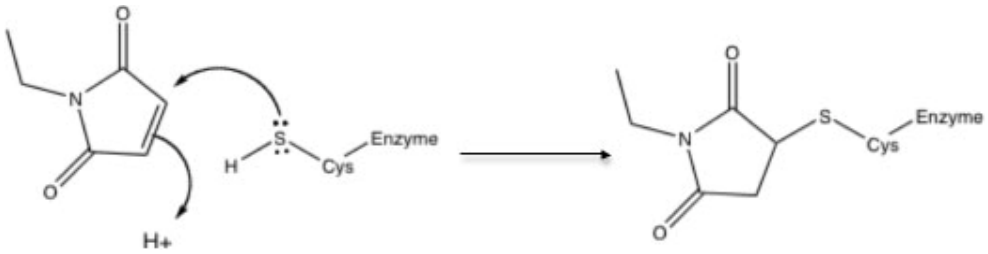

Figure 1-7. **Mechanism of irreversible inhibition of a cysteine peptidase with NEM** (reproduced from reference (173))

1.5.7.2 Ubiquitin C-terminal hydrolases (UCHs)

UCHs were the first discovered DUBs. Four proteins, which are highly homologous in their catalytic domains, form the human UCH subclass of DUBs.

Their functions have the following features:

(1) When ubiquitins are captured by small cellular nucleophiles, such as glutathione, polyamines, inappropriately, UCHs act in the recycling of these wrongly conjugated ubiquitin.

(2) UCHs may be involved in the processing of newly synthesized Ub, which is translated either as a polyubiquitin precursor or fused to a ribosomal protein (170).

(3) Based on the biochemical and structural results, UCHs prefers to cleave relatively small protein substrates, which contain less than 20 to 30 amino acids, from ubiquitin (174).

(4) UCHs cleave poly-Ub variants with varying efficiency. For example, the yeast DUB Ubp2 prefers to cleave K63- over K48-linked Ub chains as a substrate (175). UCH-L5 cleaves various types of polyubiquitin chains except linear dimers.

1.5.7.3 Ubiquitin-specific proteases (USPs)

USPs consist of 58 members, which are the largest subclass of DUBs. The catalytic domain of USPs is composed of Cys and His boxes, which are two short and well-conserved motifs. However, this catalytic domain is not sufficient to carry out its DUB function. It must work together with large unrelated, regulatory sequences, which are interspersed between Cys and His boxes. With different size of regulator, the size of complete catalytic domains of USPs varies from around 300 to 800 amino acids.

Not all members of USPs have complete catalytic triad. Take the USP30 and USP16 for example; they lack the aspartate, which are important to polarize the histidine. Nevertheless, they retain the catalytic function. This conflict indicates that some of USPs may use a different residue to stabilize the active site. Significantly, some members of USPs, such as USP16, USP30, USP39, USP45, or USP52, which lack the important Cys or His, indeed cannot cleave ubiquitin. So they are renamed as ubiquitin-specific protease variant (USPV), which are not real DUBs. The functions of these variants with respect to ubiquitin need to be further investigated (170).

Different members of USPs prefer different types of polyubiquitin conjugated substrates. For example, USP8 and USP14 can cleave K48- but not K63-linked Ub polymers (90, . In vitro assay reveals that some members of USPs, such as IsoT, USP2, USP15, and CYLD can cleave linear ubiquitin chains (177). It should be noted that in vivo assay for the above activity is not yet available. In vivo, only proteins, RIP1 and NEMO, which are involved in TNF-α-induced NF-κB signaling pathway, have been found to be substrate of linear ubiquitin chains. In this signaling pathway, ubiquitination of NEMO by K63 and linear ubiquitin, ubiquitination of RIP1 by K63, K11 and linear ubiquitin (147), are essential for NF-κB activation. CYLD can remove ubiquitin chains from NEMO (178) and RIP1 (179), thereby inactivating NF-κB activation. However, whether CYLD can remove the linear ubiquitin chains from NEMO and RIP1 has not been studied, needing further investigation (179, 180).

1.5.7.4 Machado-Joseph disease protein domain proteases (MJDs)

Ataxin-3 mutation is involved in a neurodegenerative poly-glutamine expansion disease called spinocerebellar ataxia type 3. Ataxin-3 and some Ataxin-3-like proteins constitute the MJDs subclass, which are characterized by a domain called Josephin. The similarity between this domain and other DUBs is quite low (181, 182). Ataxin-3 preferentially cleaves K63- over K48-linked polyubiquitin chains. It prefers to cleave longer over shorter chains (183).

1.5.7.5 Ovarian tumor proteases (OTUs)

The first named OUT members are Otubain-1 and Otubain-2, which are found to be able to cleave ubiquitin chains in vitro (184). After that, another OUT domain-containing protein, Cezanne was identified to harbor DUB activity in vitro and in a yeast two-hybrid assay (185). A20, a potent inhibitor of NF-κB signaling, is a well-known member of OUTs. In vitro, A20 can cleave both K48- and K63-linked Ub polymers with similar efficiency. However it only works for K63-linked but not K48-linked polyubiquitinated RIP in vivo (186). For most of the OTUs, their physiological functions remain to be investigated further. Unlike other cysteine protease DUBs, the OUTs lack the complete catalytic triad and their active site is stabilized by another means, which is related to a hydrogen bonding network (187).

1.5.7.6 JAMM motif proteases

JAMM is a widely expressed subclass, which can be found in all three major kingdoms of life, bacteria, archaea, and eukarya. Although bacteria have JAMM, they lack both ubiquitin protease activity and ubiquitin-like system. This phenomenon points out two indications:

(1) During evolution, JAMM domains have received some new protease functions.

(2) Some of human JAMM proteases may have diverse set of functions apart from DUB function.

Not all members containing JAMM harbor DUB function. The ones with at least one amino acid changed in the conserved Zn^{2+} ion-stabilizing residues are not a de novo DUBs (170).

Some members of this type are K63 selective DUBs. For example: AMSH, a K63-selective DUB , participates in multivesicular body sorting. Poh1, which is a stoichiometric subunit of 19S (PA700) proteasome regulatory complex, is also a K63 selective DUB (188). The specific disassembly of K63-linked chains is a property of BRCC36, which is one member of BRISC and BRCA1-A complex (188). Jab1 is anther JAMM type DUB. It is one member of CO9 signalosome (CSN). The CSN also contains a K63-selective DUB activity, which is due to its association with BRCC36 (188).

1.6 Background of BRE

1.6.1 DNA and RNA of BRE

1.6.1.1 Transcript variant of human and mouse BRE

BRE, brain and reproductive organ-expressed, also named TNFRSF1A modulator, BRCC4 or BRCC45. Its gene (NCBI gene ID 9577) is located at 2p23.2, from telomere to centromere. It starts from 28,113,557 to 28,561,767 bp, containing a total of 448,284 bases. It has two flanking genes, which are RBKS 2p23.3 and RPL23AP34 2p23.2. They are located in minus strand orientation and positive strand orientation, respectively.

The gene of human BRE contains fifteen exons (1 to 12, X, Y, and Z). See Figure 1-8 (189). Exons X, Y, and Z are alternatively spiced. The exon X is located between exon 1 and 2 at the 5' end, while the exon Y and Z are located between exon 11 and 12 at the 3' end. By alternative splicing predominantly at 5' or 3' end, a total of six transcript variants are produced. Three of them (αa, αb, αc) are produced by alternative splicing at the 3' end and one splicing between the exon 1 and 2 at the 5' end. Only these three transcripts are functional, which produce 3 protein isoforms with distinct C-terminus. The other three (βa, βb, βc) involve splicing in an additional exon between the exon 1 and 2 at the 5' end. These three transcripts are expected to be nonfunctional. The main BRE protein is encoded by the major transcript αa (also named as variant 3 by NCBI). This protein is 383 amino-acids long, named 'protein isoform 2 (NP-954661.1)' by NCBI. In the major transcript αa, the alternative exons X, Y, and Z are not present. The exon 1 is non-coding. Its translation starts from ATG in the exon 2 (190). In human cells, all of the predominant splice variants are found to be co-expressed at different ratios. The normal cells lines express lower level of BRE than the cancer cell lines (190).

In the mouse, alternative splicing only occurs to the 5' end, which results in putative protein isoforms with different N-terminus. Some of these transcripts are predicted to be functional. The major transcript is named as variant 5 by NCBI. The protein encoded by this major transcript is a ubiquitous 383 amino-acids protein. It shares 99% similarity with human BRE. The other minor transcript variants are not co-expressed with the main one in all tissues, and are expressed differentially in different tissues. The mouse BRE alternative transcripts are generally in low abundance except in the heart (189, 191). No pseudogene of BRE has been found.

1.6.1.2 Transcription

The transcription start site is located differently over the region between 35 to 112 bases upstream of the last base of exon 1. The most frequent transcription start site is located at 40 bases upstream of the last base of exon 1. Initially, the mRNA of BRE was found to be highly

expressed in brain and reproductive organs. This is why it was named 'BRE'. Now it has been determined that the mRNA of BRE is expressed ubiquitously. The highest mRNA of BRE is expressed in adrenal and heart (189, 192).

1.6.1.3 Mutations

Based on the data of 4 populations (Europe, China, Japan, and Yoruba), the number of SNP in BRE gene is 453. This number is consistent with the size of BRE gene (448284 bases), as the observed frequency of SNP is 1 per 1000 bp of contig sequences (193). However, none of the SNPs is located in the coding exons of BRE. One SNP is located in the 5' UTR while the rest are in the introns. Two recombination hotspots have been located in the introns of BRE. One is from position 28271535 to 28276573, while the other is from position 28338948 to 28341210.

BRE gene contains a large CNP (copy number polymorphism) with losses and gains at different segments, and some small CNP regions (three-copy losses and two-copy gains). The large CNP region, containing 163295 bases, is at the 5' end. The most downstream small CNP region in the 3' end is located near exon Z. (The data is obtained from International Hap Map Consortium, 2003 (189). Two mutations of BRE in cell lines have been found in lung carcinoma and clear cell renal cell carcinoma, respectively.

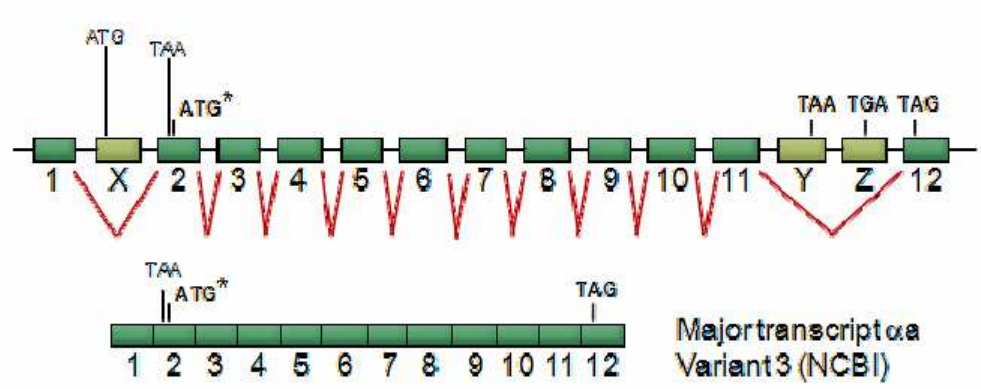

Figure 1-8. **Human BRE gene and the major transcript variant** (reproduced from reference (189))

1.6.2 Protein

The major isoform of BRE (isoform 2) contains 383 amino acids with a molecular weight of 44 kDa. It is a highly conserved protein. No homolog has been found within the same species. The crystal structure of BRE is not available. The 333 residues at the N-terminus are considered as a unique domain pfam06113. Besides, it has two UEV domains. One is located from residues 30 to 147 at the N-terminus and the other from residues 275 to 363 at the C-terminus (194). UEV domain is an Ub interaction motif, which strongly resembles the

catalytic domain of E2. Although it has the ability to bind ubiquitin, it lacks catalytic activity because of the lack of a cysteine necessary for the formation of a thioester-ubiquitin intermediate (195). UEV domains of BRE are important for interactions with other members of the BRE-containing complex (196, 197), and for binding to polyubiquitin chain (194).

All of examined mammalian cell lines express high level of BRE. These included HeLa, HepG2, HL60, Jurkat, KRC/Y, MCF7, NIH3T3, NS0, THP-1, and lymphoblastoid CB14022 cells, etc. (189). Among different mouse tissues, the expression level of BRE is different. The order is: lungs = spleen = thymus > adrenal > testis = kidney > brain > heart = liver (198).

1.6.3 BRE in two complexes

BRE is expressed in cytosolic and nuclear compartments (199). In nucleus, BRE is one part of the BRCA1-A complex. This complex has the following functions:

(1) It is an E3 ubiquitin ligase. For example, the C-terminus of p53 can be ubiquitinated by BRCA1-A complex (200).

(2) It is also a deubiquitination enzyme. For example, it can specifically remove K63-linked polyubiquitin chains from K63-linked ubiquitinated H2A and H2AX.

Through the functions as E3 and DUB, BRCA1-A complex is important in DNA repair and cell cycle regulation (194, 200).

The components of BRCA1-A complex are BRCA1, BARD1, Abraxas/Abra1/CCDC98, RAP80, BRCC36, BRE, and MERIT40/NBA1 (194, 200-203). See Figure 1-9. The interactions of these components are as follows:

(1) RAP80 contains a tandem ubiquitin-interacting motif domain (UIM) at its N-terminus, which is required for its binding with ubiquitin (204).

(2) RAP80 interacts with the BRCT domain of BRCA1 (201).

(3) MERIT40 interacts with BRE directly and robustly via the C-terminal UEV domain of BRE and C-terminal PxxR of MERIT40 (197).

(4) BRCC36 interacts with the N-terminal UEV domain of BRE (196).

(5) Abraxas and BRCC36 interact with each other through the coiled-coil domains on both proteins, positioning a MPN+MPN-domain pair in the complex (194, 205).

(6) RAP80 associates with a large region of Abraxas. This region contains N-terminal three-fourths of Abraxas, including ABR domain and coiled-coil domain (205, 206).

(7) BRCT domain of BRCA1 binds directly to C-terminal SPxF motif of Abraxas in a phosphorylation-dependent manner (205-207).

(8) BRE interacts with Abraxas directly via the N-terminus (residues 1-200) of BRE and the N-terminal ABR region of Abraxas (197).

The functions of each component are as follows:

(1) Rap80 contains UIM domain, Abraxas-interacting region (AIR) and Zn finger (194). It acts upstream of BRCA1. It recruits BRCA1 to MDC1-γH2AX-dependent K63-linked ubiquitin polymers at DSBs (201, 204). Furthermore, it is necessary for recruiting BRCC36 to its K63-linked polyubiquitinated substrates, such as histones H2A and H2AX at DSBs (201, 205, 208, 209).
(2) MERIT40 contains a VWA domain at the N-terminus (194). It is important for maintaining BRE and Abraxas abundance (194). It regulates BRCA1-A retention at DNA breaks primarily via a role in maintaining the stability of BRE (202, 203).
(3) Abraxas possesses MPN-domain at its N-terminus, coiled-coil domain and SPxF domain at its C-terminus (194). It is essential for the integrity of BRCA1-A complex (194). The interaction between Abraxas and BRE and interaction between Abraxas and BRCC36 can influence the whole complex formation (202). Abraxas mediates the interactions of both Rap80 and BRCC36 with BRCA1 (205).
(4) BRCC36 is a deubiquitinating enzyme (202). It specifically catalyzes K63-linked polyubiquitin chains (188). It contains MPN+ and coiled-coil domains (194). It is mainly associated with deubiquitination of H2A/H2AX K63-linked polyubiquitination during DNA repair (201, 210, 211). Through DUB function towards its histone substrates, it may work to release the BRCA1-A machinery from these foci once the necessary repairs have been made (188). Besides, BRCC36 also exerts K63 specific DUB function toward some other unspecified yet non-histone substrates (188, 201, 211).
(5) BRE is essential in maintaining the integrity and the DNA-repair function of this complex (197, 200, 202).
Taken together, each member of BRCA1-A complex is responsible for the integral functions of BRCA1-A complex (194).

In cytoplasm, BRE is one part of the BRISC (BRCC36 isopeptidase) complex. The components of this complex are ABRO1/KIAA0157, BRCC36, MERIT40/NBA1, and BRE. See Figure 1-9. BRE is critical for maintaining the integrity and function of the BRISC (197). This complex specifically cleaves K63-linked polyubiquitin chains (188). The K63-Ub substrate of BRISC is unknown. Which protein in the BRISC can target the complex to its substrate is also unknown. (196). Unlike RAP80, ABRO1 does not contain the BRCA1-interacting motif. Thus, the BRISC complex does not interact with BRCA1 (197). This complex lacks E3 ubiquitin ligase activity. It is not known whether BRISC is related with the anti-apoptotic function of BRE.

BRISC and BRCA1-A complexes are differentially regulated by protein-protein interactions in cytoplasm and nucleus, respectively. The abundance of one complex is counterbalanced in part by the abundance of the other complex (196). BRE is found critical for maintaining the integrity and function of these two complexes.

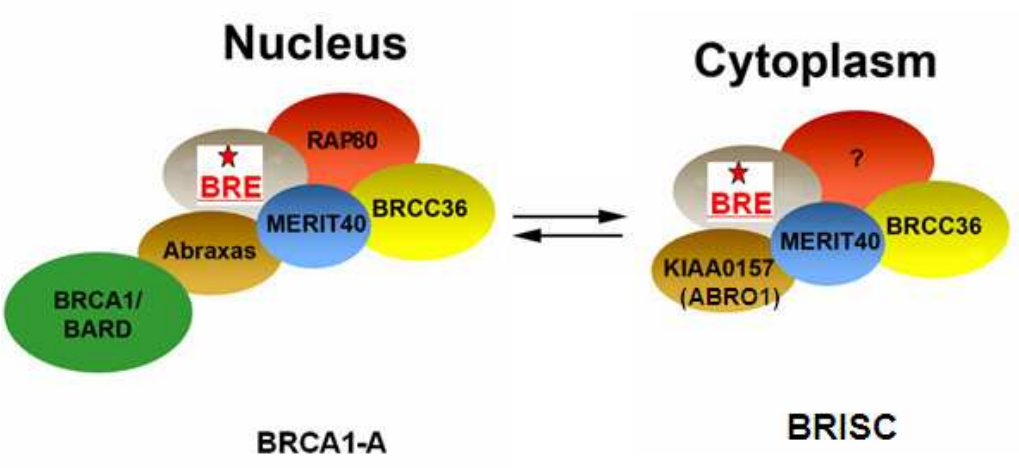

Figure 1-9. **BRE is expressed in cytosolic and nuclear compartments.** (reproduced from reference (196))

1.6.4 The anti-apoptotic function of BRE

1.6.4.1 In cell lines

BRE is an anti-apoptotic protein in the extrinsic apoptotic pathway. BRE can bind to the intracellular domains of TNF-R1 and Fas. Besides, it can also conjugate with DISC complex during apoptosis (199, 212). The decreased apoptotic response to TNF-α and anti-Fas agonist antibody has been identified in Jurkat and HeLa cell lines when BRE is overexpressed. The increased apoptotic response to TNF-α has been identified in HeLa cell line when BRE is knocked down by siRNA (199).

BRE is also an anti-apoptotic protein in the intrinsic apoptotic pathway when cells are stimulated by stress-related and genotoxic stimuli. The decreased apoptotic response to cycloheximide (inhibitor of protein biosynthesis in eukaryotic organisms), 4-nitroquinoline-1-oxide (DNA-damaging agent), etoposide (Topoisomerase II inhibitor), and staurosporine (broad-spectrum protein kinase inhibitor) has been observed when BRE is overexpressed (199).

In contrast to tBID, which transfers the apoptotic signal from the extrinsic pathway to the mitochondrial pathway, BRE inhibits the crosstalk between the two pathways by inhibiting the release of pro-apoptotic mitochondrial proteins. BRE is not translocated to mitochondria or nucleus during apoptosis, and it does not affect the level of tBID (199). The anti-apoptotic function of BRE has been examined in CD95 type II cell line, such as HeLa, Jurkat, and hepatocyte. This type of cell line has a feature that it needs mitochondrial apoptotic pathway to amplify the apoptotic signal emanated from the death receptor (213, 214).

1.6.4.2 In vivo

1.6.4.2.1 Human sample

In a collection of 123 human hepatocellular carcinoma (HCC) samples, the tumoral regions of 74% of these samples showed BRE overexpression. In contrast, little BRE was detected in the non-liver regions, cirrhotic regions or otherwise (198). Furthermore, the BRE overexpression levels correlated with poor differentiation of HCC and therefore poor prognosis (198).

1.6.4.2.2 Mouse model

The mouse Lewis lung carcinoma D122 stable transfectants of human BRE developed into local tumor faster than the stable transfectants of empty vector and parental D122. This was found in both syngeneic C57BL/6 host and nude mice in footpad injection model. However, in culture condition, the ectopic expression of human BRE in D122 does not affect cell proliferation (215). The anti-apoptotic function of BRE in vivo has been demonstrated by attenuation of Fas agonist antibody-induced acute fulminant hepatitis in transgenic mice expressing human BRE in the liver (198). Recent work on the transgenic mouse model shows significantly faster growth of diethylnitrosamine-induced liver tumors, but not the initiation of tumor formation. Of note, in the DEN-induced liver tumors of the control mice, the expression of endogenous BRE was also increased. This phenomenon indicates that BRE is important in the liver cancer (216). Taken together, BRE overexpression promotes tumor survival in liver instead of initiating tumor formation. BRE overexpression is not sufficient to initiate spontaneous tumor, but it can promote the growth of tumor by its anti-apoptotic activity.

1.6.4.3 Seemingly opposing data

A recent study showed that overexpression of BRE occurs predominantly in MLL-rearranged AML (acute myeloid leukemia) with a t(9;11)(p22;q23). Moreover, high BRE expression has been identified as an independent favorable prognostic factor for reduced cancer relapse in pediatric AML (217). Another study also reported correlation of high BRE expression with FAB M5 morphology and the MLL-AF9 fusion. This study demonstrated that high BRE expression predicts favorable outcome in adult acute myeloid leukemia, in particular among MLL-AF9–positive patients (218). These data seem to be contradictory with our reports that BRE attenuates apoptosis and promotes tumor survival. However, the above observations were based on microarray-based gene expression profiling and RT–PCR, which detect only the mRNA expression levels. Western blot analysis of BRE was carried out only by the first study which showed in fact no change in BRE protein expression between t(9;11)(p22;q23) (n=6) and other MLL-rearranged AML cases (n=5), despite the significant difference in mRNA expression levels found between the 2 groups. Owing to the contradictory findings between BRE mRNA and protein expression shown in the above study, further work is required to achieve a better understanding of the data reported in the 2 papers.

1.6.5 BRE and ubiquitin

1.6.5.1.1 E3 and DUB functions of BRCA1-A complex

BRCA1-A complex works as an E3 ubiquitin ligase (200). Rap80 recruits BRCA1-A to its K63-linked ubiquitin polymers tagged substrates at DSBs (204). BRE is necessary for the E3 activity of BRCA1-A complex (200). BRCA1-A complex also possesses deubiquitinase activity that specifically removes K63-linked ubiquitin chains, rather than K6-, K11-, K29-, K48-, or linear-linked ubiquitin chains, on its substrates. BRCC36 in this complex processes this specificity (200-202). The substrates of BRCC36 include H2A/H2AX and some other unspecified yet non-histone substrates (188, 201, 211). RAP80 targets BRCC36 to its K63-linked polyubiquitinated substrates (208, 209). BRE may regulate the K63 DUB function of BRCC36 (201). This DUB function facilitates the complex to be released from the DSB sites once necessary repairs have been made (188). Taken together, BRCA1-A has both of ubiquitinating and deubiquitinating activities. The functions of DNA-repair and anti-apoptosis of BRCA1-A are regulated by amplifying and removing the ubiquitin chains (194).

1.6.5.1.2 DUB function of BRISC

BRISC also specifically cleaves K63-linked polyubiquitin chains, rather than K6-, K11-, K29-, K48- or linear-linked polyubiquitin chains, mainly due to BRCC36 (188). The K63-Ub substrate of BRISC is unknown (196). The DUB effect of BRISC towards its substrate only occurs to hydrophobic patch of the distal ubiquitin at a ubiquitin-ubiquitin cleavage site (219). Because ABRO1 lacks the BRCA1-interacting motif, the BRISC complex does not interact with BRCA1. Thus, BRISC lacks the E3 ubiquitin ligase activity (197).

1.6.5.1.3 BRE

The UEV domains of BRE enable it to bind ubiquitin (189, 194). BRE was shown to bind K48- and K63-linked polyubiquitin chains in vitro (194). Therefore, these domains of BRE may be involved in deubiquitinating activity of BRCC36 in the BRCA1-A and BRISC complexes. Furthermore, it is conceivable that the UEV domains may have a role in potentiating the E3 ligase activity of BRCA1/BARD1 in BRCA1-A complex (194, 196, 197). It is possible that the UEV domains of BRE may play a role in holding the polyubiquitin chains in an appropriate position (194). Furthermore, increased association of BRE with ubiquitinated proteins after death receptor stimulation was also detected. These results indicate that the anti-apoptotic function of BRE is closely related to ubiquitin (199).

1.7 RNA interference

1.7.1 Mechanism of RNA interference

RNA interference (RNAi) is a process within living cells that moderates the activity of their genes. Two types of small ribonucleic acid (RNA) molecules, microRNA (miRNA) and small

interfering RNA (siRNA) are central to RNA interference. RNAs are the direct products of genes, and these small RNAs can bind to other specific messenger RNA (mRNA) molecules and either increase or decrease their activity, for example by preventing an mRNA from producing a protein. See Figure 1-10.

The RNAi pathway is initiated by the enzyme Dicer, which cleaves long double-stranded RNA (dsRNA) molecules into short fragments of ~20 nucleotides. When the dsRNA is exogenous (coming from infection by a virus with an RNA genome or laboratory manipulations), the RNA is imported directly into the cytoplasm and cleaved to short fragments by the Dicer (220). The short fragments from the exogenous dsRNA are called siRNAs. The initiating dsRNA can also be endogenous (originating in the cell), as in pre-microRNAs expressed from RNA-coding genes in the genome. The primary transcripts from such genes are first processed to form the characteristic stem-loop structure of pre-miRNA in the nucleus, and then exported to the cytoplasm to be cleaved by Dicer. The cleaved fragments from endogenous dsRNA (pre-microRNA) are called mature miRNAs, which are structurally similar to siRNAs (221).

Next, siRNA or mature miRNA is unwound into two single-stranded (ss) ssRNAs, namely the passenger strand and the guide strand. Here the double-stranded siRNA can derive from cleaved dsRNA or be transfected directly into cell. After the unwounding, the passenger strand is degraded, and the guide strand is incorporated into the RNA-induced silencing complex (RISC) (222). The most well studied outcome is post-transcriptional gene silencing, which occurs when the guide strand base pairs with a complementary sequence in a messenger RNA molecule and induces cleavage by Argonaute, the catalytic component of the RISC complex. Nowadays, RNAi has become a valuable research tool, both in cell culture and in living organisms, to induce suppression of specific genes of interest (223).

1.7.2 Small hairpin RNA

A small hairpin RNA or short hairpin RNA (shRNA) is a sequence of RNA that makes a tight hairpin turn that can be used to silence target gene expression via RNA interference (RNAi). shRNA is an advantageous mediator of RNAi in that it has a relatively low rate of degradation and turnover. Expression of shRNA in cells is typically accomplished by delivery of plasmids or through viral or bacterial vectors (224). Once the plasmids or vectors have integrated into the host genome, the shRNA is then transcribed in the nucleus by polymerase II or polymerase III depending on the promoter choice. This product mimics pre-microRNA (pre-miRNA) and is processed by Drosha. The pre-shRNA is exported from the nucleus by Exportin 5. This product is then processed by dicer and loaded into the RNA-induced silencing complex (RISC). The sense (passenger) strand is degraded. The antisense (guide) strand directs RISC to mRNA that has a complementary sequence. In the case of perfect complementarily, RISC cleaves the

mRNA. In the case of imperfect complementarily, RISC represses translation of the mRNA. In both of these cases, the shRNA leads to target gene silencing (225).

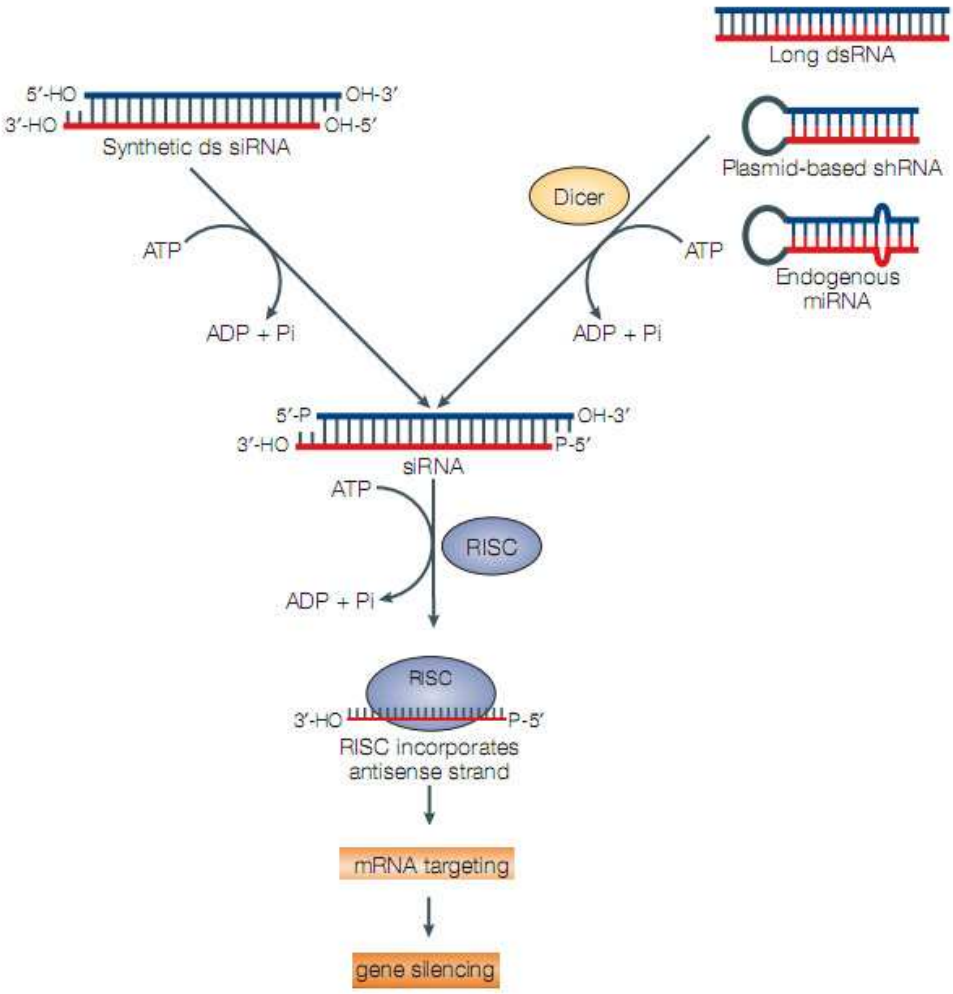

Figure 1-10. **Mechanism of RNA interference** (modified from reference (223))

CHAPTER 2: Materials and methods

2.1 Materials

2.1.1 Primers used for cloning

All of primers were produced by Invitrogen.

Table 2-1. **Primers used for cloning**

Names	Sequences
V5For	5’ GGG GAT CCG CCA CCA TGG CGA TCC CTA ACC CTC TCC TCG GTC TCG A 3’
V5Rev	5’ GGG TCG ACC TAC GTA GAA TCG AGA CCG AGG AGA GGG TTA 3’
BREFor	5’ GGG GAT CCG CCA CCA TGT CCC CAG AAG TGG CCT TGA A 3’
BRERev	5’ GGG TCG ACC TAG AGC TTT CCA TTG GCA AAT GCT 3’
BREForAd	5’ GGG GTA CCG CCA CCA TGT CCC CAG AAG TGG CCT TGA A 3’
BRERevAd	5’ GGA AGC TTC TAG AGC TTT CCA TTG GCA AAT GCT 3’
V5ForAd	5’ GGG GTA CCG CCA CCA TGG CGA TCC CTA ACC CTC TCC TCG GTC TCG A 3’
V5RevAd	5’ GGA AGC TTC TAC GTA GAA TCG AGA CCG AGG AGA GGG TTA 3’
BREForEBB	5’ GGG GAT CCA TGT CCC CAG AAG TGG CCT TGA A 3’
BRERevEBB	5’ GGG CGG CCG CTA GAG CTT TCC ATT GGC AAA TGC T 3’

2.1.2 DNA clones used in the studies

1. pBABEpuro, pBABEpuro-BRE, pBABEpuro-BREV5, pBABEpuro-V5BRE

pBABEpuro is a mammalian expression, retroviral expression vector from Addgene (#1764) (Figure 2-1). It has a puromycin selectable marker. Three targets (BRE, BRE tagged by V5 at the C-terminus, BRE tagged by V5 at the N-terminus) were cloned into pBABEpuro separately, via the cloning sites of Sal I and BamH I, generating three pBABEpuro-based retroviral expression vectors, which were named as pBABEpuro-BRE, pBABEpuro-BREV5, and pBABEpuro-V5BRE. These retroviral expression vectors were used with the retroviral package vector, pCL-Ampho to generate retrovirus.

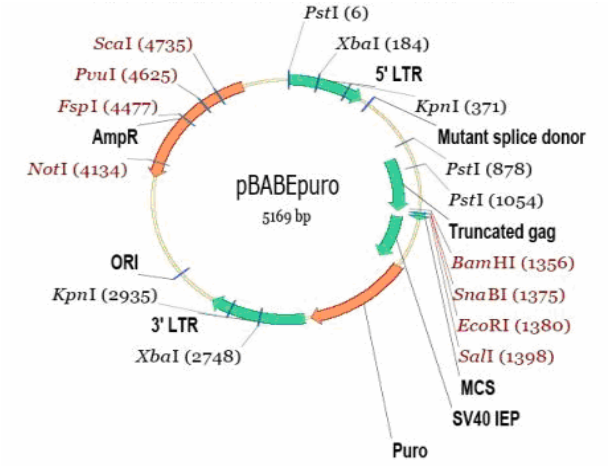

Figure 2-1. **Map of pBABEpuro** (reproduced from reference (48))

2. pBABEneo, pBABEneo-BREV5

pBABEneo is a mammalian expression, retroviral expression vector from Addgene (#1767) (Figure 2-2). It has a neomycin selectable marker. One target (BRE tagged by V5 at the C-terminus) was cloned into pBABEneo, via the cloning sites of Sal I and BamH I, generating a pBABEneo-based retroviral expression vector, which was named as pBABEneo-BREV5. pBABEneo-BREV5 was used with the retroviral package vector, pCL-Ampho to generate retrovirus.

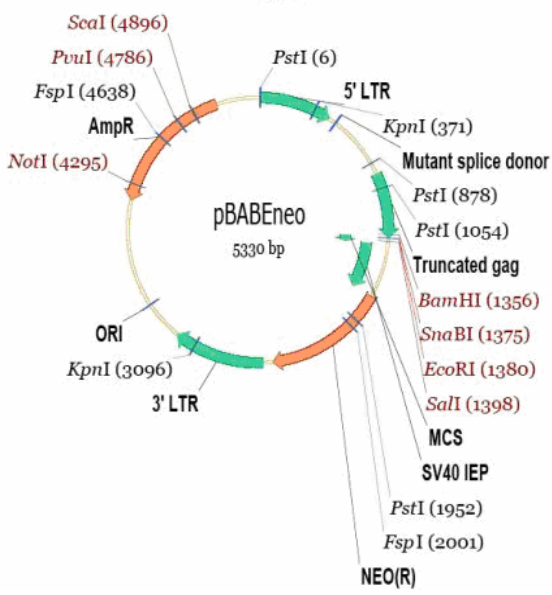

Figure 2-2. **Map of pBABEneo** (reproduced from reference (48))

3. pBABEhygro, pBABEhygro-BRE

pBABEhygro is a mammalian expression, retroviral expression vector from Addgene (#1765)

(Figure 2-3). It has a hygromycin selectable marker. One target (BRE) was cloned pBABEhygro via the cloning sites of Sal I and BamH I, generating a pBABEhygro-based retroviral expression vector, which was named as pBABEhygro-BRE. pBABEhygro-BRE was used with the retroviral package vector, pCL-Ampho to generate retrovirus.

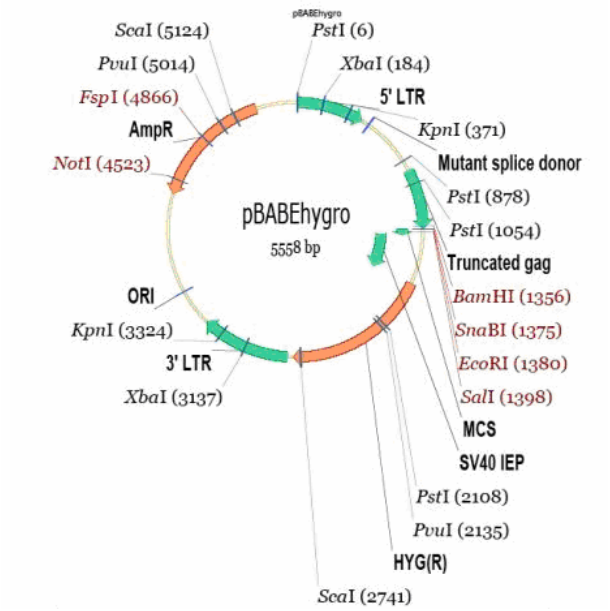

Figure 2-3. **Map of pBABEhygro** (reproduced from reference (48))

4. pCL-Ampho

pCL-Ampho is a retroviral package vector, commercially available from Imgenex (#10046P). It is safety-modified and can express a high-level expression of gap, pol, and env proteins. It is suitable for most mammalian cells (but not hamster). It was used for retrovirus generation together with retroviral expression vectors, such as pBABEpuro, pBABEpuro-BRE, pBABEpuro-BREV5, pBABEpuro-V5BRE, pBABEneo-BREV5, and pBABEhygro-BRE.

Figure 2-4. **Structure of pCL-Ampho** (reproduced from reference (226))

5. pAdTrack-CMV, pAdTrack-CMV-BRE, pAdTrack-CMV-BREV5, pAdTrack-CMV-V5BRE

pAdTrack-CMV is a mammalian expression, adenoviral shuttle vector in the AdEasy system, which is for adenovirus generation, commercially available from Addgene (#16405) (Figure 2-5). It has a kanamycin selectable marker and a GFP monitor. Three targets (BRE, BRE tagged by V5 at the C-terminus, BRE tagged by V5 at the N-terminus) were cloned into

pAdTrack-CMV separately, via the cloning sites of Kpn I and Hind III, generating three pAdTrack-CMV-based adenoviral shuttle vectors, which were named as pAdTrack-CMV-BRE, pAdTrack-CMV-BREV5, and pAdTrack-CMV-V5BRE. Recombinant of pAdTrack-CMV-BREV5 and pAdEasy®-1 was used for adenovirus generation.

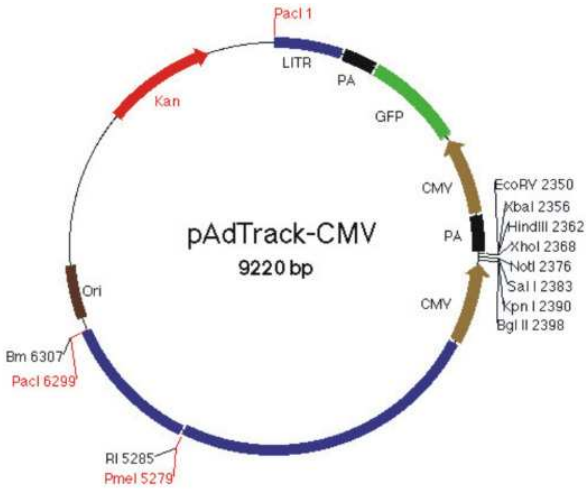

Figure 2-5. **Map of pAdTrack-CMV** (reproduced from reference (48))

6. pAdEasy®-1

It is a mammalian expression, adenoviral backbone vector in the AdEasy system, which is for adenovirus generation, commercially available from Addgene (#16400) (Figure 2-6). It has an ampicillin selectable marker. Recombination occurred between the adenoviral backbone vector (pAdEasy®-1) and the adenoviral shuttle vector containing BRE tagged by V5 at the C-terminus (pAdTrack-CMV-BREV5). This recombinant was packaged into HEK293T cells to make adenovirus. Besides, the AdEasier®-1 bacterial cells are BJ5183 derivatives, which already contain this pAdEasy®-1 plasmid.

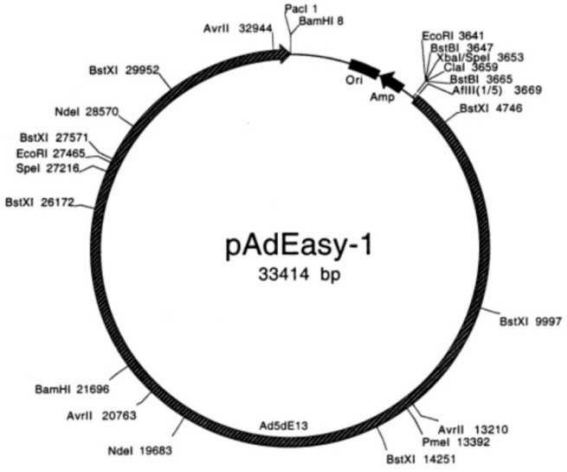

Figure 2-6. **Map of pAdEasy®-1** (reproduced from reference (48))

7. pcDNA3 and V55K

pcDNA3 is a mammalian expression vector, commercially available from Invitrogen (Figure 2-7). It contains a neomycin selectable marker. It was used as a vehicle control in gene transfection. In V55K, BRE tagged with V5 at the N-terminus was cloned into pcDNA3 vector. V55K was used as PCR template for the insert containing BRE tagged with V5 at the N-terminus. This V5BRE insert was cloned into pBABEpuro to generate a pBABEpuro-based retroviral expression vector, which was named as pBABEpuro-V5BRE. Similarly, this V5BRE insert was cloned into pAdTrack-CMV to generate a pAdTrack-CMV-based adenoviral shuttle vector, which was named as pAdTrack-CMV-V5BRE.

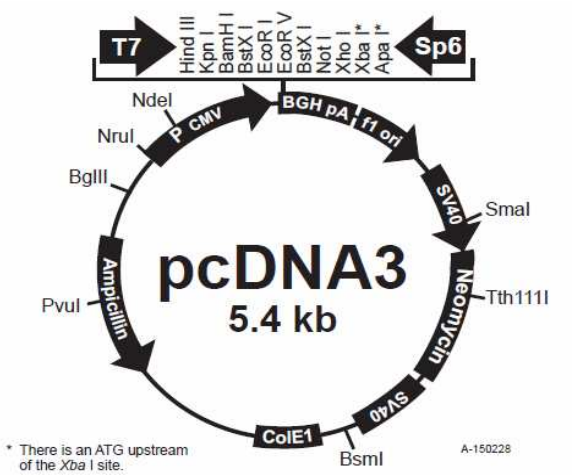

Figure 2-7. **Map of pcDNA3** (reproduced from reference (40))

8. pEBB-FLAG-XIAP and pEBB-FLAG-BRE

pEBB-FLAG-XIAP is a pEBB-based mammalian expression vector containing full length of XIAP tagged by FLAG, commercially available from Addgene (#11558) (Figure 2-8). The backbone size of pEBB is 5353 bp, while the size of the insert (XIAP tagged by FLAG) is 1500 bp. It contains a neomycin selectable marker. It was used for high level of XIAP expression. Besides, XIAP in pEBB-FLAG-XIAP was replaced by BRE to generate a pEBB-based plasmid, which can express high level of BRE. This pEBB-based plasmid, containing BRE tagged by FLAG, was named as pEBB-FLAG-BRE.

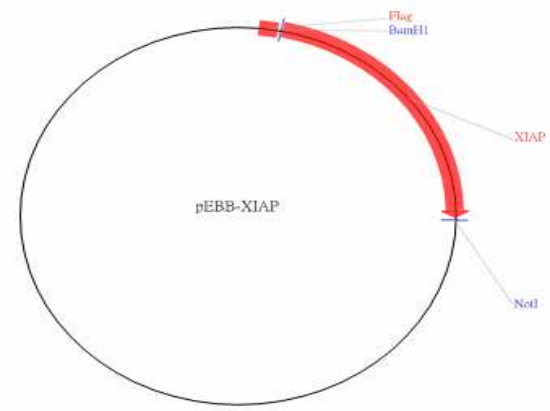

Figure 2-8. **Map of pEBB-FLAG-XIAP** (reproduced from reference (48))

9. pcDNA3.1/GS and GS-BRE

pcDNA3.1/GS is a Gene Storm® empty vector, commercially available from Invitrogen (#H-K1000) (Figure 2-9). GS-BRE, ResGen Gene Storm® Clone for accession number L38616, was purchased from Invitrogen. In GS-BRE, BRE tagged with V5 and 6x His at the C-terminus was cloned into the pcDNA3.1/GS empty vector. GS-BRE was used as PCR template for the inserts containing BRE alone and BRE tagged with V5 at the C-terminus. These inserts were cloned into pBABEpuro, pBABEneo, and pBABEhygro separately, to generate pBABEpuro-BRE, pBABEpuro-BREV5, pBABEneo-BREV5, and pBABEhygro-BRE for retrovirus generation. Similarly, these inserts were cloned into pAdTrack-CMV separately to generate pAdTrack-CMV-based adenoviral shuttle vectors, which were named as pAdTrack-CMV-BRE and pAdTrack-CMV-BREV5. GS-BRE was also used as PCR template for the insert containing BRE alone to generate the pEBB-based plasmid, pEBB-FLAG-BRE, which can express high level of BRE. Besides, pcDNA3.1/GS and GS-BRE were used to generate stable transfectants of Jurkat A3 cell, which were named as GSV1 and GSB2.

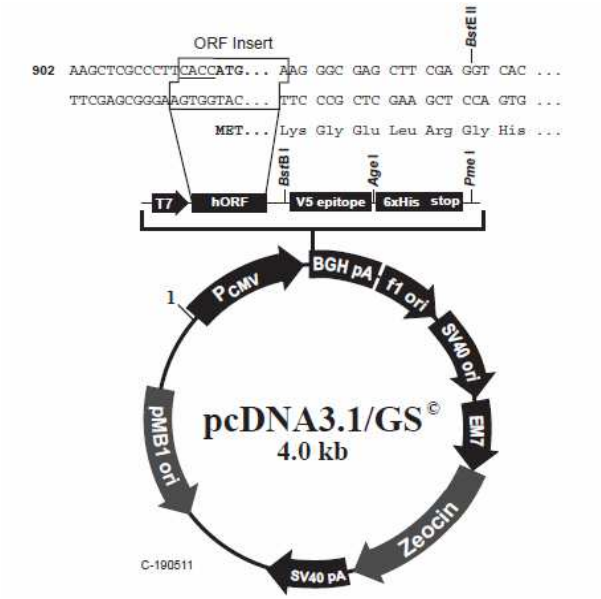

Figure 2-9. **Map of pcDNA3.1/GS** (reproduced from reference (41))

10. pRK5-HA-Ubiquitin-K48

pRK5-HA-Ubiquitin-K48 is a pRK5-HA-based mammalian expression vector containing K48 only ubiquitin with all of the other lysines mutated to arginines, commercially available from Addgene (#17605). The backbone size of pRK5-HA is 4800 bp, while the size of the insert (K48 ubiquitin) is 220 bp. It was used for high level HA tagged K48-linked ubiquitin expression.

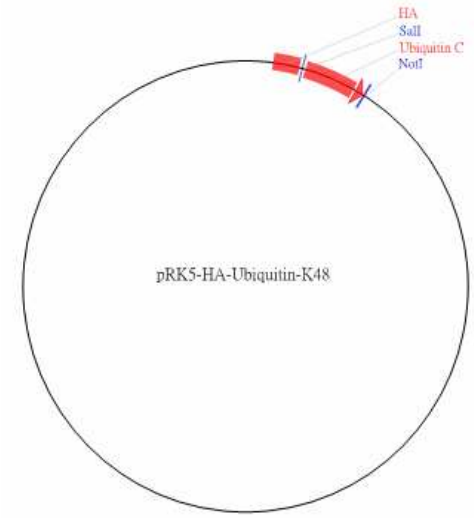

Figure 2-10. **Map of pRK5-HA-Ubiquitin-K48** (reproduced from reference (48))

11. pRK5-HA-Ubiquitin-K63

pRK5-HA-Ubiquitin-K63 is a pRK5-HA-based mammalian expression vector containing K63 only ubiquitin with all of the other lysines mutated to arginines, commercially available from Addgene (#17606). The backbone size of pRK5-HA is 4800 bp, while the

size of the insert (K63 ubiquitin) is 220 bp. It was used for high level HA tagged K63-linked ubiquitin expression.

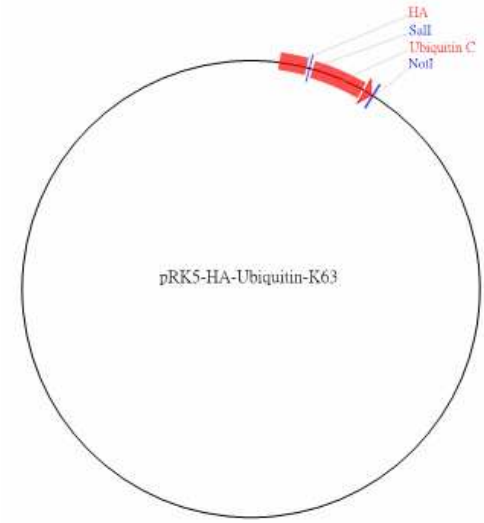

Figure 2-11. **Map of pRK5-HA-Ubiquitin-K63** (reproduced from reference (48))

12. pRK5-HA-Ubiquitin-K0

pRK5-HA-Ubiquitin-K0 is a pRK5-HA-based mammalian expression vector containing K0 ubiquitin with all of the lysines mutated to arginines, commercially available from Addgene (#17603). The backbone size of pRK5-HA is 4800 bp, while the size of the insert (K0 ubiquitin) is 220 bp. It was used for high level HA tagged K0-linked (linear) ubiquitin expression.

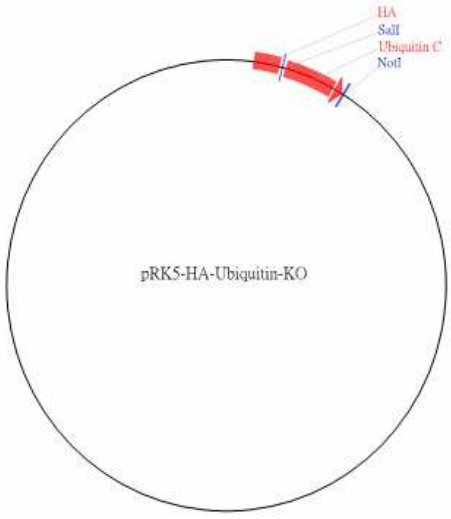

Figure 2-12. **Map of pRK5-HA-Ubiquitin-K0** (reproduced from reference (48))

13. BRE shRNA and empty shRNA vector

Empty shRNA vector is negative control shRNA pGFP-V-RS non-effective tGFP plasmid,

commercially available from Origene (#TR30008) (Figure 2-13). It contains kanamycin and puromycin resistance markers for easy selection. BRE shRNA is shRNA construct against Mus musculus BRE in pGFP-V-RS vector, from Origene (#GI536607). The sequence against BRE is CAT CTT TGG AGA GGA TGC TGA GTT TCT GC. BRE shRNA and empty shRNA were cloned into the pGFP-V-RS vector under U6 polymerase III promoter for shRNA expression, respectively. BRE shRNA was used to generate stable BRE-depleted cell lines of D122, which were named as B07. Empty shRNA vector was used to generate negative control cell lines of D122, which were named as T8.

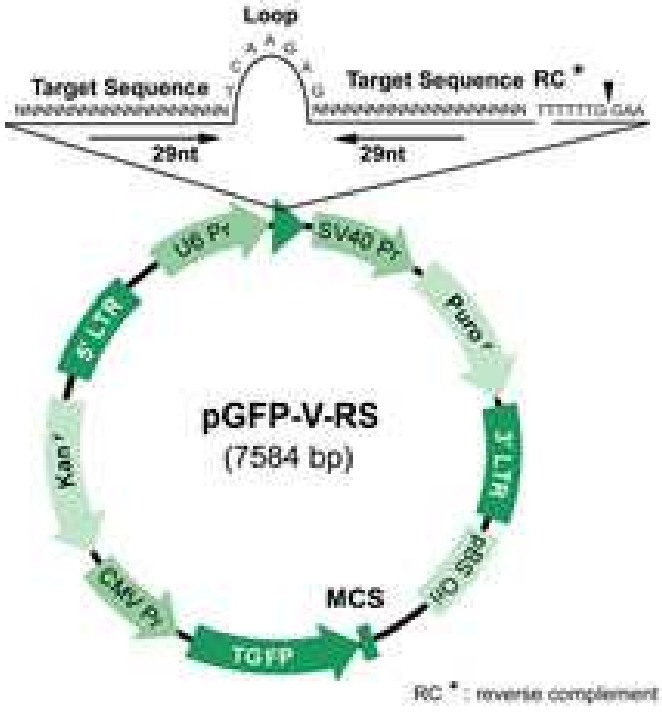

Figure 2-13. **Map of pGFP-V-RS** (reproduced from reference (44))

2.1.3 Materials for DNA manipulation

Table 2-2. **Materials for DNA manipulation**

Chemicals and enzymes	Manufactures
Platiunm® pfx DNA polymerase	Invitrogen (Carlsbad, CA)
dNTP	
10× pfx amplification buffer	
$MgSO_4$ (50 mM)	
T4 DNA ligase	
5× T4 DNA ligase buffer	
DNA MW marker (1 kb plus)	

Quick-Load® DNA ladder (1 kb, 100 bp)	New England Biolabs (Beverly, MA)
Restriction enzyme and buffer	
CHROMA SPIN™-1000 column	Clontech Laboratories (Palo Alto, CA)
Glycerol	Sigma (St. Louis, MO)
SeaKem® LE agarose	Cambrex Bio Science Rockland (Rockland, ME)

2.1.4 Materials for protein manipulation

Table 2-3. **Materials for protein manipulation**

Materials	Manufactures
rec-Protein G-Sepharose® 4B conjugate	Invitrogen (Camarillo, CA)
10× cell lysis buffer (#9803)	Cell Signaling (Danvers, MA)
Complete mini EDTA-free protease inhibitor cocktail tablet	Roche (Mannheim, Germany)
Phosphatase inhibitor cocktail tablet	
Phenylmethanesulfonyl fluoride (PMSF)	Sigma (St. Louis, MO)
Trizma® base	
Sodium chloride	
Ethylene diamine tetraacetic acid (EDTA)	
Triton X-100	
Glycine	
Sodium dodecyl sulfate (SDS)	
PBS	
TWEEN® 20	
Ammonium persulfate (APS)	
30% Acrylamide/Bis solution	Bio-Rad Laboratories (Hercules, CA)
Immun-Blot™ PVDF membrane (0.2 μm)	
Methanol	Merk (Darmstadt, Germany)
Isopropanol	
Lumingen™ PS-3 detection reagent	GE healthcare (little Chalfont, Buckinghamshire, UK)
Lumingen™ TMA-6 detection reagent	
Amersham hyperfilm™ ECL high performance chemiluminescence film	
ECL advance blocking milk	
PageRuler™ prestained protein molecular weight ladder	Fermentas (Ontario, Canada)
Calcium plus skimmed milk	Nestle (Vevey, Switzerland)

2.1.5 Materials for virus manipulation

Table 2-4. **Materials for virus manipulation**

Materials	Manufactures
Sodium chloride	Sigma (St. Louis, MO)
Polyethylene glycol 8'000 (PEG)	
Polybrene	
Ammonium acetate	
Isoamyl alcohol	
100% ethanol	Merk (Darmstadt, Germany)

Nucleic acid purification grade, phenol/water/chloroform	Applied Biosystems (Foster City, CA)
Pellet paint co-precipitant	EMD Chemicals (San Diego, CA)
E.coli pulser cuvette (0.1 cm electrode gap)	BIO-RAD Laboratories (Hercules, CA)
Ultra-pure glycerol	Invitrogen (Camarillo, CA)

2.1.6 Antibodies

Table 2-5. **Antibodies**

Antibodies	Manufactures	Catalog #
Anti-GAPDH	US-Biological (Swampscott, MA)	G8140-11A
Anti-β-actin	Sigma (St. Louis, MO)	AC-74
HRP-anti-HA		H6533
HRP-anti-FLAG		A8592
Anti-FLAG		F3165
Anti-biotinylated XIAP	R&D (Minneapolis, MN)	BAF8221
Anti-cFLIP	Cell Signaling (Danvers, MA)	3210
Mouse (G3A1) IgG1 Isotype Control		5415S
Anti-PARP		9542S
Anti-cleaved caspase 3		9661S
Anti-cIAP-1	IMGENEX (San Diego, CA)	IMG-5716
Anti-cIAP-2	R&D (Minneapolis, MN)	MAB817
HRP-anti-V5	Invitrogen (Camarillo, CA)	46-0708
Anti-XIAP	BD Transduction Laboratories (San Diego, CA)	610717
Anti-ubiquitin	BD Phamingen (San Diego, CA)	550944
Anti-Mouse Ig-HRP		554002
Streptavidin-HRP		554060
Anti-BRE	Clinical Immunology Laboratory, CUHK	Mab489-7
Anti-BRE		Mab246
Anti-Rabbit Ig-HRP	Promega (Madison, MI)	W401B

2.1.7 Chemicals

Table 2-6. **Chemicals**

Chemicals	Manufactures
TNF-α	Invitrogen (Camarillo, CA)
Etoposide	Sigma (St. Louis, MO)
N-Ethylmaleimide (NEM)	
MG132	
Caspase family inhibitor, Z-VAD-FMK (VAD)	BIovision (Mountain View, CA)
Cycloheximide (CHX)	Merk (Darmstadt, Germany)

2.1.8 Kits

Table 2-7. **Kits**

Kits	Manufactures
BCA protein assay kit	Pierce (Rockford, IL)
Plasmid miniprep kit	Qiagen Inc. (QIAGEN GmbH, Hilden)
Plasmid midiprep kit	
QIAquick gel extraction kit	
Annexin V-PE apoptosis detection kit	BD Phamingen (San Diego, CA)
Platiunm® pfx DNA polymerase kit	Invitrogen (Carsbad, CA)
T4 DNA ligase kit	
Lumingen ^{TM} PS-3 detection kit	GE healthcare (little Chalfont, Buckinghamshire, UK)
Lumingen ^{TM} TMA-6 detection kit	

2.1.9 Culture media and reagents

Table 2-8. **Culture media and reagents**

Products	Manufactures
DMEM	GIBCO BRL Life Technologies (Gaithersburg, MD)
RPMI	
Fetal bovine serum	
Trypsin-EDTA	
Penicillin/streptomycin	
Opti-MEM® I	
Puromycin dihydrochloride	Sigma (St. Louis, MO)
Hygromycin	
Kanamycin monosulfate	
G418	
Zeocin	Invitrogen (Carlsbad, CA)
Lipofectamine 2000	
Ampicillin sodium	Medochemie Ltd. (Limassol, Cyprus)

2.1.10 Bacterial strains used for transformation and cloning

TOP 10 E. coli

DH5α

AdEasier®-1: they are BJ5183 derivatives, which already contain the AdEasy®-1 plasmid.

2.1.11 Instrumentation

Table 2-9. **Instrumentation**

Instruments	Manufactures
Thermal Cyclers PTC-200	MJ research, Inc. (South San Francisco, CA)
Thermal Cyclers C1000	BIO-RAD Laboratories (Hercules, CA)
FAScan Calibur	Becton Dickinson (Franklin Lakes, NJ)
Platform Vari Mix Shaker	Barnstead/Thermolyne (Dubuque, IA)
Type 37600 mixer	

MIRAK ™ digital 4 place Multi Mixer	
Model 200/2.0 power supply	BIO-RAD Laboratories (Hercules, CA)
Mini-PROTEAN® Tetra cell	
Trans-Blot® SD Semi-dry transfer cell	
Power supply for Gel Electrophoresis Chamber	Pharmacia (little Chalfont, Buckinghamshire, UK)
FOTODYNE Gel Electrophoresis Chamber	Carolina Biological Supply Company (Burlington, NC)
FOTODYNE FotoDyne Phoresis I	
FOTODYNE 5-5334	
FOTODYNE exposer	
Video Copy Processor P67E	Mitsubishi (Tokyo, Japan)
Capacitance Extender	BIO-RAD Laboratories (Hercules, CA)
Pulse Controller	
Gene pulser	
Inverted microscope	Olympus (Tokyo, Japan)
Fluorescence microscope DMIRB	Leica Microsystems (Wetzlar, Germany)
Centrifuge 5415D	Eppendorf (Hamburg, Germany)
Centrifuge 5424	
Centrifuge J6-MI	Beckman Coulter (Fullerton, CA)
Centrifuge Avanit J-25I	
Centrifuge Multifuge X3R	Thermo Fisher Scientific (Billerica, MA)
DU® 800 spectrophotometer	Beckman Coulter (Fullerton, CA)
DTX 800 Multimode Detector	
NanoDrop® ND-1000 Spectrophotometer	Thermo Fisher Scientific (Billerica, MA)
Balance TE3102S	Sartorius (Bradford, MA)
Electronic balance ER-180A	A&D (San Jose, CA)
GEMINI twin shaking water bath	Robbins Scientific (Billerica, MA)
Water bath	Clifton company (Clifton, NJ)
Haake Heating Circulator	Haake (Overland Park, KS)
BINDER constant temperature incubator	BINDER Inc. (Bohemia, NY)
Water Jacked CO_2 Incubator	Forma Scientific (Billerica, MA)
Orion 2 star PH Bench top detector	Thermo Fisher Scientific (Billerica, MA)
OPTIMAX X-Ray film Processor	Optimax Company (Oberstenfeld, Germany)

2.2 Methods

2.2.1 Construction of plasmids

2.2.1.1 Polymerase chain reaction (PCR)

Table 2-10. **Reaction mixer for PCR**

Names	Volumes
10× pfx amplification buffer	5 µl
$MgSO_4$ (50 mM)	1 µl
dNTP (2.5 mM)	6 µl
Primer 1 (10 pmol/µl)	1 µl
Primer 2 (10 pmol/µl)	1 µl
H_2O	34.6 µl
Template (50 ng/µl)	1 µl
Platiunm® pfx DNA polymerase	0.4 µl
Total volume	50 µl

Table 2-11. **Cycling parameters for PCR**

Segments	Number of cycles	Temperature (℃)	Duration
1	1	94	3 min
2	35	94	15 sec
		Annealing temperature	30 sec
		68	2 min
3	1	68	5 min
4	1	12	Forever

Nine constructs were prepared for later usage. The differences of their inserts in PCR manipulation were as follows.

Table 2-12. **Differences of inserts of nine constructs in PCR manipulation**

Names of constructs	Template	Primer 1	Primer 2	Annealing temperature
pBABEpuro-BRE	GS-BRE	BREFor	BRERev	63℃
pBABEpuro-BREV5	GS-BRE	BREFor	V5Rev	65℃
pBABEpuro-V5BRE	V55K	V5For	BRERev	63℃
pBABEneo-BREV5	GS-BRE	BREFor	V5Rev	65℃
pBABEhygro-BRE	GS-BRE	BREFor	BRERev	63℃
pAdTrack-CMV-BRE	GS-BRE	BREForAd	BRERevAd	63℃
pAdTrack-CMV-BREV5	GS-BRE	BREForAd	V5RevAd	65℃
pAdTrack-CMV-V5BRE	V55K	V5ForAd	BRERevAd	63℃
pEBB-FLAG-BRE	GS-BRE	BREForEBB	BRERevEBB	63℃

2.2.1.2 Enzyme digestion and purification

PCR products were purified by agarose gel electrophoresis, using the QIAquick gel extraction kit according to the manufacture's instruction. The purified PCR products and corresponding vectors were digested by enzymes according to the cloning sites. The digestion condition was set according to the manufacture's instruction. After digestion, the digested insert was purified, using the QIAquick gel extraction kit according to the manufacture's instruction. The digested vector was purified by CHROMA SPIN ^{TM}-1000 column according to the manufacture's instruction or by agarose gel electrophoresis, using the QIAquick gel extraction kit. The differences of the nine constructs in enzyme digestion manipulation were as follows.

Table 2-13. **Differences of nine constructs in enzyme digestion manipulation**

Names of constructs	Digestion enzymes	Vectors	Digested vectors purification
pBABEpuro-BRE	Sal I and BamH I	pBABEpuro	CHROMA SPIN ^{TM}-1000 column
pBABEpuro-BREV5	Sal I and BamH I	pBABEpuro	CHROMA SPIN ^{TM}-1000 column
pBABEpuro-V5BRE	Sal I and BamH I	pBABEpuro	CHROMA SPIN ^{TM}-1000 column

pBABEneo-BREV5	Sal I and BamH I	pBABEneo	CHROMA SPIN™-1000 column
pBABEhygro-BRE	Sal I and BamH I	pBABEhygro	CHROMA SPIN™-1000 column
pAdTrack-CMV-BRE	Kpn I and Hind III	pAdTrack-CMV	CHROMA SPIN™-1000 column
pAdTrack-CMV-BREV5	Kpn I and Hind III	pAdTrack-CMV	CHROMA SPIN™-1000 column
pAdTrack-CMV-V5BRE	Kpn I and Hind III	pAdTrack-CMV	CHROMA SPIN™-1000 column
pEBB-FLAG-BRE	Not I and BamH I	pEBB-FLAG-XIAP	Agarose gel electrophoresis

2.2.1.3 Ligation

Table 2-14. **Ligation condition**

Names	Conditions
5× T4 DNA ligase buffer	4 μl
Purified digested insert	100 ng
Purified digested vector	100 ng
T4 DNA ligase (5 U/μl)	1 μl
H_2O	To 20 μl
Total volume	20 μl
Temperature	14℃
Time	Overnight

2.2.1.4 Heat shock transformation

Five μl of ligation product was added into an eppendorf containing 50 μl of competent cells (DH5α). The eppendorf was incubated in ice for 30 min. Then it was incubated in 42℃ water bath for 30 sec and then on ice for 2 min. Two hundred and fifty μl of LB medium was add into the cells. The eppendorf was shaked at 37℃ at 250 rpm for 1 hour. LB plates containing 100 μg/ml of ampicillin or 50 mg/ml of kanamycin were pre-warmed to room temperature. All of the bacteria were spreaded on these antibiotic-containing plates. Then the plates were incubated at 37℃ for overnight.

Table 2-15. **Differences of nine constructs in heat shock transformation**

Names of constructs	Antibiotics
pBABEpuro-BRE	Ampicillin (100 μg/ml)
pBABEpuro-BREV5	Ampicillin (100 μg/ml)
pBABEpuro-V5BRE	Ampicillin (100 μg/ml)
pBABEneo-BREV5	Ampicillin (100 μg/ml)
pBABEhygro-BRE	Ampicillin (100 μg/ml)
pAdTrack-CMV-BRE	Kanamycin (50 mg/ml)
pAdTrack-CMV-BREV5	Kanamycin (50 mg/ml)
pAdTrack-CMV-V5BRE	Kanamycin (50 mg/ml)
pEBB-FLAG-BRE	Ampicillin (100 μg/ml)

2.2.1.5 Check of plasmids

Several single colonies of bacteria on the antibiotic-containing plates were collected for PCR check and miniprep separately. The plasmids of miniprep were used for digestion check. The colony whose PCR check and digestion check were both positive was picked to prepare midiprep. The concentration of plasmids was measured by NANODrop and confirmed by agarose gel electrophoresis. Then the plasmids of midiprep were sent for sequencing. cDNA and amino acid sequences of gene of interests of the nine constructs were as follows.

Table 2-16. **cDNA and amino acid sequences of gene of interests of the nine constructs**

Names of constructs	Genes of interest	Shown in
pBABEpuro-BRE	BRE	Figure 2-14
pBABEpuro-BREV5	BREV5 (BRE tagged by V5 at the C-terminus)	Figure 2-15
pBABEpuro-V5BRE	V5BRE (BRE tagged by V5 at the N-terminus)	Figure 2-16
pBABEneo-BREV5	BREV5 (BRE tagged by V5 at the C-terminus)	Figure 2-15
pBABEhygro-BRE	BRE	Figure 2-14
pAdTrack-CMV-BRE	BRE	Figure 2-14
pAdTrack-CMV-BREV5	BREV5 (BRE tagged by V5 at the C-terminus)	Figure 2-15
pAdTrack-CMV-V5BRE	V5BRE (BRE tagged by V5 at the N-terminus)	Figure 2-16
pEBB-FLAG-BRE	BRE	Figure 2-14

A)

ATGTCCCCAGAAGTGGCCTTGAACCGAATATCTCCAATGCTCTCCCCTTTCATATCT
AGCGTGGTCCGGAATGGAAAAGTGGGACTGGATGCTACAAACTGTTTGAGGATAA
CTGACTTAAAATCTGGCTGCACATCATTGACTCCTGGGCCCAACTGTGACCGATTT
AAACTGCACATACCATATGCTGGAGAGACATTAAAGTGGGATATCATTTTCAATGCC
CAATACCCAGAACTGCCTCCCGATTTTATCTTTGGAGAAGATGCTGAATTCCTGCCA
GACCCCTCAGCTTTGCAGAATCTTGCCTCCTGGAATCCTTCAAATCCTGAATGTCTC
TTACTTGTGGTGAAGGAACTTGTGCAACAATATCACCAATTCCAATGTAGCCGCCT
CCGGGAGAGCTCCCGCCTCATGTTTGAATACCAGACATTACTGGAGGAGCCACAGT
ATGGAGAGAACATGGAAATTTATGCTGGGAAAAAAAACAACTGGACTGGTGAATT
TTCAGCTCGTTTCCTTTTGAAGCTGCCCGTAGATTTCAGCAATATCCCCACATACCT
TCTCAAGGATGTAAATGAAGACCCTGGAGAAGATGTGGCCCTCCTCTCTGTTAGTT
TTGAGGACACTGAAGCCACCCAGGTGTACCCCAAGCTGTACTTGTCACCTCGAATT
GAGCATGCACTTGGAGGCTCCTCAGCTCTTCATATCCCAGCTTTTCCAGGAGGAGG
ATGTCTCATTGATTACGTTCCTCAAGTATGCCACCTGCTCACCAACAAGGTGCAGT
ACGTGATTCAAGGGTATCACAAAAGAAGAGAGTATATTGCTGCTTTTCTCAGTCAC
TTTGGCACAGGTGTCGTGGAATATGATGCAGAAGGCTTTACAAAACTCACTCTGCT
GCTGATGTGGAAAGATTTTTGTTTTCTTGTACACATTGACCTGCCTCTGTTTTTCCC
TCGAGACCAGCCAACTCTCACATTTCAGTCCGTTTATCACTTTACCAACAGTGGAC
AGCTTTACTCCCAGGCCCAAAAAAATTATCCGTACAGCCCCAGATGGGATGGAAAT
GAAATGGCCAAAAGAGCAAAGGCTTATTTCAAAACCTTTGTCCCTCAGTTCCAGG
AGGCAGCATTTGCCAATGGAAAGCTC

B)

MSPEVALNRISPMLSPFISSVVRNGKVGLDATNCLRITDLKSGCTSLTPGPNCDRFKLHI
PYAGETLKWDIIFNAQYPELPPDFIFGEDAEFLPDPSALQNLASWNPSNPECLLLVVKE
LVQQYHQFQCSRLRESSRLMFEYQTLLEEPQYGENMEIYAGKKNNWTGEFSARFLLK

LPVDFSNIPTYLLKDVNEDPGEDVALLSVSFEDTEATQVYPKLYLSPRIEHALGGSSAL
HIPAFPGGGCLIDYVPQVCHLLTNKVQYVIQGYHKRREYIAAFLSHFGTGVVEYDAEG
FTKLTLLLMWKDFCFLVHIDLPLFFPRDQPTLTFQSVYHFTNSGQLYSQAQKNYPYSP
RWDGNEMAKRAKAYFKTFVPQFQEAAFANGKL

Figure 2-14. **cDNA and amino acid sequences of BRE**

A)

ATGTCCCCAGAAGTGGCCTTGAACCGAATATCTCCAATGCTCTCCCCTTTCATATCT
AGCGTGGTCCGGAATGGAAAAGTGGGACTGGATGCTACAAACTGTTTGAGGATAA
CTGACTTAAAATCTGGCTGCACATCATTGACTCCTGGGCCCAACTGTGACCGATTT
AAACTGCACATACCATATGCTGGAGAGACATTAAAGTGGGATATCATTTTCAATGCC
CAATACCCAGAACTGCCTCCCGATTTTATCTTTGGAGAAGATGCTGAATTCCTGCCA
GACCCCTCAGCTTTGCAGAATCTTGCCTCCTGGAATCCTTCAAATCCTGAATGTCTC
TTACTTGTGGTGAAGGAACTTGTGCAACAATATCACCAATTCCAATGTAGCCGCCT
CCGGGAGAGCTCCCGCCTCATGTTTGAATACCAGACATTACTGGAGGAGCCACAGT
ATGGAGAGAACATGGAAATTTATGCTGGGAAAAAAAACAACTGGACTGGTGAATT
TTCAGCTCGTTTCCTTTTGAAGCTGCCCGTAGATTTCAGCAATATCCCCACATACCT
TCTCAAGGATGTAAATGAAGACCCTGGAGAAGATGTGGCCCTCCTCTCTGTTAGTT
TTGAGGACACTGAAGCCACCCAGGTGTACCCCAAGCTGTACTTGTCACCTCGAATT
GAGCATGCACTTGGAGGCTCCTCAGCTCTTCATATCCCAGCTTTTCCAGGAGGAGG
ATGTCTCATTGATTACGTTCCTCAAGTATGCCACCTGCTCACCAACAAGGTGCAGT
ACGTGATTCAAGGGTATCACAAAAGAAGAGAGTATATTGCTGCTTTTCTCAGTCAC
TTTGGCACAGGTGTCGTGGAATATGATGCAGAAGGCTTTACAAAACTCACTCTGCT
GCTGATGTGGAAAGATTTTTGTTTTCTTGTACACATTGACCTGCCTCTGTTTTTCCC
TCGAGACCAGCCAACTCTCACATTTCAGTCCGTTTATCACTTTACCAACAGTGGAC
AGCTTTACTCCCAGGCCCAAAAAAATTATCCGTACAGCCCCAGATGGGATGGAAAT
GAAATGGCCAAAAGAGCAAAGGCTTATTTCAAAACCTTTGTCCCTCAGTTCCAGG
AGGCAGCATTTGCCAATGGAAAGCTCAAGGGCGAGCTTCGAGGTCACCCATTCGA
AGGTAAGCCTATC**CCTAACCCTCTCCTCGGTCTCGATTCTACG**

B)

MSPEVALNRISPMLSPFISSVVRNGKVGLDATNCLRITDLKSGCTSLTPGPNCDRFKLHI
PYAGETLKWDIIFNAQYPELPPDFIFGEDAEFLPDPSALQNLASWNPSNPECLLLVVKE
LVQQYHQFQCSRLRESSRLMFEYQTLLEEPQYGENMEIYAGKKNNWTGEFSARFLLK
LPVDFSNIPTYLLKDVNEDPGEDVALLSVSFEDTEATQVYPKLYLSPRIEHALGGSSAL
HIPAFPGGGCLIDYVPQVCHLLTNKVQYVIQGYHKRREYIAAFLSHFGTGVVEYDAEG
FTKLTLLLMWKDFCFLVHIDLPLFFPRDQPTLTFQSVYHFTNSGQLYSQAQKNYPYSP
RWDGNEMAKRAKAYFKTFVPQFQEAAFANGKLKGELRGHPFEGKPI**PNPLLGLDST**

Figure 2-15. **cDNA and amino acid sequences of BREV5**

Sequence of BRE is shown in underlined letters. Sequence of V5 epitope is shown in bold.

A)

CCTAACCCTCTCCTCGGTCTCGATTCTACGCGTACCGGTTCCCCAGAAGTGGCC
TTGAACCGAATATCTCCAATGCTCTCCCCTTTCATATCTAGCGTGGTCCGGAATGGA
AAAGTGGGACTGGATGCTACAAACTGTTTGAGGATAACTGACTTAAAATCTGGCTG
CACATCATTGACTCCTGGGCCCAACTGTGACCGATTTAAACTGCACATACCATATGC
TGGAGAGACATTAAAGTGGGATATCATTTTCAATGCCCAATACCCAGAACTGCCTC
CCGATTTTATCTTTGGAGAAGATGCTGAATTCCTGCCAGACCCCTCAGCTTTGCAG
AATCTTGCCTCCTGGAATCCTTCAAATCCTGAATGTCTCTTACTTGTGGTGAAGGA
ACTTGTGCAACAATATCACCAATTCCAATGTAGCCGCCTCCGGGAGAGCTCCCGCC
TCATGTTTGAATACCAGACATTACTGGAGGAGCCACAGTATGGAGAGAACATGGA
AATTTATGCTGGGAAAAAAAACAACTGGACTGGTGAATTTTCAGCTCGTTTCCTTT
TGAAGCTGCCCGTAGATTTCAGCAATATCCCCACATACCTTCTCAAGGATGTAAATG
AAGACCCTGGAGAAGATGTGGCCCTCCTCTCTGTTAGTTTTGAGGACACTGAAGC
CACCCAGGTGTACCCCAAGCTGTACTTGTCACCTCGAATTGAGCATGCACTTGGAG
GCTCCTCAGCTCTTCATATCCCAGCTTTTCCAGGAGGAGGATGTCTCATTGATTACG

TTCCTCAAGTATGCCACCTGCTCACCAACAAGGTGCAGTACGTGATTCAAGGGTAT
CACAAAAGAAGAGAGTATATTGCTGCTTTTCTCAGTCACTTTGGCACAGGTGTCGT
GGAATATGATGCAGAAGGCTTTACAAAACTCACTCTGCTGCTGATGTGGAAAGATT
TTTGTTTTCTTGTACACATTGACCTGCCTCTGTTTTTCCCTCGAGACCAGCCAACTC
TCACATTTCAGTCCGTTTATCACTTTACCAACAGTGGACAGCTTTACTCCCAGGCCC
AAAAAAATTATCCGTACAGCCCCAGATGGGATGGAAATGAAATGGCCAAAAGAGC
AAAGGCTTATTTCAAAACCTTTGTCCCTCAGTTCCAGGAGGCAGCATTTGCCAATG
GAAAGCTC

B)

PNPLLGLDSTRTGSPEVALNRISPMLSPFISSVVRNGKVGLDATNCLRITDLKSGCTSL
TPGPNCDRFKLHIPYAGETLKWDIIFNAQYPELPPDFIFGEDAEFLPDPSALQNLASWN
PSNPECLLLVVKELVQQYHQFQCSRLRESSRLMFEYQTLLEEPQYGENMEIYAGKKN
NWTGEFSARFLLKLPVDFSNIPTYLLKDVNEDPGEDVALLSVSFEDTEATQVYPKLYL
SPRIEHALGGSSALHIPAFPGGGCLIDYVPQVCHLLTNKVQYVIQGYHKRREYIAAFLS
HFGTGVVEYDAEGFTKLTLLLMWKDFCFLVHIDLPLFFPRDQPTLTFQSVYHFTNSGQ
LYSQAQKNYPYSPRWDGNEMAKRAKAYFKTFVPQFQEAAFANGKL

Figure 2-16. **cDNA and amino acid sequences of V5BRE**

Sequence of BRE is shown in underlined letters. Sequence of V5 epitope is shown in bold.

2.2.2 Plasmids preparation

When preparing plasmids initially from the stab culture, several single colonies were isolated first. Then the sterile liquid LB containing the suitable antibiotic (100 μg/ml of ampicillin or 50 mg/ml of kanamycin), according to the antibiotic resistant gene of the plasmid, was prepared. One single colony was transferred into 100 ml of liquid LB containing the suitable antibiotic by using a sterile pipette tip. Bacterial culture was shaked for around 16 hours at 250 rpm in a 37℃ shaking incubator. After that, 900 μl of bacterial culture was aspirated into 250 μl of sterile 80% Glycerol as long term storage, which was kept in a -80℃ freezer. The plasmids in the left bacterial culture were extracted using a Qiagen midiprep kit. When preparing plasmids, whose long term storage was already prepared, a few bacteria were picked from the -80℃ long term storage into 100 ml of liquid LB containing suitable antibiotic by using a sterile pipette tip. The latter steps were the same with the above-mentioned steps.

2.2.3 Cell culture

2.2.3.1 Monolayer cells

Table 2-17. **Monolayer cells**

Names	Descriptions	Catalog #
HeLa	Human cervical carcinoma	ATCC #CCL-2
NIH3T3	Mus musculus (mouse) NIH/Swiss strain embryonic fibroblast	ATCC #CRL-1658
HEK293T	Human embryonic kidney 293 cells	ATCC #CRL-11268

D122	The poorly immunogenic and highly metastatic D122 clone of 3LL Lewis lung carcinoma of C57BL/6 origin (227)	/
B07	BRE-depleted cell line of D122 with stable BRE shRNA (#GI536607, Origene) transfection.	/
E7, C6	Subclone of B07 cell line	/
T8	Negative control cell line of D122 with stable empty shRNA vector (#TR30008, Origene) transfection.	/
C6-neo-BREV5	Cell line of C6 with stable pBABEneo-BREV5 retrovirus infection	/

These cells were grown in DMEM medium supplemented with 10% fetal bovine serum and 100 U/ml of penicillin and streptomycin. Cultures were maintained at 37℃ with 5% CO_2.

2.2.3.2 Suspension cell

Table 2-18. **Suspension cells**

Names	Descriptions	Catalog #
Jurkat A3	Human acute T cell leukemia subclone selected for high sensitivity to anti-Fas agonist antibody	ATCC #CRL-2570
GSV1	Jurkat A3 with stable empty vector pcDNA3.1/GS transfection	/
GSB2	Jurkat A3 with stable GS-BRE transfection	/

The cells were grown in RPMI medium supplemented with 10% fetal bovine serum and 100 U/ml of penicillin and streptomycin. Cultures were maintained at 37℃ with 5% CO_2.

2.2.4 Cell transfection

Cells, such as D122, C6, and HEK293T, were washed twice in the DMEM with 10% fetal bovine serum only. Appropriate number of cells (usually 2×10^5 cells for D122 and C6, 1×10^6 cells for HEK293T) were seeded in one well of a 6-well plate. After overnight incubation, cells were around 80-90% confluent. The cells were washed twice in DMEM only. Two ml of DMEM only was added to the cells as plating medium. Four μg of DNA was diluted in 250 μl of Opti-MEM® I medium. Ten μl of Lipofectamine 2000 was diluted in another 250 μl of Opti-MEM® I medium. The diluted Lipofectamine 2000 was incubated for 5 min at room temperature. The diluted DNA was combined with the diluted Lipofectamine 2000 by gently mixing. The mixture was incubated for 20 min at room temperature. Five hundred μl of DNA-Lipofectamine complexes were added to the well. Cells were incubated after a gentle mix. After 4 to 6 hours, medium containing DNA-Lipofectamine complexes was changed with serum- and penicillin/streptomycin-containing fresh DMEM medium. Forty-eight hours after transfection, cells were used for further analysis.

For performing transfection in a 25-cm^2 flask to generate adenovirus, 2×10^6 HEK293T cells were seeded. Three ml of DMEM only was added to the cells as plating medium. Four μg of DNA was diluted in 500 μl of Opti-MEM® I medium. Twenty μl of Lipofectamine 2000 was diluted in 500 μl of Opti-MEM® I medium. The other details were the same with the above-mentioned steps.

2.2.5 Generation of stable transfectants

One day before transfection, 2×10^5 D122 cells per well were seeded in two wells of a 6-well plate,. After overnight incubation, they were transfected with BRE and negative control shRNA, respectively. Twenty-four hours after transfection, cells in each well were trypsinized and resuspended in 24 wells of a 24-well plate with medium containing 5 μg/ml of puromycin. Around 10 days later, the puromycin resistant cells in each well of the 24-well plate were trypsinized and resuspended in one well of a 6-well plate. Cells were harvested for check when they were around 80-90% confluent. The expression level of target gene was checked by Western blot analysis. Cell lines of D122 with stable BRE shRNA and empty shRNA transfection were named as B07 and T8, respectively.

2.2.6 Western blot analysis

2.2.6.1 BCA™ protein assay

A set of diluted albumin standards and BCA™ working reagents were prepared according to the manufacture's instruction. The sample, whose protein concentration was unknown, was diluted. BCA™ working reagents were added to the diluted albumin standards and the diluted sample. They were incubated at 37℃ for 30 min. The absorbance values of them at 595 nm were tested by the DTX 800 multimode detector. The protein concentration of the sample was calculated according to the relationship between the protein concentrations and absorbance values of the albumin standards.

2.2.6.2 SDS-PAGE

The same quantities of samples (5 μg or 10 μg) were resolved on 9% sulphate-polyacrylamide gel. Electrophoresis was carried out at 85 V at room temperature. The gel was calibrated with protein marker. After electrophoresis, protein was transferred onto PVDF membrane using a Semi-Dry transferring cell at 20 V for 30 min.

2.2.6.3 Immunoblotting

The PVDF membrane containing the transferred protein was blocked for 2 hours at room temperature. The blocking powder was dissolved in TBS. Primary antibody was then added to the membrane. After overnight incubation with shaking, the membrane was subsequently washed with PBST (PBS, 0.05% Tween-20) for three times at 10 minutes each. The bound

primary antibody was visualized with appropriate HRP-conjugated secondary antibody for 3 hours. Lumingen detection reagent was applied to the membrane. Then the membrane was exposed to X-ray film. The following table showed the details of the blocking milk, antibodies, and detection reagents. M meant calcium plus skimmed milk. EM meant ECL advance blocking milk.

Table 2-19. **Details of the Immunoblotting**

Names	Blocking milk	Primary antibodies	Secondary antibodies	Detection reagents (Lumingen)
Anti-GAPDH	5% M	1:6000 (in 5% M)	1:30000 Anti-Mouse Ig-HRP (in 2% M)	PS-3
Anti-β-actin	5% M	1:6000 (in 5% M)	1:30000 Anti-Mouse Ig-HRP (in 2% M)	PS-3
HRP-anti-HA	5% M	1:4000 (in 5% M)	/	PS-3
HRP-anti-FLAG	5% M	1:30000 (in 5% M)	/	PS-3
Anti-biotinylated XIAP	2% M	1:2000 (in 2% EM)	1:40000 Streptavidin-HRP (in 2% M)	PS-3
Anti-cFLIP	2% M	1:4000 (in 2% EM)	1:80000 Anti-Rabbit Ig-HRP (in 5% M)	TMA-6
Anti-PARP	5% M	1:10000 (in 5% M)	1:80000 Anti-Rabbit Ig-HRP (in 5% M)	TMA-6
Anti-cleaved caspase 3	2% M	1:4000 (in 2% EM)	1:80000 Anti-Rabbit Ig-HRP (in 5% M)	TMA-6
Anti-cIAP-1	2% M	1:4000 (in 2% EM)	1:80000 Anti-Rabbit Ig-HRP (in 5% M)	TMA-6
Anti-cIAP-2	2% M	1:4000 (in 2% EM)	1:30000 Anti-Mouse (in 2% M)	TMA-6
HRP-anti-V5	5% M	1:1000 (in 5% M)	/	PS-3
Anti-XIAP	2% M	1:4000 (in 2% EM)	1:30000 Anti-Mouse (in 2% M)	TMA-6
Anti-ubiquitin	2% M	1:4000 (in 2% EM)	1:30000 Anti-Mouse (in 2% M)	TMA-6
Anti-BRE (Mab489-7)	2% M	1:10 (in 2% EM)	1:30000 Anti-Mouse (in 2% M)	TMA-6
Anti-BRE (Mab246)	2% M	1:5 (in 2% EM)	1:30000 Anti-Mouse (in 2% M)	TMA-6

2.2.7 Chemical treatment

2.2.7.1 Etoposide, TNF-α, MG132, CHX, VAD, and DMSO

For monolayer cells:

(1) Direct treatment of monolayer cells

One day before chemical treatment, 2×10^5 cells, such as D122, C6, E7, T8, and C6-neo-BREV5 were seeded in one well of a 6-well plate. Around 16 hours later, culture

medium of cells was changed to 3 ml of fresh medium containing suitable chemical, such as etoposide, TNF-α, MG132, CHX, VAD, and solvent control DMSO. Cells were incubated with the chemical containing medium for the indicated time. After that, they were harvested for further analysis.

(2) Treatment of monolayer cells after transfection

Forty-eight hours after transfection, culture medium of cells, such as C6 and HEK293T, was changed to 3 ml of fresh medium containing suitable chemical, such as TNF-α, MG132, and solvent control DMSO. The latter steps were the same with (1).

For suspension cells:

Two hundred thousand cells, such as GSV1 and GSB2 in 3 ml of fresh medium containing suitable chemical, such as etoposide, MG132, VAD, and solvent control DMSO, were seeded in one well of a 6-well plate. The cells were incubated with the chemical containing medium for the indicated time. After that, they were harvested for further analysis.

2.2.7.2 NEM

In NEM treatment experiments, NEM was used in the following two ways:

(1) Addition of NEM into lysis buffer for subsequent cell lysis

Before cell harvest, NEM was added to fresh routine lysis buffer (Cell Signaling, #9803). Cells were lysed by this NEM-containing lysis buffer and routine lysis buffer separately.

(2) Addition of NEM to cell lysate

Cells were lysed in routine lysis buffer (Cell Signaling, #9803) first. Protein concentration of this lysate was tested. The same quantities of proteins (5 μg) were allocated to several eppendorfs. NEM was added into some of these eppendorfs. H_2O was added into one eppendorf as solvent control. There was another eppendorf with nothing added into it as negative control. These eppendorfs were incubated in ice for 10 min. Next, they were vortexed for 10 sec and rotated on a rolling platform for 1 hour at 4℃. After that, these eppendorfs were centrifuged at 13200 rpm for 10 min at 4℃. Then they were used for Western blot analysis.

2.2.8 Apoptosis assays by the flow cytometry

BRE-depleted cells, B07 and negative shRNA control line, T8 were treated with TNF-α in the absence of cycloheximide for the indicated time duration. Cells were harvested for flow cytometric analysis using Annexin V-FITC and Propidium Iodide staining. Cells were trypsinized and washed twice with ice-cold PBS. Next, cells were pelleted by centrifuge at 1000 rpm for 5 min at 4℃, and then resuspended in 100 μl of 1× binding buffer. Five μl of Annexin V-FITC and 5 μl of Propidium Iodide were added into the solution. Solution was

mixed gently and incubated for 15 min at room temperature in dark. Four hundred μl of 1× binding buffer was added to the solution. Flow analysis was conducted using FACS Calibur flow cytometry and CellQuest software.

2.2.9 Immunoprecipitation

Around 2 × 10^6 cells were harvested. Cells were washed twice with 1 ml of PBS in an eppendorf and spinned at 4000 rpm for 1 min. Next, supernatant was removed completely and cell pellet was resuspended in 0.5 ml of ice-cold IP lysis buffer (20 mM Tris PH 7.4, 50 mM NaCl, 2 mM EDTA, 1 mM PMSF, 1× protease inhibitor cocktail, 1× phosphatase inhibitor cocktail, 1% Triton X-100, 5 μM MG132). The eppendorf was vortexed gently, and placed on a rolling platform for 1 hour at 4℃. After centrifuge at 3000 rpm for 15 min, supernatant was carefully collected without disturbing the pellet, and transferred to a clean eppendorf. Protein concentration was measured by BCA assay. A total of 200 μg of each sample was transferred to a new eppendorf and pre-cleared with 20 μl of Protein G-Sepharose for 1 hour. Then beads were pelleted by centrifuge 10,000 g for 1 min and supernatant was removed to another new eppendorf. Five μg of antibody was added to each eppendorf containing lysate. The eppendorf was placed on a rolling platform at 4℃ for 1 hour. Fifty μl of washed Protein G-Sepharose in pre-chilled lysis buffer was added into each eppendorf. The mixture was continually incubated on a rolling platform at 4℃ for overnight. After incubation, the eppendorf was centrifuged at 10000 g for 2 min at 4℃. The supernatant was removed completely and the beads were washed 5 times with 400 μl of lysis buffer each. After the last wash, supernatant was aspirated. Seven point five μl of 4× SDS loading buffer (200 mM Tris-HCl pH 6.8, 8% SDS, 40% glycerol, 4% β-mercaptoethanol, 50 mM EDTA, 0.08% bromophenol blue) and 22.5 μl of IP lysis buffer were added to the beads. Beads were vortexed and heated to 100 ℃ for 5 min. Then beads were pelleted by centrifuge at 10000 g for 5 min. Supernatant, considered as elute, was collected to load onto the gel.

2.2.10 BRE containing retrovirus generation and transduction

2.2.10.1 Retrovirus generation

2.2.10.1.1 Production of retrovirus by transient transfection of packaging cells

Five pBABE-based retroviral expression vectors containing gene of BRE were generated according to a standard molecular cloning procedure. The retrovirus was named after the name of corresponding pBABE-based retroviral expression vector.

Table 2-20. **Retroviral expression vectors and corresponding retrovirus**

Names of retroviral expression vectors	Genes of interest	Selectable markers	Names of corresponding retrovirus
pBABEpuro-BRE	BRE	Puromycin	pBABEpuro-BRE
pBABEpuro-BREV5	BRE tagged by V5 at the C-terminus	Puromycin	pBABEpuro-BREV5
pBABEpuro-V5BRE	BRE tagged by V5 at the N-terminus	Puromycin	pBABEpuro-V5BRE
pBABEneo-BREV5	BRE tagged by V5 at the C-terminus	Neomycin	pBABEneo-BREV5
pBABEhygro-BRE	BRE	Hygromycin	pBABEhygro-BRE

HEK293T cells were co-transfected with one of the above-mentioned retroviral expression vector containing the gene of BRE and the retroviral package vector, pCL-Ampho. Forty-eight h after the transfection, retrovirus-containing supernatant was harvested. It was filtered by 0.45 mm syringe filters. After that, any cells in the supernatant were removed. The retrovirus-containing supernatant was used directly or stored at -80℃.

2.2.10.1.2 Production of retrovirus by stable transfection of packaging cells

HEK293T cells were co-transfected with one of the above-mentioned retroviral expression vector containing the gene of BRE and the retroviral package vector, pCL-Ampho. Forty-eight h after the transfection, cells were selected according to the selectable marker of the retroviral expression vector (Table 2-20). Five μg/ml of puromycin was used for pBABEpuro-BRE, pBABEpuro-BREV5, and pBABEpuro-V5BRE, 2 mg/ml of neomycin for pBABEneo-BREV5, 100 μg/ml of hygromycin for pBABEhygro-BRE. Two weeks later, many cells died, leaving only antibiotic-resistant cells alive. Antibiotic-resistant cells were expanded into large cultures in medium without antibiotic. When cells were around 80-90% confluent, retrovirus-containing supernatant was harvested and filtered. It was used directly or stored at -80℃.

2.2.10.2 Retrovirus concentration

Retrovirus is usually produced at low titer. It often needs to be concentrated for storage or further applications. To concentrate virus, using PEG (Polyethylene glycol) is a convenient and timesaving method without ultra-centrifugation. Ten ml of sterile PEG solution (40% PEG, 2.4% NaCl) was added to 40 ml of the filtered retrovirus-containing supernatant in a 50 ml tube. This tube was rotated on a rolling platform at 4℃ overnight. After overnight rotation, retrovirus was pelleted by centrifuge at 3500 rpm at 4℃ for 90 min. Supernatant was removed completely. Pellet was resuspended in 400 μl of PBS. One hundred μl of retrovirus-containing PBS was allocated to four eppendorfs each. This concentrated retrovirus

was used directly or stored at -80℃.

2.2.10.3 Retrovirus titering

Two hundred thousand NIH3T3 cells per well were seeded in six wells of a 6-well plate. Around 16 hours later, a serial dilutions (five 10-fold dilutions) of retrovirus in culture medium containing 8 μg/ml of polybrene were prepared. Polybrene (hexadimethrine bromide) is a cationic polymer used to increase the efficiency of infection of cells with a retrovirus in cell culture. Polybrene acts by neutralizing the charge repulsion between virions and sialic acid on the cell surface (228). These five 10-fold dilutions were used to infect five wells of NIH3T3 cells, respectively. Cells without retrovirus infection were negative control. After 24 hours infection, 1/20 of cells of each well were splitted onto a 10-cm plate. One day later, cells were selected according to the selectable marker of the retroviral expression vector (Table 2-20). Five μg/ml of puromycin was used for pBABEpuro-BRE, pBABEpuro-BREV5 and pBABEpuro-V5BRE, 2 mg/ml of neomycin for pBABEneo-BREV5, 100 μg/ml of hygromycin for pBABEhygro-BRE. Around 10 days later, antibiotic resistant cells formed several colonies. The cells of negative control were all dead.

Number of colonies was counted on one of the 10-cm plate, which had ten to fifty evenly distributed colonies.

Titer (CFU/ml) = number of colonies / (virus volume × replication factor × fraction of infected cell plated)

Beside, after titer assay, antibiotic resistant NIH3T3 cells were harvested for Western blot analysis to confirm the gene of BRE in the retrovirus.

2.2.10.4 Retrovirus transduction

Ten thousand cells of C6 were seeded in one well of a 6-well plate. Around 16 hours later, 2×10^5 CFU retrovirus of pBABEneo-BREV5 was used to infect the cells in 8 μg/ml of polybrene. After 24 hours infection, cells were trypsinized and resuspended in 24 wells of a 24-well plate. One day later, cells were selected by 2 mg/ml of neomycin. Around 10 days later, neomycin-resistant cells in each well of the 24-well plate were trypsinized and resuspended in one well of a 6-well plate. The concentration of neomycin in the medium was halved to 1 mg/ml at the same time. Cells were trypsinized when they were around 80-90% confluent. Half-cells were used for Western blot analysis, half-cells were kept growing.

2.2.11 BRE containing adenovirus generation and transduction

2.2.11.1 Adenovirus generation

2.2.11.1.1 Subclone BRE into a adenoviral shuttle vector, pAdTrack-CMV

AdEasy technology system was used to generate adenovirus. Three pAdTrack-CMV-based adenoviral shuttle vectors containing gene of BRE were generated according to a standard molecular cloning procedure.

Table 2-21. **Shuttle vectors**

Names	Genes of interest	Selectable markers
pAdTrack-CMV-BRE	BRE	Kanamycin
pAdTrack-CMV-BREV5	BRE tagged by V5 at the C-terminus	Kanamycin
pAdTrack-CMV-V5BRE	BRE tagged by V5 at the N-terminus	Kanamycin

2.2.11.1.2 Generation of recombinant adenovirus plasmids

(1) Characterization of the pAdEasy®-1 plasmids in AdEasier®-1 cells with extensive restriction digestions

AdEasier®-1 bacterial cells are BJ5183 derivatives, which already contain the supercoiled backbone vector, pAdEasy®-1. As BJ5183 cells have a relatively high frequency of homologous recombination, unwanted or detrimental rearrangement and/or recombination of the pAdEasy®-1 sequences in AdEasier®-1 cell can occur. Thus, it is important for characterizing the pAdEasy®-1 plasmids in AdEasier®-1 with extensive restriction digestions. Plasmids in AdEasier®-1 cells and pAdEasy®-1 stock DNA, which was made in a strain incapable of homologous recombination, were digested by Hind III and Pst I. The digestion patterns of these two plasmids were the same. Thus, the unwanted or detrimental rearrangement and/or recombination of the pAdEasy®-1 did not occur.

(2) Preparation of electro-competent AdEasier®-1 cells

Frozen stock of AdEasier®-1 cells was inoculated into 10 ml of LB medium with 100 μg/ml of ampicillin in a 50 ml tube. Cells were incubated in a shaker at 37 ℃ overnight. One ml of bacterial culture was diluted into 1000 ml of LB medium with 100 μg/ml of ampicillin in eight 1 liter flasks (125 ml each). They were incubated for 4 to 5 hour with vigorous aeration at 37℃, until the absorbance value at 550 nm was around 0.8. This was done by DU® 800 spectrophotometer. Then bacterial culture was collected in four 250-ml conical centrifuge tubes. These tubes were incubated in ice for 1 hour. Cells were pelleted by centrifuging at 3,000 rpm (2,600 g) at 4℃ for 10 min. All of the pellets were washed by resuspending in

1000 ml of sterile, ice-cold WB (WB = 10% ultra-pure glycerol, 90% distilled water, v/v). Cell suspension was centrifuged at 3,000 rpm (2500 g) at 4℃ for 30 min. Then the wash and centrifuge steps were repeated once. After that, most of the supernatant was poured roughly. Only about 20 ml of supernatant was left. Cells were resuspended in the left 20 ml of supernatant and were transferred to a 50 ml tube. Then cells were spinned at 3,000 rpm at 4℃ for 10 min. All but 3 ml supernatant was pipetted out. Cells were resuspended in left WB in the tube. Cell suspension was allocated to 150 eppendorfs (20 µl each), which had been pre-chilled at -80°C. These aliquots were stored at -80℃.

(3) Linearization of adenoviral shuttle vector

The adenoviral shuttle vector pAdTrack-CMV-BREV5 was picked for adenovirus generation. The corresponding adenovirus was named as adenovirus-BREV5. A little of pAdTrack-CMV-BREV5 bacterial frozen stock was grown in 5 ml of LB containing 50 mg/ml of kanamycin in a 15 ml tube in a shaker at 37℃ at 250 rpm. After overnight shaking, plasmids in the bacterial culture were extracted using a Qiagen miniprep kit. Four µg of plasmids was linearized by Pme I in 100 µl of digestion solution. One hundred µl of H_2O, 100 µl of 7.5 M ammonium acetate, and 4 µl of pellet paint co-precipitant were added into the digestion solution. DNA was extracted with 300 µl of 25:24:1 phenol/chloroform/isoamyl alcohol (pH 8.0). Top layer of DNA solution was transferred to a clean tube. DNA was precipitated with 600 µl of 100% ethanol by centrifuging for 5 min at 16000 g at room temperature. Pellets were washed three times with 70% ethanol to eliminate residual salt. Washed DNA pellets were resuspended in 8 µl of H_2O.

(4) Electro-transformation

Eight µl of linearized pAdTrack-CMV-BREV5 was added into an eppendorf containing 20 µl of competent AdEasier®-1 cells. The bacteria/DNA mix was incubated in ice for 30 min. It was transferred to an ice-cold E.coli pulser cuvette (0.1 cm electrode gap), carefully avoiding formation of bubbles. The cuvette was kept in ice for 5 min. The pulse at 2500 V, 200 Ω, and 25 µF in a Bio-Rad Gene pulser electroporator was delivered to the cuvette. It was kept in ice for 5 min. Five hundred µl of sterile LB medium was added into it. The transformation mix was resuspended and transferred into a new eppendorf. The eppendorf was incubated at 250 rpm for 1 hour at 37℃. Then all of the transformation mix was spreaded into one LB plate with 50 mg/ml of kanamycin. The plate was incubated overnight in a 37℃ incubator.

(5) Identification of the correct recombinants

There were five kanamycin resistant colonies on the plate. DNA of these five colonies was prepared using a Qiagen miniprep kit, and digested by Pac I. After digesting the recombinant

with Pac I, correct recombinant should yield a large fragment (approximately 30 kb) and a small fragment of 3.0 kb or 4.5 kb. The reason of the two possible small fragments is that the homologous recombination can occur between two ori regions or two homologous left arms on pAdTrack-CMV-BREV5 and pAdEasy®-1, respectively. In my case, after Pac I digestion check, two possible correct recombinants, which yielded a smaller fragment of 3.0 kb and 4.5 kb separately, were picked out among the five kanamycin resistant colonies. The one, which yielded a smaller fragment of 3.0 kb, was used for later adenovirus generation. This colony was named as recombinant 3.

(6) Re-transformation of recombinant 3 into a recombination-defective strain

Because of the high frequencies of recombination and rearrangement of large plasmids in BJ5183 cells, after checking by the Pac I restriction endonuclease digestion, the recombinant 3 was re-transformed into a recombination-defective strain (DH5α) by heat shock transformation. The re-transformed plasmids in DH5α were digested again by Pac I. They still yielded a large fragment (approximately 30 kb) and a small fragment of 3.0 kb.

2.2.11.1.3 Generation of recombinant adenovirus in HEK293T packaging cells

Recombinant 3 was digested with Pac I in 100 µl of digestion solution. One hundred µl of H_2O, 100 µl of 7.5 M ammonium acetate and 600 µl of 100% ethanol were added into it. This mix was incubated at -20℃ for 2 hours. DNA was precipitated by centrifuging for 10 min at 16000 g. Pellets were washed three times with 70% ethanol to eliminate residual salt. Washed DNA pellets were resuspended in 20 µl of EB buffer. Purified linearized recombinant 3 was transfected to HEK293T cells on a 25-cm^2 tissue culture flask using Lipofectamine 2000. The transfected cells were maintained in 37℃, 5% CO_2 incubator for two weeks. One to two ml of fresh complete DMEM was added into the flask every 3 days. Since pAdTrack-CMV-BREV5 contained a GFP monitor, the green fluorescence was observed under fluorescence microscopy. The obvious GFP plaques were observed under fluorescence microscopy from 4 days after transfection.

Around 2 weeks after the transfection, HEK293T cells were harvested from flask by rinsing. Cells were centrifuged at 750 rpm for 5 min. All but 2 ml medium was removed. Pellets were resuspended by vortex and transferred into two eppendorfs (1 ml each). Four freeze-thaw-vortex cycles were performed to release adenovirus from cells. Cells were froze in liquid nitrogen bath, thawed in a 37 ℃ water bath, and mixed by vigorous vortex for 30 sec. Three more cycles of the freezing-thawing-vortex were repeated.

2.2.11.1.4 Stepwise amplification

(1) The first round of amplification

One day before infection, HEK293T cells were seeded in two 25-cm^2 tissue culture flasks (approximately 3×10^6 cells per flask in 7 ml of complete DMEM). After 16 hours incubation, cells in each flask with 80-90% confluence were infected by 50% of the primary transfection viral supernatant (i.e., 1.0 ml of viral lysate per flask). Usually at 4 days after infection, 50% of the infected cells were detached. Cells were rinsed off and transferred into a 50 ml tube. Cells were almost all GFP positive at this moment. Cells were centrifuged at 750 rpm for 5 min. All but 4 ml medium was removed. Pellets were resuspended by vortex. Four freeze-thaw-vortex cycles were performed to release adenovirus from cells.

(2) The second round of amplification

One day before infection, HEK293T cells were seeded in two 75-cm^2 tissue culture flasks (approximately 6×10^6 cells per flask in 15 ml of complete DMEM). After 16 hours incubation, cells with 90% confluence in each flask were infected by 2 ml of viral lysate. Four days after infection, 50% of the infected cells were detached. Cells were rinsed off and centrifuged. Pellets were resuspended in 8 ml of medium. Four freeze-thaw-vortex cycles were performed to release adenovirus from cells.

(3) The third round of amplification

Four 75-cm^2 tissue culture flasks of HEK293T cell were seeded. Cells in each flask were infected by 2 ml of viral lysate. Infected cells were resuspended in 16 ml of medium. Four freeze-thaw-vortex cycles were performed. Adenovirus-containing medium was allocated into 32 eppendorfs (500 μl each). These aliquots were stored at -80℃.

2.2.11.2 Titer assay

Two hundred thousand NIH3T3 cells per well were seeded in twelve wells of 6-well plate. Around 16 hours later, serial dilutions (twelve 10-fold dilutions) of adenovirus were prepared. They were used to infect NIH3T3 for 24 hours. GFP positive cells were counted on one of the twelve wells, which had one to ten evenly, distributed GFP positive cells.

Titer (CFU/ml) = number of GFP positive cells / (virus volume × replication factor)

$= 4 \text{ CFU} / (10^{-10} \text{ ml} \times 2)$

$= 2 \times 10^{10} \text{ CFU/ml}$

2.2.11.3 Adenovirus transduction

Two hundred thousand target cells, such as C6, were seeded in one well of a 6-well plate. Four million CFU diluted adenovirus in 3 ml of fresh medium was used to infect the cells. After 48 hours infection, cells were harvested for Western blot analysis.

CHAPTER 3: BRE attenuates apoptosis through maintaining the cellular level of an apoptotic inhibitor XIAP

3.1 Establishment of cell lines with BRE expression stably knocked down by shRNA

BRE is a death receptor-associated protein, which can attenuate extrinsic apoptosis initiated by activation of death receptors, TNFR-1 and Fas, and intrinsic apoptosis activated by DNA-damaging agents or by the potent protein kinase inhibitor, staurosporine (199, 212). In vivo anti-apoptotic function of BRE has been demonstrated by attenuation of Fas agonist antibody-induced acute fulminant hepatitis in transgenic mice over-expressing human BRE in the liver. Consistent with the common association of reduced apoptosis with tumorigenesis, protein level of BRE is up-regulated in human hepatocellular carcinoma (198). Transgenic mice with overexpression of human BRE in the liver showed significantly faster growth of diethylnitrosamine-induced liver tumors (216). Despite the functional characterization of BRE as an anti-apoptotic protein, and its implication in tumorigenesis, the molecular and biochemical mechanisms by which this protein inhibits mitochondrial apoptotic pathway remain completely unknown.

To begin addressing the above issues, we have recently generated D122 cell lines with BRE expression stably depleted by shRNA. These cell lines are named with the prefix ‘B07’. The negative control shRNA stable transfectant lines are named with the prefix ‘T8’. D122 is a mouse Lewis lung carcinoma cell line, which we have previously employed to study the effect of BRE overexpression on apoptosis, tumor growth, and metastasis (199, 215). As shown, the BRE expression in B07 cell lines (Figure 3-1, lane 2, 4, 6, 8) was efficiently knocked down. The BRE expression in the negative control cell lines T8 (Figure 3-1, lane 3, 5, 7, 9) was unaffected.

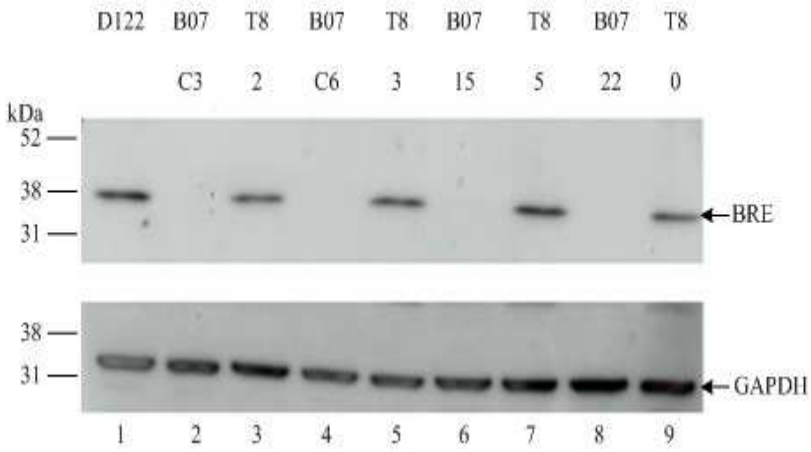

Figure 3-1. **Establishment of cell lines with BRE expression stably knocked down by shRNA.**

B07 (C3, C6, 15, 22) were independent lines of D122 with stable BRE shRNA transfection. T8 (0, 2, 3, 5) were independent lines of D122 with stable empty shRNA vector transfection as negative controls. The protein loading was visualized by the GAPDH. This experiment was performed in duplicate.

3.2 BRE-depleted cells are more sensitive to apoptosis

Decreased apoptotic response to TNF-α in the presence of cycloheximide and anti-Fas agonist antibody has been observed in Jurkat and HeLa cell lines upon ectopic expression of BRE. By contrary, siRNA-mediated depletion of BRE in HeLa rendered the cells more susceptible to the above TNF-α treatment (199). BRE overexpression could also lead to attenuation of intrinsic apoptosis induced by cycloheximide, 4-nitroquinoline-1-oxide, etoposide, and staurosporine (199).

In order to determine whether increased apoptotic response can be detected in the stable BRE-depleted cell lines B07 upon treatment with extrinsic and intrinsic apoptotic stimuli, B07 and E7, a subclone of B07, together with the parent cell D122 and negative shRNA control lines T8 were treated with TNF-α in the presence of cycloheximide (CHX) for extrinsic apoptosis, and etoposide for intrinsic apoptosis. When cells were subjected to apoptotic stimulation by TNF-α and CHX, the parent cell D122, negative control shRNA counterpart T8 showed apoptosis, as indicated by cleavage of PARP and caspase 3, starting from 9 hours of the treatment. Apoptosis of B07 and E7 started as early as 5 hours (Figure 3-2, A). When cells were subjected to apoptotic stimulation by etoposide, the parent cell D122, negative control shRNA counterpart T8 just began to show apoptosis at 16 hours of the treatment. In contrast, B07 and E7 already showed strong apoptosis at this time point (Figure 3-2, B).

Thus, the BRE-depleted cells are more sensitive to apoptosis induced by death receptor (Figure 3-2, A) and genotoxic stimulus (Figure 3-2, B) than the non-depleted counterparts, parent D122 and negative control shRNA transfectants. This result corroborates the previous finding that BRE is an anti-apoptotic protein for both the extrinsic and intrinsic pathways.

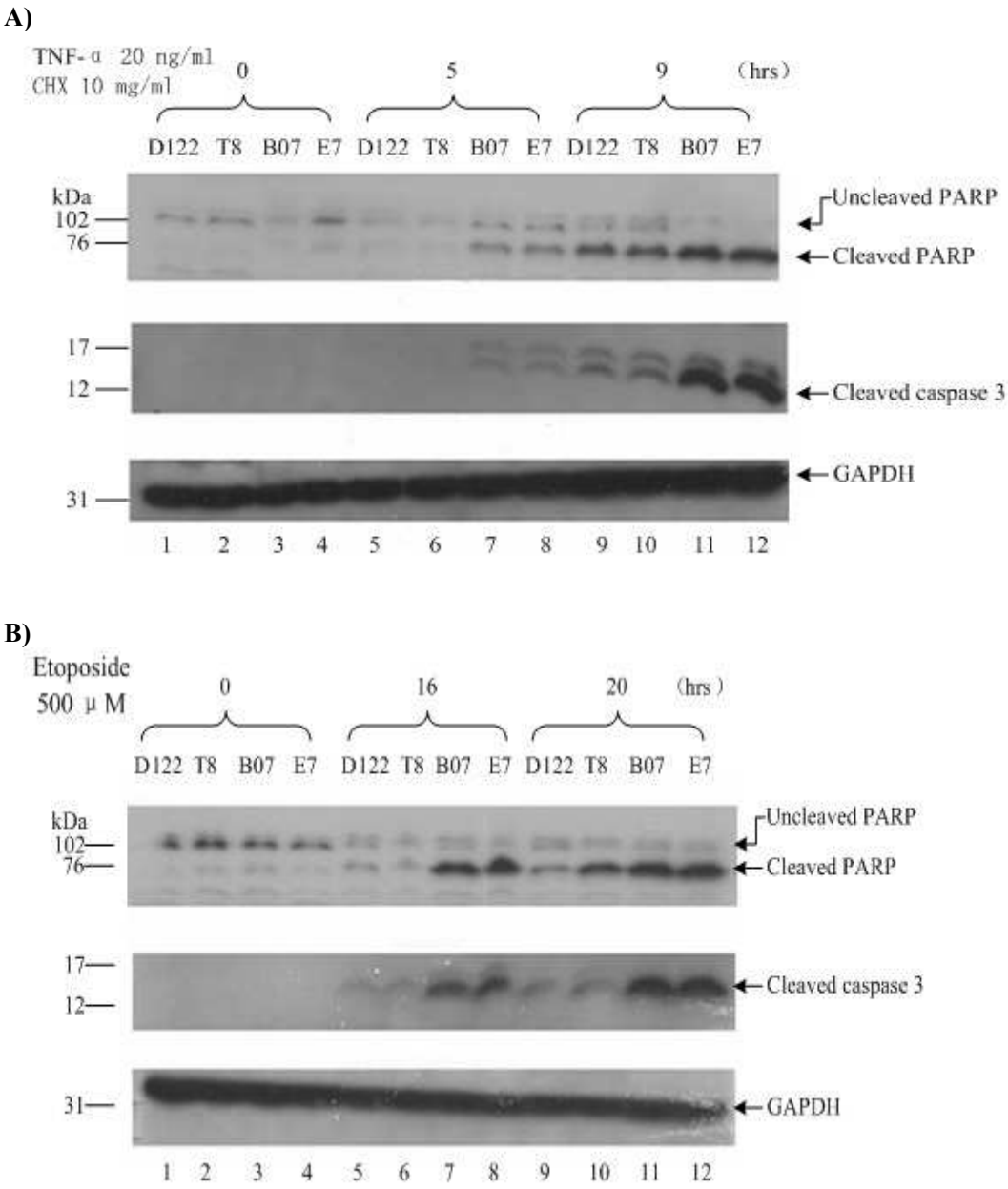

Figure 3-2. **BRE-depleted cells are more sensitive to apoptosis.**

BRE-depleted cells, B07 and E7, parent D122, and negative shRNA control line, T8, were treated with 20 ng/ml of TNF-α in the presence of 10 mg/ml of cycloheximide (CHX) (panel A), and 500 μM of etoposide (panel B), respectively. DMSO was used as solvent control. After the indicated time duration, cells were harvested for Western blot analysis. Apoptosis was indicated by the appearance of cleaved PARP and cleaved caspase 3. Protein loading was visualized by GAPDH. This experiment was performed in duplicate.

3.3 BRE-depleted cells are susceptible to TNF-α induced apoptosis in the absence of cycloheximide

In most cell types including D122, apoptotic induction by TNF-α requires concurrent inhibition of protein synthesis. This is because activation of TNFR-1 by its ligand TNF-α, triggers both pro- and anti-apoptotic signaling pathways, the latter of which functions by de novo synthesis of more of the anti-apoptotic proteins through NF-κB activation to counter the former (229). Cycloheximide (CHX) is a commonly used inhibitor of protein synthesis when TNF-α is used to induce apoptosis.

To determine whether the BRE-depleted cells are susceptible to TNF-α even in the absence of cycloheximide, the BRE-depleted cells B07 and E7 together with the parent cell D122 and negative shRNA control lines T8 were treated with TNF-α alone for the indicated time duration and then harvested for Western blot analysis of apoptosis. Apoptosis was found to occur to B07 and E7, but not the non-depleted cells, at 16 and 24 hours of the treatment (Figure 3-3). Flow cytometric analysis also revealed apoptosis of B07 but not T8 treated with TNF-α alone for 16 and 23 hours (Figure 3-4).

Both of the Western blot and flow cytometric analyses showed that the BRE-depleted cells are susceptible to TNF-α even in the absence of cycloheximide, indicating the absence of BRE has the same functional consequence as the presence of CHX in TNF-α-induced apoptosis, which is the inhibition of the up-regulation of anti-apoptotic proteins by TNFR1-activated NF-κB pathway. The next step was therefore to identify if there is any NF-κB-up-regulated anti-apoptotic proteins whose expression can be inhibited by BRE-depletion.

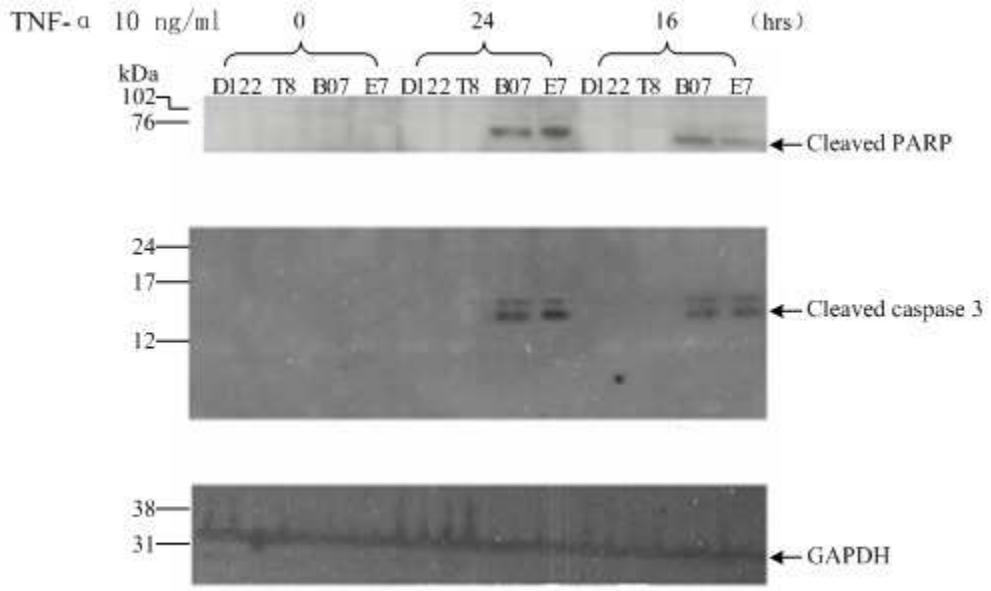

Figure 3-3. **BRE-depleted cells are susceptible to TNF-α induced apoptosis in the absence of cycloheximide (Western blot analysis).**

BRE-depleted cells, B07 and E7, parent D122 and negative shRNA control line, T8, were treated with 10 ng/ml of TNF-α in the absence of CHX. DMSO was used as solvent control. After the indicated time duration, cells were harvested for Western blot analysis. Apoptosis was indicated by the appearance of cleaved PARP and cleaved caspase 3. Protein loading was visualized by GAPDH. This experiment was performed in duplicate.

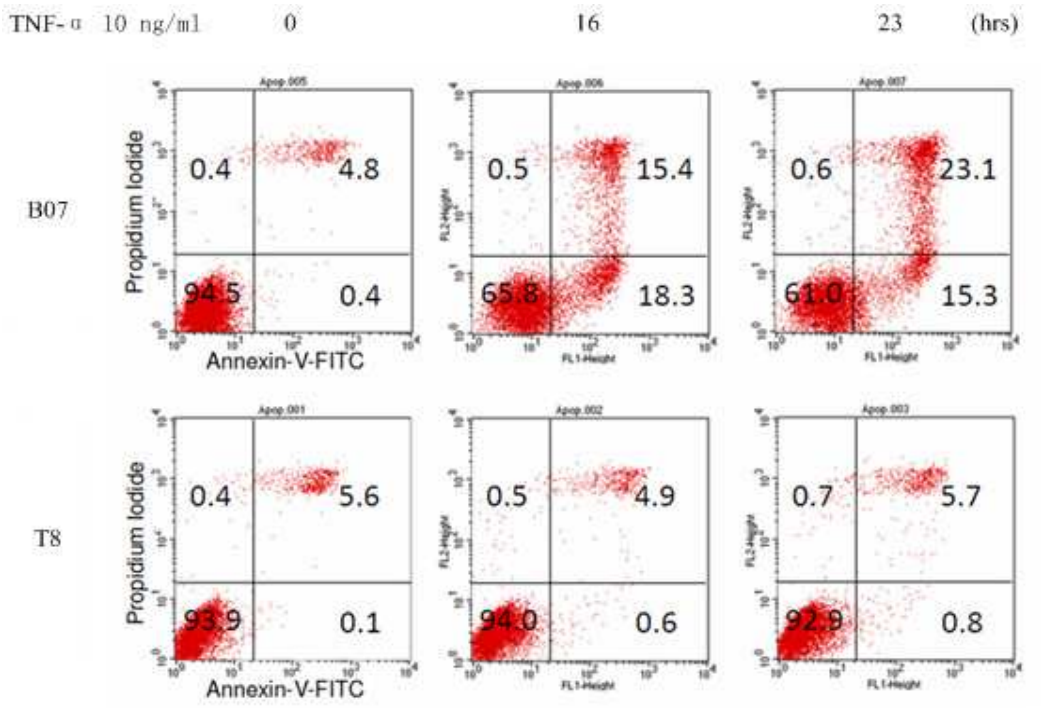

Figure 3-4. **BRE-depleted cells are susceptible to TNF-α induced apoptosis in the absence of cycloheximide (flow cytometric analysis).**

BRE-depleted cells B07 and negative shRNA control line, T8, were treated with 10 ng/ml of TNF-α in the absence of CHX. DMSO was used as solvent control. After the indicated time duration, cells were harvested for flow cytometric analysis using Annexin V-FITC and Propidium Iodide staining. Viable cells were indicated in lower left quadrant; apoptotic cells upper and lower right; necrotic cells upper left. This experiment was performed once.

3.4 Reduction of XIAP in BRE-depleted cells

The apoptotic susceptibility of the BRE-depleted cells to TNF-α alone suggests the absence of some of the anti-apoptotic proteins, which are up-regulated following NF-κB activation. We followed this lead to investigate the expression levels of four anti-apoptotic proteins, among others, known to be up-regulated following NF-κB activation, cIAP-1, cIAP-2, XIAP, and cFLIP (229, 230). Depletion of BRE had no effect on the protein levels of cIAP-1, cIAP-2, $cFLIP_L$, and $cFLIP_S$ (Figure 3-5, A). However, XIAP protein expression was remarkably reduced in the BRE-depleted cells (Figure 3-5, B).

XIAP is the most potent inhibitor of caspases of IAP family. In contrast to cIAP-1, cIAP-2, and cFLIP, which inhibit only the extrinsic apoptosis, XIAP inhibits the initiator caspase 9 of the intrinsic pathway, as well as effector caspase 3 and 7 common to both of the intrinsic and extrinsic pathways (231, 232). Thus, cells depleted of XIAP are expected to be sensitized to both of the death receptor ligands, and genotoxic stimuli. This finding fits well to the anti-apoptotic characteristics of BRE, which attenuates both the extrinsic and intrinsic apoptosis.

A)

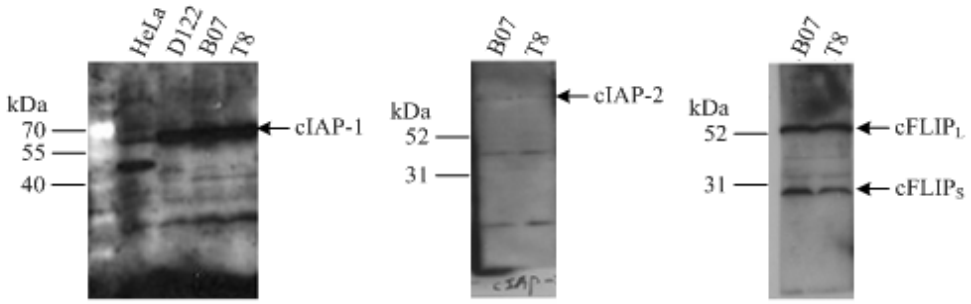

B)

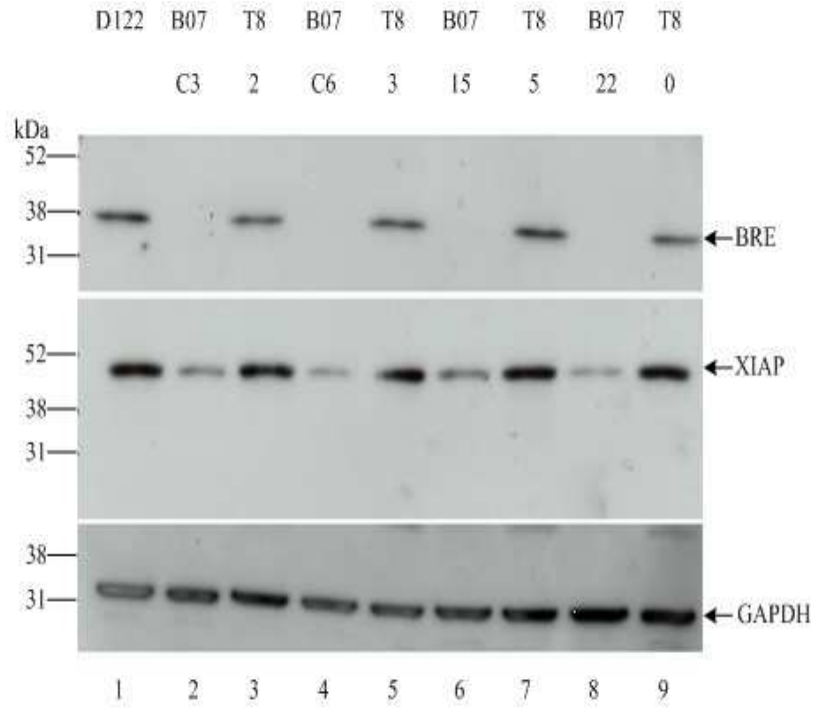

Figure 3-5. **Reduction of XIAP in BRE-depleted cells**

(A) Left panel: parent cell D122, BRE-depleted cells B07, negative control T8, together with anther cell line HeLa were lysed for Western blot analysis and probed by anti-cIAP-1 antibody. Middle panel: BRE-depleted cells B07 and negative control T8 were lysed for Western blot analysis and probed by anti-cIAP-2 antibody. Right panel: BRE-depleted cells B07 and negative control T8 were lysed for Western blot analysis and probed by anti-cFLIP antibody. This experiment was performed once.

(B) B07 (C3, C6, 15, 22) are independent lines of D122 with stable BRE shRNA transfection. T8 (0, 2, 3, 5) are independent lines of D122 with stable empty shRNA vector transfection as negative controls. These cells were lysed for Western blot analysis and probed by anti-BRE and anti-XIAP antibodies. The protein loading was visualized by GAPDH. This experiment was performed in duplicate.

3.5 Recovery of BRE restores XIAP in BRE-depleted cells

Taken the above data together, it is highly likely that I have already identified a molecular mechanism for the anti-apoptotic activity of BRE. I hypothesize that BRE through maintaining the cellular XIAP level attenuates apoptosis. To test the above hypothesis, BRE level was restored via the retrovirus infection in the stable BRE-depleted cell line, C6, which is one of B07 cell lines. In C6, the protein level of XIAP, as shown in Figure 3-5, B, was less than the parent cell lines D122. However, when the V5-tagged BRE was introduced into C6, via the retrovirus transduction, the XIAP level was also restored. The level of XIAP recovery was related to the level of BRE expression (Figure 3-6). Thus, it is confirmed that BRE has a critical role in maintaining the cellular XIAP level. Next, the issue of whether C6 cells with XIAP or BRE level restored showed increased resistance to apoptosis was tested.

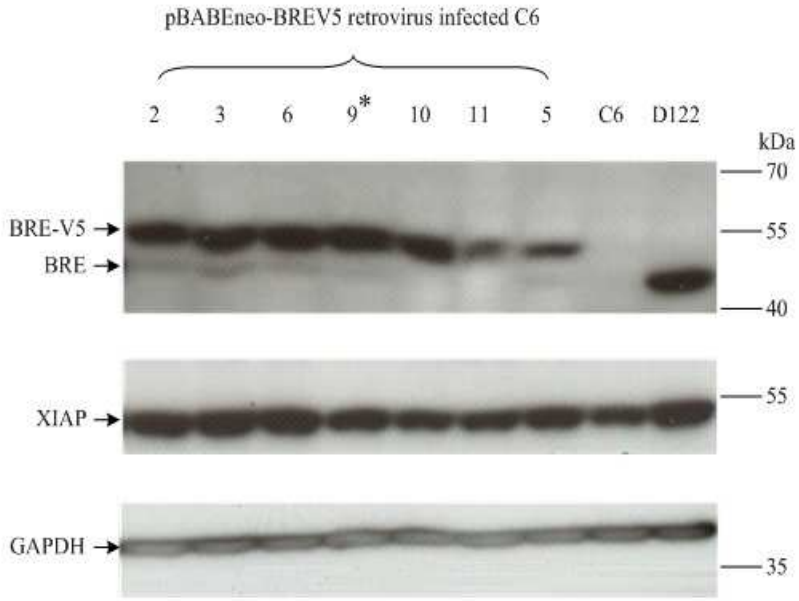

Figure 3-6. **Recovery of BRE restores XIAP in BRE-depleted cells.**
pBABEneo-BREV5 retroviruses were generated by the co-transfection of retroviral expression vector pBABEneo-BREV5 and the package vector pCL-Ampho to the package cell line HEK293T. The exogenous BRE was tagged by V5 at the C-terminus. The parent cell line was mouse Lewis lung carcinoma D122. C6 was a subclone of B07, which was the line of D122 with stable BRE shRNA transfection. Clone 2, 3, 6, 9, 10, 11, and 5 were independent lines of C6 with stable pBABEneo-BREV5 retrovirus infection, whose BRE level were restored at different levels. Clone 9 (asterisked) is unstable with ongoing apoptosis. Protein loading was visualized by GAPDH. This experiment was performed in duplicate.

3.6 Recovery of XIAP or BRE to BRE-depleted cells renders the cells less sensitive to TNF-α induced apoptosis

C6 cells with XIAP or BRE level restored were subjected to apoptotic stimulation by TNF-α. While the C6 with empty vector pcDNA3 transfection, showed apoptosis, as indicated by cleavage of PARP, starting from 3 hours of TNF-α treatment, apoptosis of the XIAP-transfected C6 cells was delayed (Figure 3-7). Similarly, C6 without BRE restoration, showed apoptosis, as indicated by cleavage of PARP, starting from 3 hours of TNF-α treatment, apoptosis of the BRE-restored counterpart was significantly attenuated (Figure 3-8). Taken together, the BRE-depleted cells with BRE level or XIAP level restored are less sensitive to the TNF-α treatment than the BRE-depleted cells.

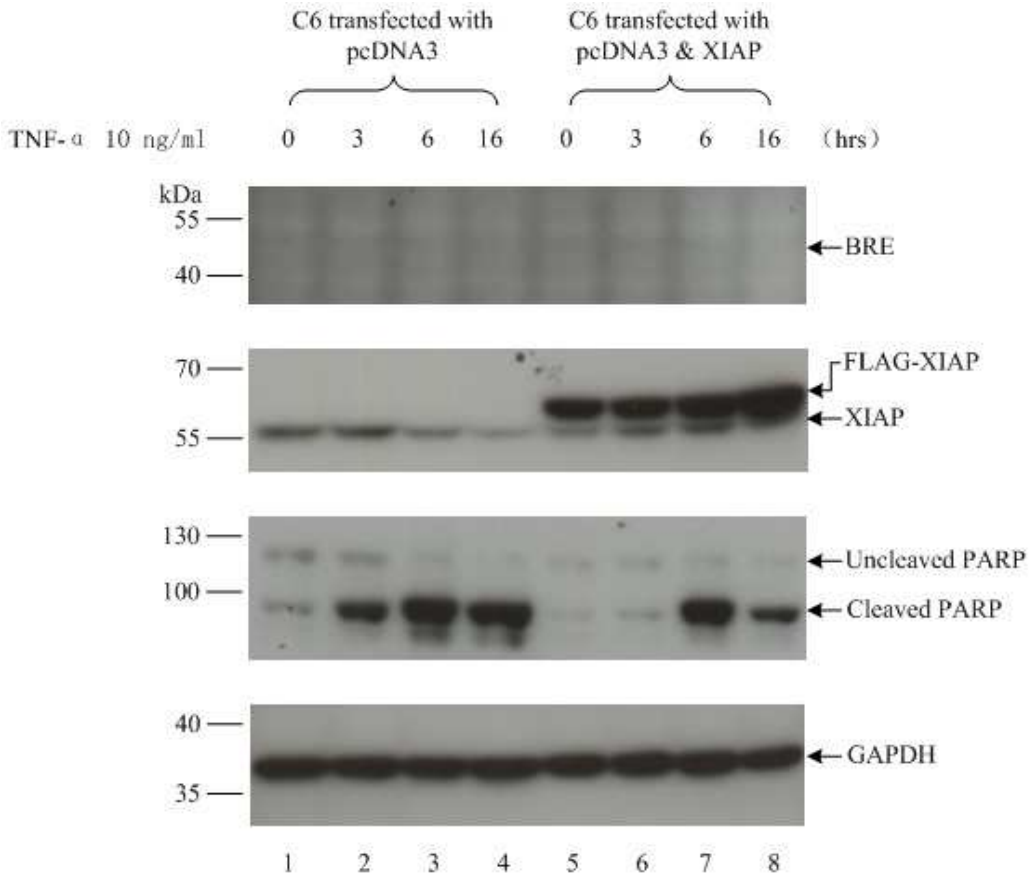

Figure 3-7. **Recovery of XIAP to BRE-depleted cells renders the cells less sensitive to TNF-α induced apoptosis.**

C6, an independent line of BRE-depleted cells B07, were transfected with the pEBB-FLAG-XIAP & pcDNA3, or pcDNA3 alone. In pEBB-FLAG-XIAP, the exogenous XIAP was tagged by FLAG. The pcDNA3 alone transfected cells were used as negative control. Forty-eight hours after transfection, the culture mediums of the cells were changed to fresh mediums containing 10 ng/ml of TNF-α. DMSO was used as solvent control. After the indicated time duration, cells were harvested for Western blot analysis. Since C6 is a stable BRE-depleted cell line, the endogenous BRE of could not be detected by our anti-BRE antibody. When C6 was transfected with pEBB-FLAG-XIAP & pcDNA3, both the FLAG-tagged and endogenous XIAP could be detected by the anti-XIAP antibody (lane 5-8). Apoptosis was indicated by the appearance of cleaved PARP. Protein loading was visualized by GAPDH. This experiment was performed once.

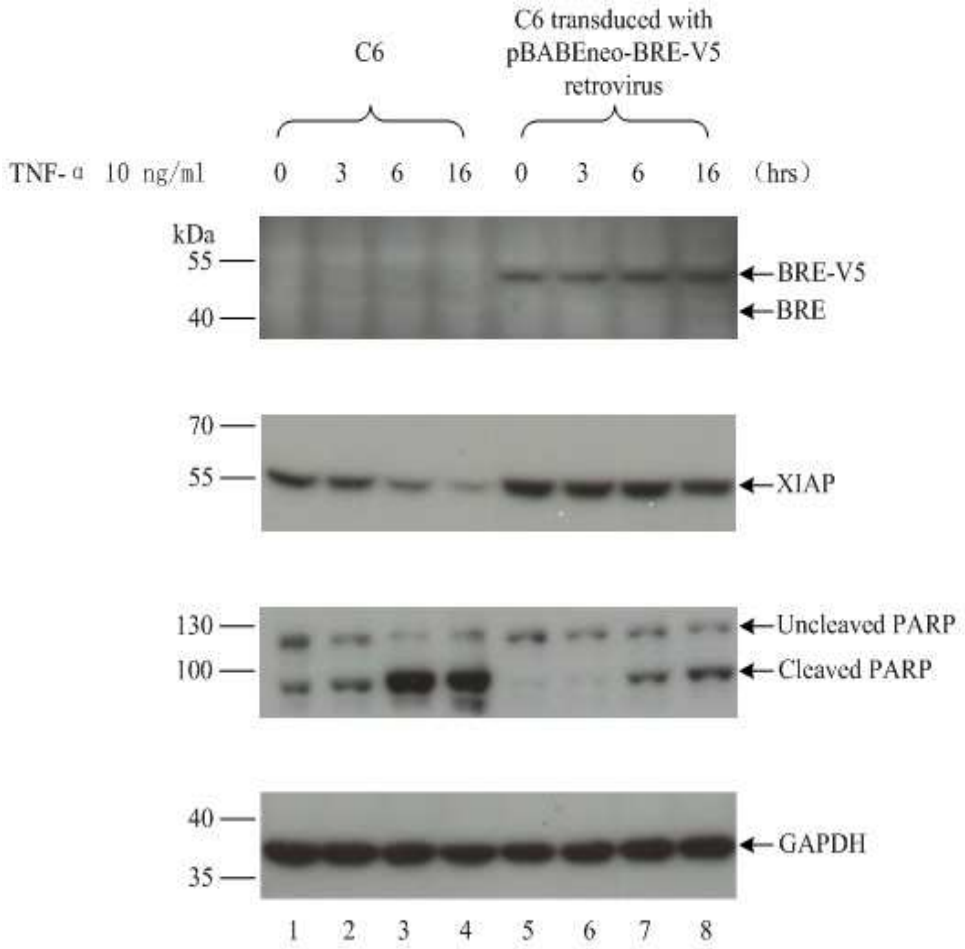

Figure 3-8. **Recovery of BRE to BRE-depleted cells renders the cells less sensitive to TNF-α induced apoptosis.**

C6, an independent line of BRE-depleted cells B07, was transduced with pBABEneo-BREV5 retrovirus for restoration of BRE and treated with 10 ng/ml of TNF-α. DMSO was used as solvent control. After the indicated time duration, cells were harvested for Western blot analysis for apoptosis to compare with un-transduced C6 treated likewise. Apoptosis was indicated by the appearance of cleaved PARP. Protein loading was visualized by GAPDH. This experiment was performed once.

3.7 N-Ethylmaleimide (NEM) affects BRE and XIAP

3.7.1 NEM affects BRE staining by anti-BRE (Mab489-7) antibody

Our team generated the first 2 monoclonal antibodies to BRE, Mab489-7 (IgG1) and Mab246 (IgG3). Mab489-7 performs better in Western blotting compared with Mab246, whereas Mab246 does better in immunohistochemistry and immunoprecipitation (198). I observed that when GSB2 cells, Jurkat A3 with stable GS-BRE (V5-tagged) transfection (199), were lysed in buffer containing 20 mM of NEM, both the endogenous and V5-tagged BRE could not be detected by Mab489-7 (Figure 3-9, lane 1). However, the endogenous and V5-tagged BRE in the same lysate remained detectable by Mab246. The use of anti-V5 antibody also detected the V5-tagged BRE. These observations indicate that NEM abolished the binding between BRE and Mab489-7, but not BRE protein level. It should be noted that both Mab489-7 and Mab246 were generated by using a human BRE protein fragment from residues 40 to 225 as the immunogen (198). This peptide contains five cysteine residues, which NEM can irreversibly bind through formation of a strong thioester bond, resulting in changes of local structure. Mab489-7, but not Mab246, may bind to the NEM-sensitive epitope, which contains or is proximal to cysteine. Next, because of the association between BRE and XIAP stability found above, I investigated whether XIAP level in the lysate containing NEM would be affected.

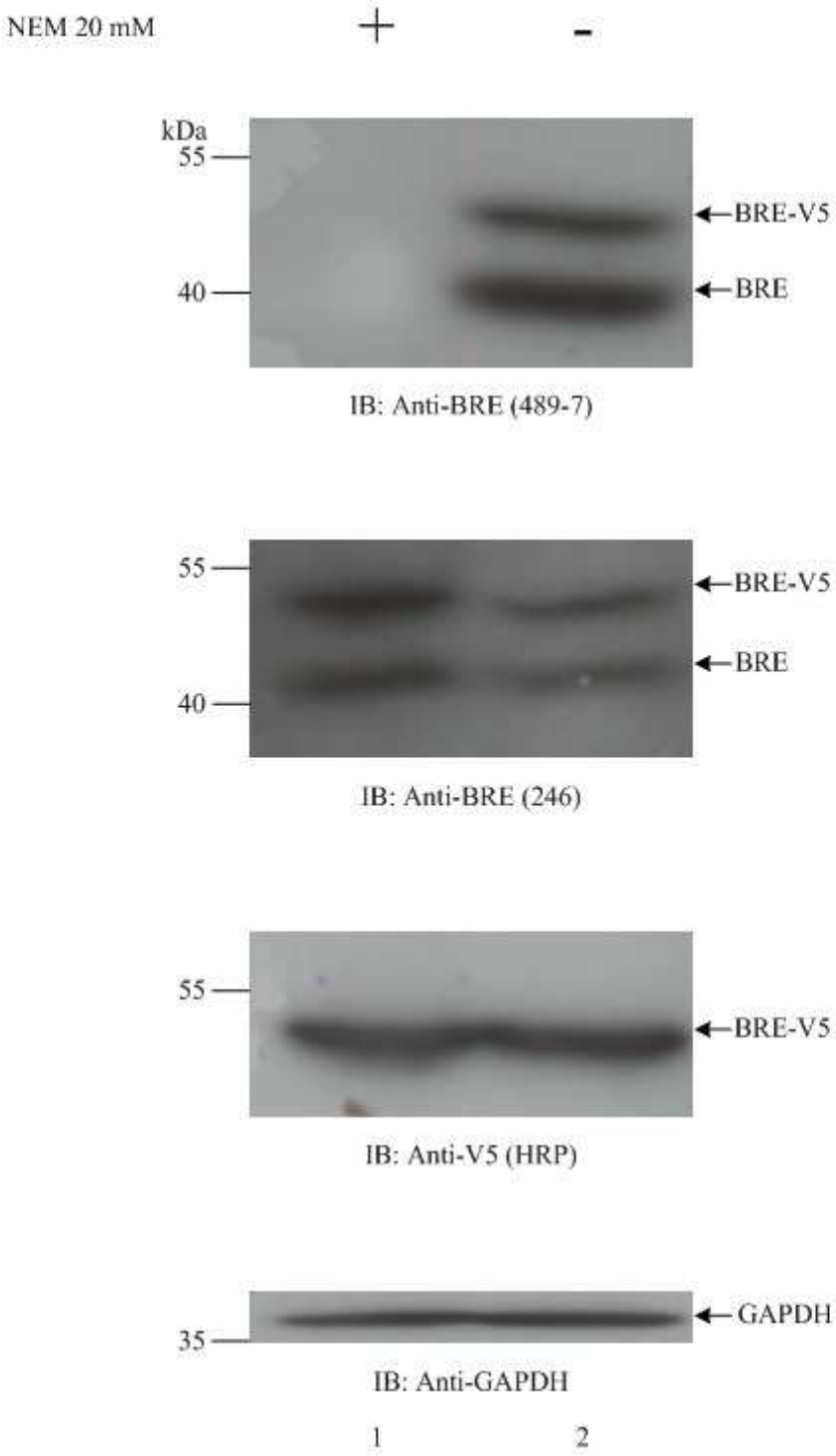

Figure 3-9. **NEM affects BRE staining by anti-BRE (Mab489-7) antibody.**

The cells were GSB2 (Jurkat A3 with stable GS-BRE transfection), expressing both of the endogenous BRE and exogenous BRE tagged by V5 at the C-terminus. Two types of fresh lysis buffer with or without 20 mM of NEM were used to lyse the cells. The lysates were probed by anti-BRE (Mab489-7), anti-BRE (Mab246), HRP-anti-V5, and anti-GAPDH antibodies. This experiment was performed in triplicate.

3.7.2 NEM affects XIAP

In this set of experiments, cell lysates were first prepared with lysis buffer containing no NEM, which was subsequently added to the cell lysates. Again, recognition of BRE by anti-BRE antibody (Mab489-7) was reduced (Figure 3-10, lane 3-5). Furthermore, XIAP level in the cell lysate, immunoblotted by anti-XIAP antibody, was also reduced. This could be caused by reduced binding of the anti-XIAP antibody to XIAP, or reduction of XIAP level.

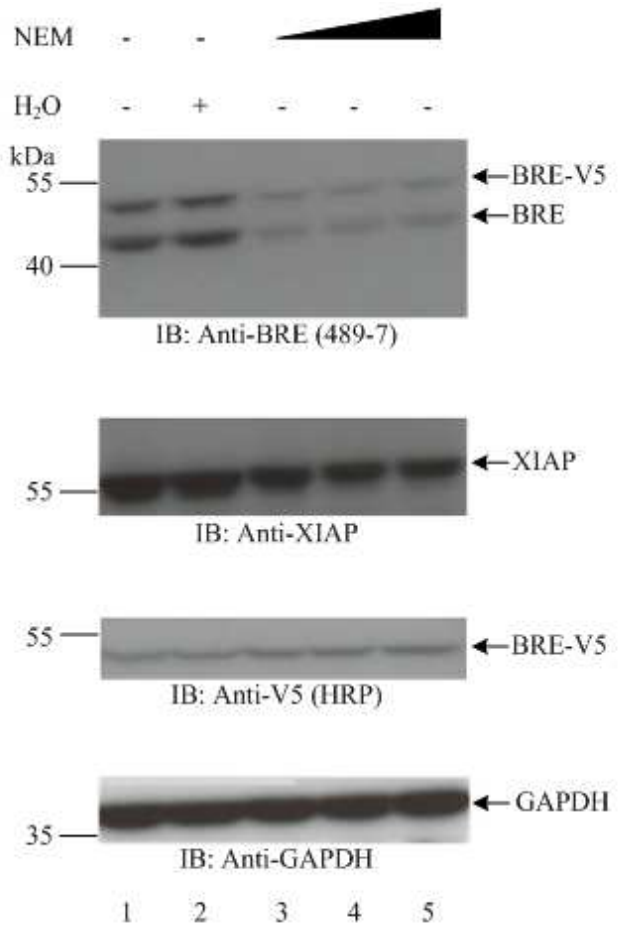

Figure 3-10. **NEM affects XIAP.**

The cells were GSB2 (Jurkat A3 with stable GS-BRE transfection), expressing both of the endogenous BRE and exogenous BRE tagged by V5 at the C-terminus. These cells were lysed in the routine lysis buffer first. The same amount of protein (5 μg) was allocated to five eppendorfs. NEM was added into three eppendorfs, making the concentration to be 20 mM, 39 mM, and 50 mM (lane 3-5). H_2O was added as solvent control (lane 2). Eppendorf with nothing added into it was negative control (lane 1). They were probed by anti-BRE (Mab489-7), HRP-anti-V5, anti-XIAP, and anti-GAPDH antibodies. This experiment was performed in duplicate.

3.7.3 NEM reduces XIAP instead of antibody-binding failure

NEM was added to the lysate of HEK293T transfected with pEBB-FLAG-XIAP. As expected, this reduced the immunoblot staining signal by Mab489-7, as well as anti-XIAP antibody. Of note is that the staining signal by anti-FLAG antibody was also reduced (Figure 3-11 lane 2, 3). As the amino acid sequence of FLAG epitope, which is DYKDDDDK, contains no cysteine. I conclude that the XIAP level in the cell lysate with added NEM was reduced. Since the BRE level in the NEM-containing cell lysate remained unchanged, I further propose that the cysteine residues of BRE may be involved in maintaining XIAP stability.

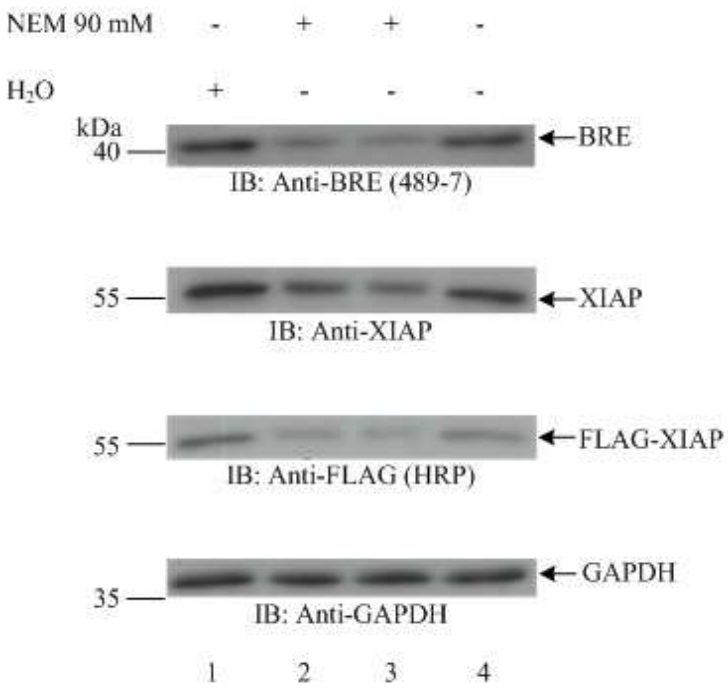

Figure 3-11. **NEM reduces XIAP instead of antibody-binding failure.**
HEK293T cells were transfected with the pEBB-FLAG-XIAP. In the pEBB-FLAG-XIAP, the exogenous XIAP was tagged by FLAG. Forty-eight hours after transfection, these cells were lysed in the routine lysis buffer first. The same amount of protein (5 μg) was allocated to four eppendorfs. NEM was added into two eppendorfs, making the concentration to be 90 mM (lane 2, 3). H_2O was added as solvent control (lane 1). Eppendorf with nothing added into it was negative control (lane 4). They were probed by anti-BRE (Mab489-7), HRP-anti-FLAG, anti-XIAP, and anti-GAPDH antibodies. This experiment was performed once.

3.8 Ubiquitination of XIAP is important for its stability

3.8.1 VAD cannot preserve XIAP upon 16 hours of etoposide treatment

From the above data, BRE can maintain cellular level of the anti-apoptotic protein XIAP. However, the mechanism is unknown. This set of experiments was carried out to identify the mechanism. The cell line used was GSV1 (Jurkat A3 with stable empty vector pcDNA3.1/GS transfection). GSV1 cells were treated with etoposide (intrinsic apoptosis stimulus), and with or without VAD (the broad-spectrum caspase inhibitor) for the indicated time duration. Upon 16 hours of etoposide treatment, the cellular XIAP was decreased to a barely detectable level. Inclusion of VAD inhibited the caspase-induced cleavage efficiently, as shown by the persistence of un-cleaved PARP during apoptotic stimulation. XIAP is known to be cleaved by caspases, which was observed in this experiment. However, inclusion of VAD cannot preserve XIAP upon 16 hours of etoposide treatment (Figure 3-12 lane 1, 2). This paradox indicates that some other mechanisms, such as the proteasome-mediated degradation, may cause degradation of XIAP during apoptosis.

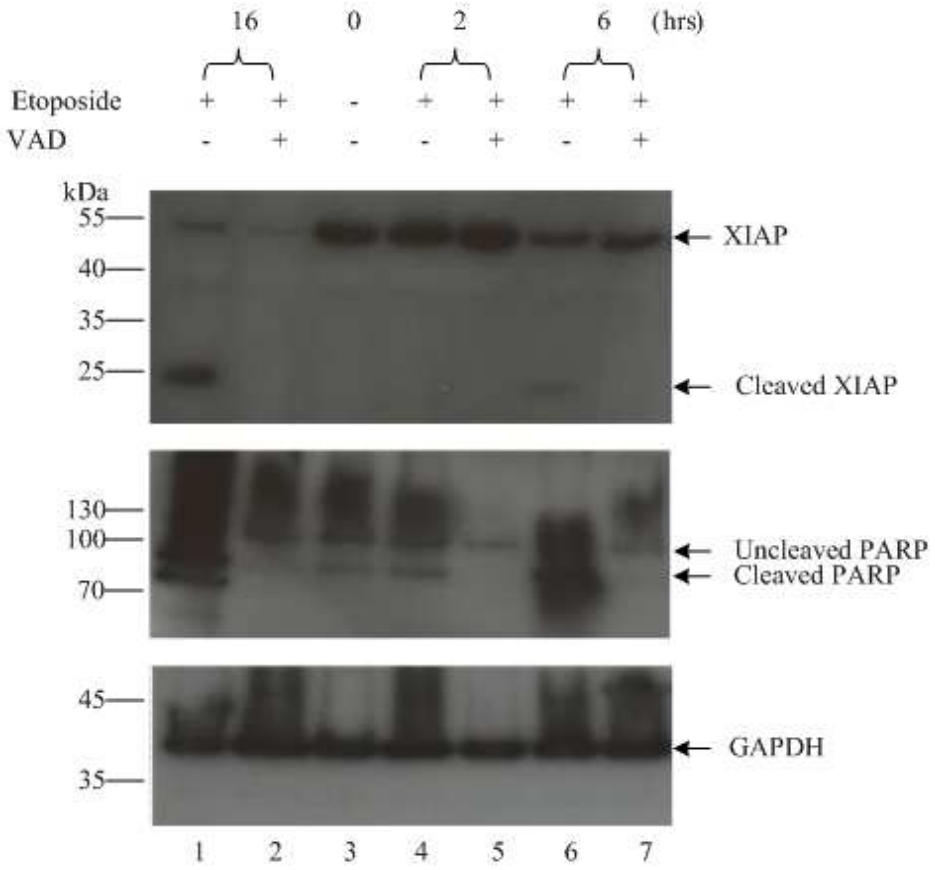

Figure 3-12. **VAD cannot preserve XIAP upon 16 hours of etoposide treatment.** GSV1 cells (Jurkat A3 with stable empty vector pcDNA3.1/GS transfection) were treated with 25 μM of etoposide (intrinsic apoptosis stimulus), and with or without 20 μM of VAD (the broad-spectrum caspase inhibitor) for the indicated time duration. DMSO treated cells were the negative control. After the indicated time duration, cells were harvested for Western blot analysis. Both of the full length XIAP and XIAP fragment cleaved by caspases were probed by anti-XIAP antibody. Apoptosis was indicated by the appearance of cleaved PARP. Protein loading was visualized by GAPDH. This experiment was performed in duplicate.

3.8.2 Degradation of XIAP in response to etoposide in the presence of VAD is due to proteasomal degradation

This experiment was carried out to determine whether the degradation of XIAP during apoptosis was caused by proteasome-mediated degradation. Cells of GSV1 were treated with MG132 (proteasome inhibitor) alone, etoposide alone, etoposide & MG132, etoposide & VAD, MG132 & VAD, or etoposide & MG132 & VAD for 16 hours. Inclusion of VAD cannot preserve XIAP upon 16 hours of etoposide treatment (Figure 3-13 lane 4), whereas MG132 can completely rescue XIAP in the presence of VAD (Figure 3-13 lane 6), indicating that the degradation of XIAP in response to etoposide in the presence of VAD is due to proteasomal degradation. Only the ubiquitin chains labeled proteins can be destroyed via proteasome. Thus, the ubiquitination of XIAP is important for its stability.

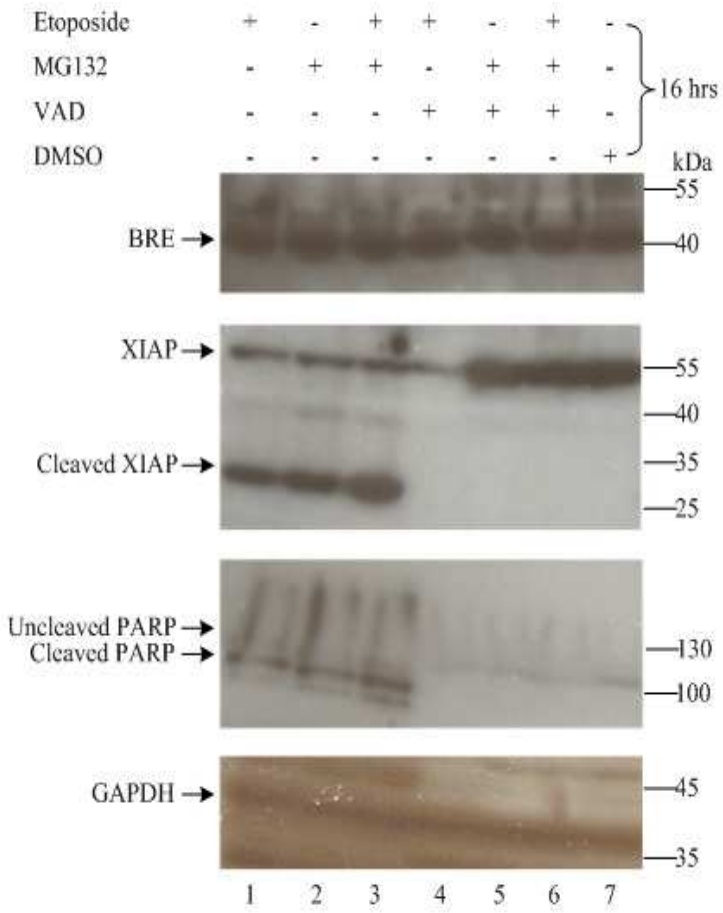

Figure 3-13. **Degradation of XIAP in response to etoposide in the presence of VAD is due to proteasomal degradation.**

GSV1 cells (Jurkat A3 with stable empty vector pcDNA3.1/GS transfection) were treated with MG132 alone, etoposide alone, etoposide & MG132, etoposide & VAD, MG132 & VAD, or etoposide & MG132 & VAD for 16 hours. The concentrations of etoposide, MG132, and VAD were 25 μM, 5 μM, and 30 μM. DMSO treated cells were negative control. After 16 hours duration, cells were harvested for Western blot analysis. Both of the full length XIAP and XIAP fragment cleaved by caspases were probed by anti-XIAP antibody. Apoptosis was indicated by the appearance of cleaved PARP. Protein loading was visualized by GAPDH. This experiment was performed once.

3.9 BRE leads to the removal of or inhibits ubiquitination of XIAP

3.9.1 Immunoprecipitation of ubiquitinated XIAP

BRE has two UEV domains, which are ubiquitin-binding domains. BRE was found to bind to K48- and K63-linked polyubiquitin chains in vitro assay (194). According to the above-mentioned result, ubiquitination of XIAP is important for its stability. Thus, I hypothesize that BRE maintains the cellular XIAP level by affecting the ubiquitination process of XIAP. There are two issues need to be solved: (1) Can BRE affect the ubiquitination of XIAP? (2) What type of ubiquitination (K48-, K63-, or K0-linked) of XIAP can be affected by BRE?

To start, I established a specific and effective system to immunoprecipitate the ubiquitinated XIAP. Two immunoprecipitation experiments were carried out. In experiment 1 (Figure 3-14), plasmids pEBB-FLAG-XIAP with or without pRK5-HA-Ubiquitin-K48 were transfected to HEK293T. In experiment 2 (Figure 3-15), plasmids pRK5-HA-Ubiquitin-K48 with or without pEBB-FLAG-XIAP were transfected to HEK293T. pRK5-HA-Ubiquitin-K48 is an expression vector containing K48-only ubiquitin with all of the other lysines mutated to arginines. Therefore, such mutant can only form poly-ubiquitin chains via K48. In these two experiments, exogenous K48-linked polyubiquitinated XIAP, immunoprecipitated by anti-FLAG antibody and probed by HRP-anti-HA antibody, only appeared in cells with pEBB-FLAG-XIAP and pRK5-HA-Ubiquitin-K48 co-transfection. Taken together, overexpressed XIAP undergoes K48-linked polyubiquitination. This immunoprecipitation system is specific and effective to immunoprecipitate ubiquitinated XIAP. Thus, this system was used in all of the later immunoprecipitation experiments.

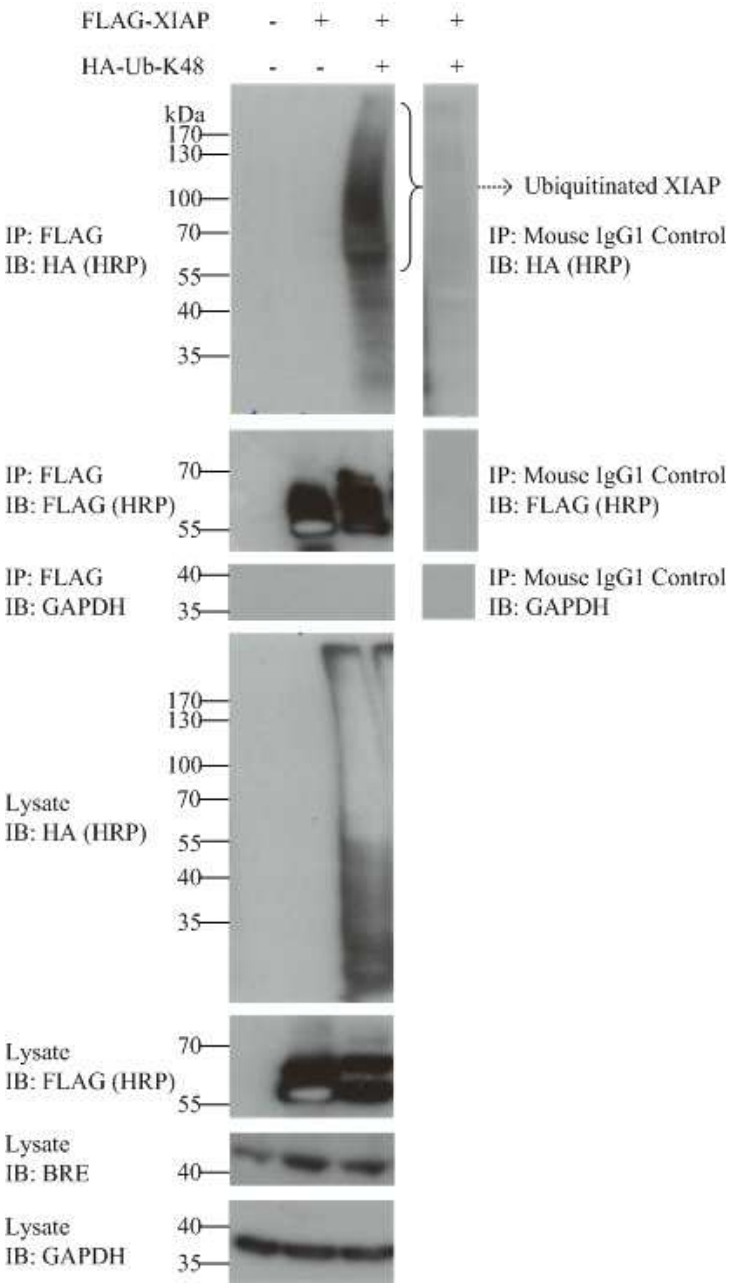

Figure 3-14. **Immunoprecipitation of ubiquitinated XIAP, experiment 1**

HEK293T cells were transfected with pEBB-FLAG-XIAP with or without pRK5-HA-Ubiquitin-K48. HEK293T cells without any transfection were used as negative control. Forty-eight hours after transfection, cells were harvested for immunoprecipitation. Anti-FLAG antibody (F3165, Sigma) was used to pull down FLAG-tagged XIAP. Anti-Mouse (G3A1) IgG1 Isotype Control (#5415S, Cell Signaling) was used as negative control. Immunoprecipitated samples together with the whole lysate were probed by HRP-anti-FLAG (A8592, Sigma), HRP-anti-HA (H6533, Sigma), and anti-GAPDH antibodies. Lysate was also probed by anti-BRE antibody. This experiment was performed once.

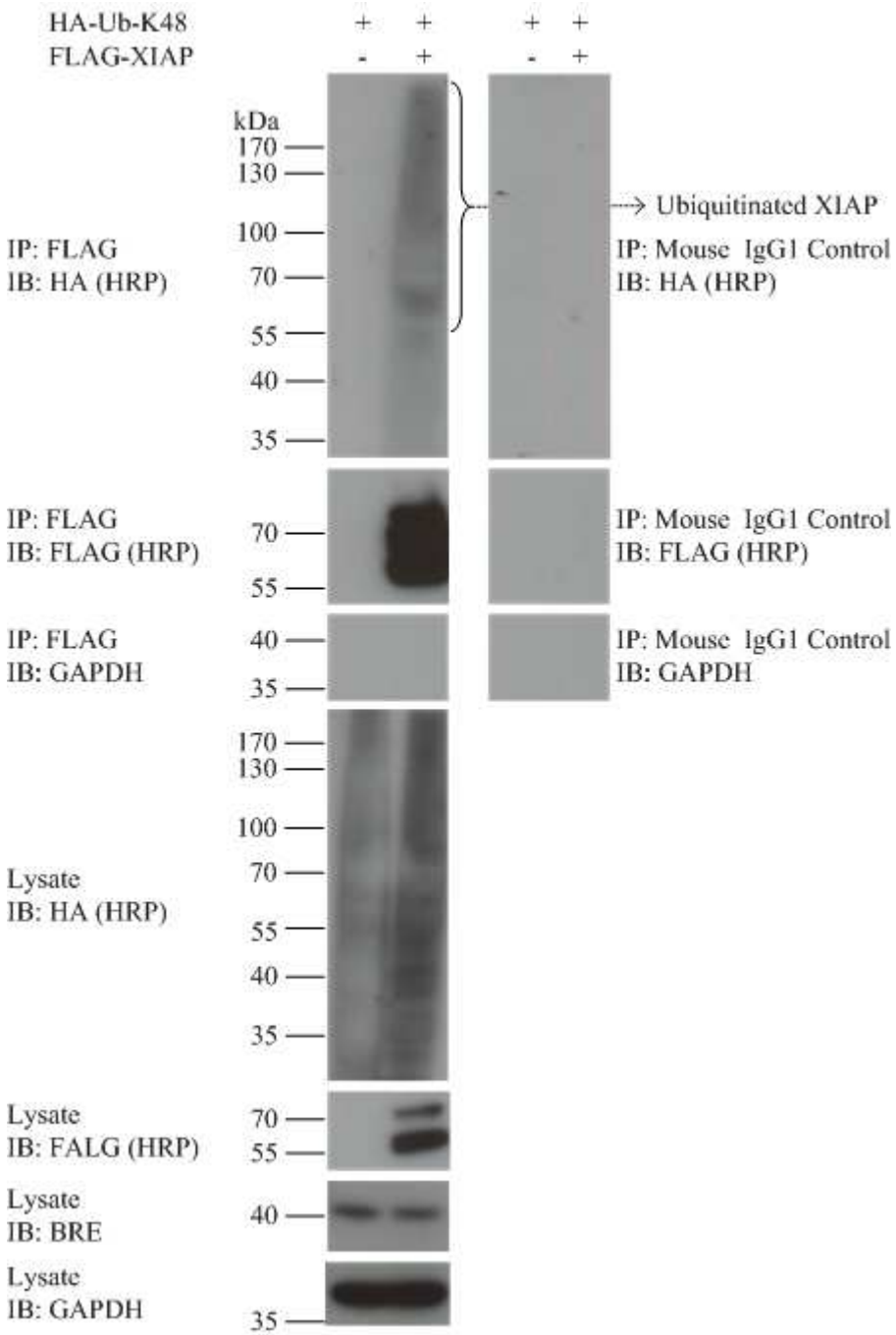

Figure 3-15. **Immunoprecipitation of ubiquitinated XIAP, experiment 2**

HEK293T cells were transfected with pRK5-HA-Ubiquitin-K48 with or without pEBB-FLAG-XIAP. HEK293T cells without any transfection were used as negative control. The later steps were the same with immunoprecipitation of ubiquitinated XIAP, experiment 1. This experiment was performed once.

3.9.2 BRE leads to the removal of or inhibits endogenous ubiquitination of XIAP

This experiment was carried out to identify whether BRE affects ubiquitination of XIAP. Plasmids pEBB-FLAG-XIAP with or without pEBB-FLAG-BRE were transfected to HEK293T. Ubiquitinated XIAP, pulled down by anti-XIAP antibody, was probed by biotinylated anti-XIAP and anti-ubiquitin antibodies. As shown, the biotinylated anti-XIAP antibody was more sensitive than anti-ubiquitin antibody to detect polyubiquitin of XIAP. Of note, the ubiquitinated XIAP formed smear was less when BRE was included. This difference was more obvious when biotinylated XIAP was used for probe (Figure 3-16). This data indicates that BRE leads to the removal of or inhibits ubiquitination of XIAP. Thus, the next question is what type of ubiquitination (K48-, K63-, or K0-linked) of XIAP can be affected by BRE.

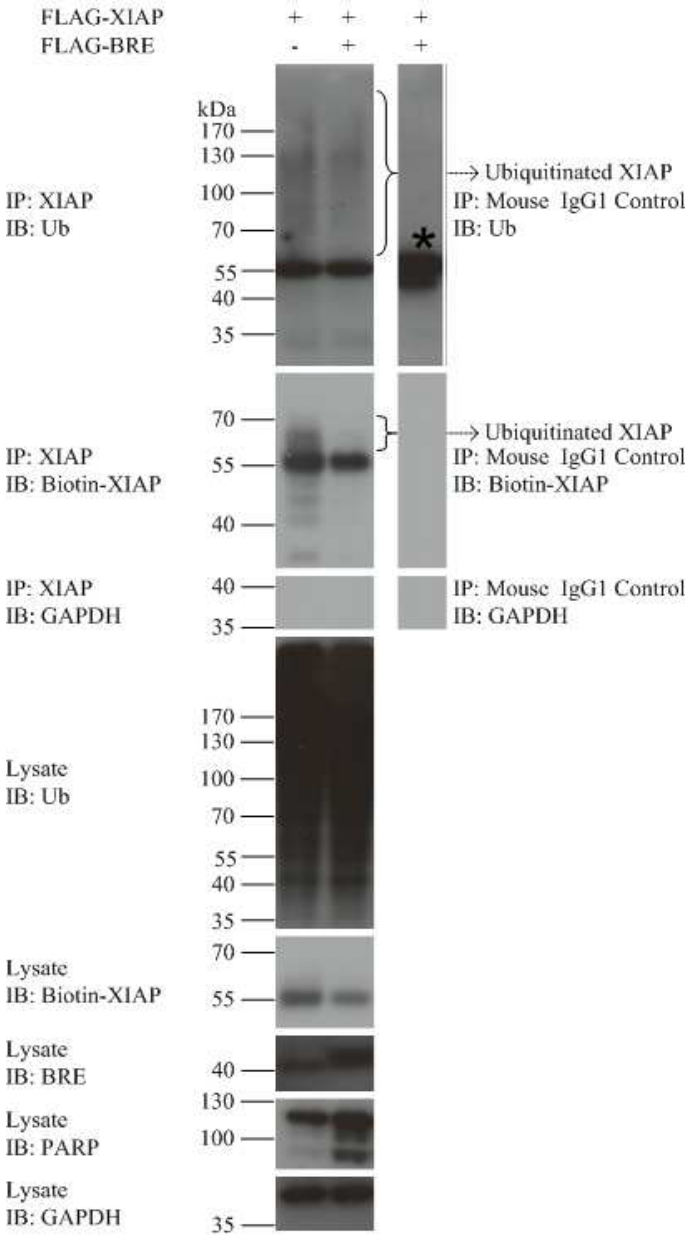

Figure 3-16. **BRE leads to the removal of or inhibits endogenous ubiquitination of XIAP.** HEK293T cells were transfected with pEBB-FLAG-XIAP with or without pEBB-FLAG-BRE. Forty-eight hours after transfection, culture medium was changed into fresh medium containing 5 μM of MG132. Two hours later, cells were harvested for immunoprecipitation. Anti-XIAP antibody (610717, BD) was used to pull down endogenous and exogenous XIAP. Anti-Mouse (G3A1) IgG1 Isotype Control (#5415S, Cell Signaling) was used as negative control. Immunoprecipitated samples together with the whole lysate were probed by biotinylated anti-XIAP (BAF8221, R&D), anti-ubiquitin (550944, BD), and anti-GAPDH antibodies. Lysate was also probed by anti-BRE and anti-PARP antibodies. The asterisked band around 55 kDa was heavy chains of anti-Mouse (G3A1) IgG1 Isotype Control. This experiment was performed once.

3.9.3 BRE does not affect exogenous K48-linked ubiquitination of XIAP

To explore the type of ubiquitination (K48-, K63-, or K0-linked) of XIAP that can be affected by BRE, the major K48-linked polyubiquitination, which labels proteins for degradation by proteasome, was investigated first. Plasmids pEBB-FLAG-XIAP and pRK5-HA-Ubiquitin-K48, with or without pEBB-FLAG-BRE were transfected to HEK293T. pRK5-HA-Ubiquitin-K48 is an expression vector containing K48-only ubiquitin with all of the other lysines mutated to arginines. Therefore, such mutant can only form poly-ubiquitin chains via K48. Exogenous K48-linked ubiquitinated XIAP, pulled down by anti-XIAP antibody, was probed by biotinylated anti-XIAP and HRP-anti-HA antibodies. Of note, the K48-linked ubiquitination of XIAP was the same regardless of co-transfection with BRE or not (Figure 3-17). Thus, although BRE can bind to K48-linked polyubiquitin chains in vitro, it does not affect the exogenous K48-linked ubiquitination of XIAP.

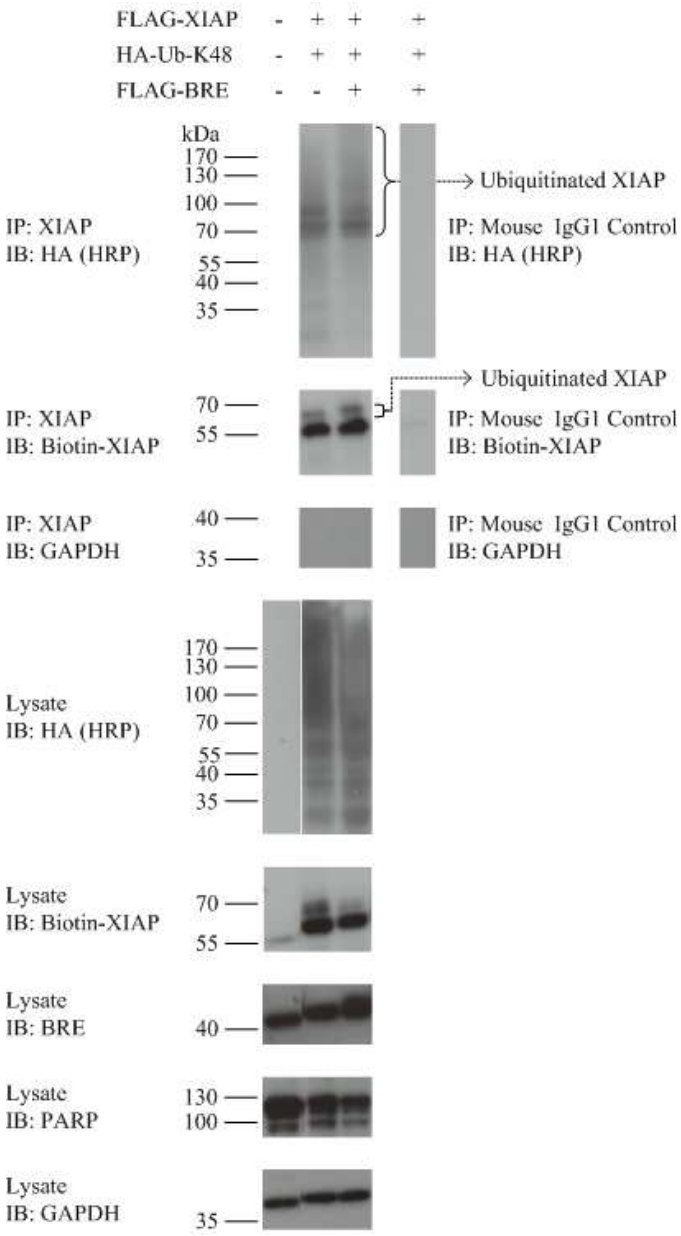

Figure 3-17. **BRE does not affect exogenous K48-linked ubiquitination of XIAP.** HEK293T cells were transfected with pEBB-FLAG-XIAP and pRK5-HA-Ubiquitin-K48, with or without pEBB-FLAG-BRE. HEK293T cells without any transfection were negative control. Forty-eight hours after transfection, culture medium was changed into fresh medium containing 5 μM of MG132. Four hours later, cells were harvested for immunoprecipitation. Anti-XIAP antibody (610717, BD) was used to pull down endogenous and exogenous XIAP. Anti-Mouse (G3A1) IgG1 Isotype Control (#5415S, Cell Signaling) was used as negative control. Immunoprecipitated samples together with the whole lysate were probed by biotinylated anti-XIAP (BAF8221, R&D), HRP-anti-HA (H6533, Sigma), and anti-GAPDH antibodies. Lysate was also probed by anti-BRE and anti-PARP antibodies. This experiment was performed in duplicate.

3.9.4 BRE does not affect exogenous K63-linked ubiquitination of XIAP

BRE can also bind K63-linked polyubiquitin chain in vitro (194), so this type of ubiquitin chain for XIAP was investigated next. Plasmids pEBB-FLAG-XIAP and pRK5-HA-Ubiquitin-K63, with or without pEBB-FLAG-BRE were transfected to HEK293T. pRK5-HA-Ubiquitin-K63 is an expression vector containing K63-only ubiquitin with all of the other lysines mutated to arginines. Therefore, such mutant can only form poly-ubiquitin chains via K63. Exogenous K63-linked ubiquitinated XIAP, pulled down by anti-XIAP antibody, was probed by both of biotinylated anti-XIAP and HRP-anti-HA antibodies. Of note, as with the K48-linked ubiquitination, K63-linked ubiquitination of XIAP was not affected by co-transfection with BRE (Figure 3-18). Thus, although BRE can bind to K63-linked polyubiquitin chains in vitro, it does not affect the K63-linked ubiquitination of XIAP.

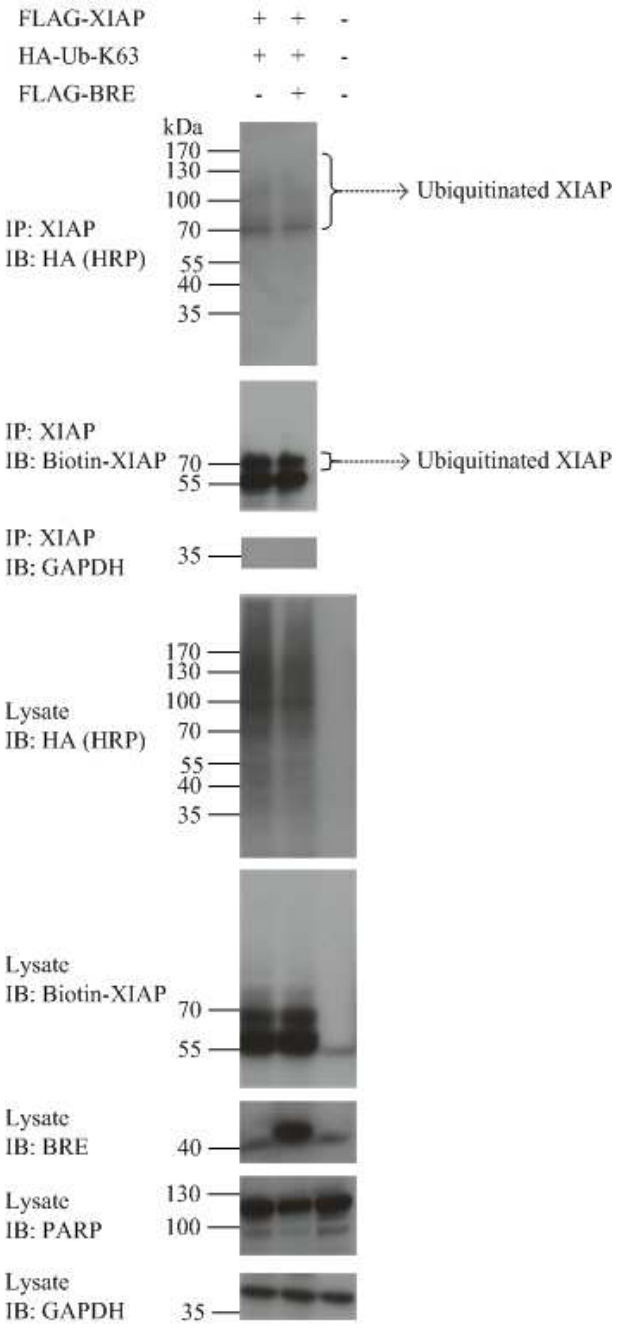

Figure 3-18. **BRE does not affect exogenous K63-linked ubiquitination of XIAP.** HEK293T cells were transfected with pEBB-FLAG-XIAP and pRK5-HA-Ubiquitin-K63, with or without pEBB-FLAG-BRE. HEK293T cells without any transfection were negative control. Forty-eight hours after transfection, culture medium was changed into fresh medium containing 5 μM of MG132. Two hours later, cells were harvested for immunoprecipitation. Anti-XIAP antibody (610717, BD) was used to pull down endogenous and exogenous XIAP. Immunoprecipitated samples together with the whole lysate were probed by biotinylated anti-XIAP (BAF8221, R&D), HRP-anti-HA (H6533, Sigma), and anti-GAPDH antibodies. Lysate was also probed by anti-BRE and anti-PARP antibodies. This experiment was performed in duplicate.

3.9.5 BRE leads to the removal of or inhibits exogenous K0-linked ubiquitination of XIAP

Linear ubiquitin chains are those linked via the C- and N-terminus of ubiquitins without involving any lysine residue of the ubiquitin. To investigate if head-to-tail linear ubiquitination occurs to XIAP, and whether the ubiquitination could be affected by BRE, plasmids pEBB-FLAG-XIAP and pRK5-HA-Ubiquitin-K0, with or without pEBB-FLAG-BRE were transfected to HEK293T. pRK5-HA-Ubiquitin-K0 is an expression vector containing K0 ubiquitin with all of the lysines mutated to arginines. Therefore, such mutant can only form head-to-tail linear poly-ubiquitin chains without involving any lysine residue. The K0-linked ubiquitinated XIAP, pulled down by anti-XIAP antibody, was probed by biotinylated anti-XIAP and HRP-anti-HA antibodies. Of note, inclusion of BRE led to weaker and shorter K0-linked ubiquitination of XIAP, indicating that overexpression of BRE may remove or inhibit head-to-tail linear ubiquitination of XIAP (Figure 3-19).

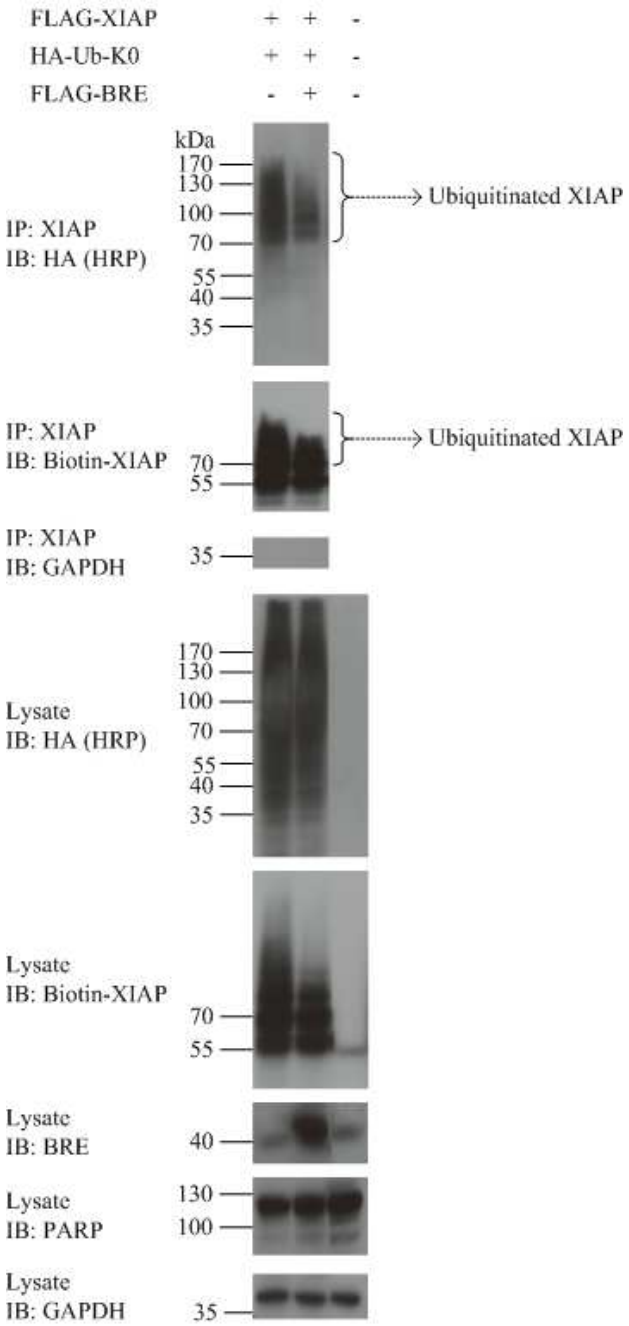

Figure 3-19. **BRE leads to the removal of or inhibits exogenous K0-linked ubiquitination of XIAP.**

HEK293T cells were transfected with pEBB-FLAG-XIAP and pRK5-HA-Ubiquitin-K0, with or without pEBB-FLAG-BRE. HEK293T cells without any transfection were negative control. Forty-eight hours after transfection, culture medium was changed into fresh medium containing 5 μM of MG132. Two hours later, cells were harvested for immunoprecipitation. Anti-XIAP antibody (610717, BD) was used to pull down endogenous and exogenous XIAP. Immunoprecipitated samples together with the whole lysate were probed by biotinylated anti-XIAP (BAF8221, R&D), HRP-anti-HA (H6533, Sigma), and anti-GAPDH antibodies. Lysate was also probed by anti-BRE and anti-PARP antibodies. This experiment was performed in duplicate.

CHAPTER 4: Discussion

4.1 Summary

Here I report identification of the molecular and biochemical mechanisms by which BRE inhibits apoptosis. BRE carries out its anti-apoptotic function through maintaining the cellular level of XIAP, which is a potent endogenous inhibitor of apoptosis. To start, we established a cell line of mouse Lewis lung carcinoma D122 with BRE expression stably depleted by shRNA. The BRE-depleted cells were indeed more sensitive to apoptosis induced by death receptor (TNF-α in the presence of cycloheximide (CHX)) and genotoxic (etoposide) stimuli than the parent and negative control shRNA counterpart. CHX plays a critical pro-apoptotic role by inhibiting synthesis of anti-apoptotic proteins, which TNF-α also up-regulates through activation of NF-κB pathway. However, BRE-depleted cells were susceptible to TNF-α-induced apoptosis even in the absence of CHX, indicating the absence of some of the anti-apoptotic proteins, which were up-regulated following NF-κB activation. We followed this to investigate the expression level of the NF-κB-driven and CHX-sensitive anti-apoptotic proteins. We observed only XIAP, but not cIAP-1, cIAP-2, or cFLIP, was down-regulated in BRE-depleted cells. Highly homologous human BRE was reconstituted in BRE-depleted mouse cells via retrovirus transduction. Correspondingly, cellular XIAP was also restored. Furthermore, reconstitution of the BRE-depleted mouse cells with human BRE or XIAP rendered the cells less sensitive to TNF-α-induced apoptosis. Addition of NEM, which binds irreversibly to cysteine residues of proteins, to cell lysates, was found to abrogate the recognition of BRE by our anti-BRE antibody (Mab489-7) in Western blot analysis. At the same time, cellular XIAP in the lysate (determined by anti-XIAP and anti-FLAG antibodies) was also found reduced. This correlation provides in vitro evidence that BRE has a protective role for XIAP, and that this role is related to cysteine residues of BRE. All of the above-mentioned results provide evidence that BRE maintains the cellular level of XIAP to exert its anti-apoptotic function. I also explore the mechanism by which BRE stabilizes XIAP. The caspase inhibitor VAD cannot preserve XIAP by 16 hours of etoposide treatment, while the proteasome inhibitor MG132 can completely rescue XIAP in the presence of VAD, indicating that, apart from caspases cleavage, proteasome-mediated degradation of XIAP is an important regulatory mechanism for its stability. BRE contains two polyubiquitin-binding UEV domains and forms complexes (BRCA1-A and BRISC) with deubiquitination activity. Polyubiquitination of endogenous and ectopically expressed XIAP as shown in Western blot using anti-ubiquitin antibody, was less when BRE was ectopically expressed. While over-expressed XIAP was found to undergo K48-linked, K63-linked, and K0-linked polyubiquitination, only the K0-linked one was affected by ectopic expression of BRE. Overexpression of BRE led to weaker and shorter K0-linked polyubiquitination of XIAP. Thus, removing or inhibiting polyubiquitination of XIAP, at least the head-to-tail linear-linked polyubiquitination, may be the mechanism by which BRE stabilizes XIAP. On the other hand,

it is possible that, as the HA-tagged Ubiquitin-K0 can be conjugated to and therefore label any lysine-linked ubiquitin chains as a terminal non-extendable ubiquitin, the observed change in the staining signal of anti-HA antibody in relation to BRE overexpression could reflect the activity of BRE on other lysine-linked ubiquitination, not necessarily the head-to-tail non-lysine-linked linear ubiquitination. However, such possibility is not likely to be true, in view of the above finding that the two major forms of ubiquitin chains, the K48- and K63-linked ones, are not affected by ectopic expression of BRE.

4.2 Shortcoming and improvement in future experiment

To delineate unequivocally the linkage-specificity of BRE on ubiquitinated XIAP, future experiments can be done using endogenous ubiquitin-depleted cell lines transfected with different type of mutants of ubiquitin. The lethal effect of depleting ubiquitin in cells can be resolved by a recently devised tetracycline-inducible RNAi system (233, 234). Three types of mutants of ubiquitin can be used. The first type is lysine (K) only mutant, such as K48, K63, K6, K11, K27, K29, and K33 ubiquitin, it can only form poly-ubiquitin chains with other Ub molecules via that single lysine, since all of other lysines are not present (235). The second type is lysine (K) to arginine (R) mutant, such as K48R, K63R, K6R, K11R, K27R, K29R, and K33R ubiquitin; it renders Ub unable to form multi-ubiquitin chains via that specific lysine with other Ub molecules. However, these proteins can still be linked to the lysine residues on target proteins formed via the remaining Ub lysine residues that have not been mutated. Thus, these K-to-R mutants can abolish formation of a specific lysine-linked ubiquitin chain (235). The third type is K0 ubiquitin, with all of the lysines mutated, enables the ubiquitin to only form linear chains via the C- and N-terminus. Transfection of XIAP, with or without BRE, to these cells, would unambiguously demonstrate the type(s) of ubiquitination that can occur to XIAP, and regulated by BRE.

To demonstrate the hypothesis that removing or inhibiting polyubiquitination of XIAP is the mechanism by which BRE stabilizes XIAP. There should be an experiment, which directly shows the relationship between the biological half-life of XIAP and ubiquitination of XIAP. To observe the half-life of a certain protein, protein synthesis inhibitor, such as cycloheximide (CHX), is often used to inhibit the newly synthesized protein. However, when we used CHX to treat cells at different time-point, the CHX also induced apoptosis, which triggered XIAP degradation. In further experiment, we can try other protein synthesis inhibitors, to solve this defect.

Furthermore, in future experiments where the effects on ubiquitination with and without BRE transfection are to be compared, an empty vector should be included to make up for the BRE expression plasmid in the latter to keep the total amount of plasmids for transfection the same as the former for better comparison.

4.3 Significance of the research findings

XIAP is a potent endogenous inhibitor of apoptosis. BRE is found to attenuate both the extrinsic and intrinsic apoptosis. Here, my report is the first to demonstrate the positive regulatory role of BRE on XIAP protein expression. Caspases are effectors of apoptosis. XIAP can inhibit caspase 3, caspase 7, and caspase 9 by direct binding or ubiquitination. XIAP also executes its anti-apoptotic function by regulating NF-κB. On the other hand, NF-κB induces the expression of XIAP. Thereby, XIAP promotes NF-κB activation in a positive feedback loop. Taken together, XIAP is a potent negative regulator of apoptosis in caspase-dependent and caspase-independent cell death pathways. Thus, how the cellular level of this protein is maintained is pivotal to cell survival. My data show that XIAP is not only cleaved by caspases during apoptosis, but also subjected to proteasomal degradation. Ubiquitination of XIAP can be catalyzed by the E3 ligase activity of the RING finger itself (46). The auto-ubiquitination sites of XIAP are localized to Lys311, Lys322, and Lys328 on the BIR3 domain (236). Modification of these sites to arginine dramatically reduces ubiquitination of XIAP, but has little effect on the ability of ectopically expressed XIAP to rescue cells from two independent apoptotic inducers (Bax and Fas) (236), suggesting that auto-ubiquitination of XIAP may have a minimal effect on XIAP protein levels. Recent studies show that ubiquitination of XIAP can be catalyzed by some other RING-bearing E3 ubiquitin ligases, such as cIAP-1 (90, 91), Siah-1 (seven in absentia homolog 1) (237), and TRIM32 (238). However, how XIAP ubiquitination is regulated physiologically remains elusive. Many antagonists of XIAP have been found. Instead of regulating ubiquitination of XIAP, these antagonists predominantly function by steric occlusion of the domains utilized by XIAP to bind caspases (83, 110, 239). Notably, the well-known antagonist Smac binds with high affinity to XIAP, cIAP-1, and cIAP-2 but stimulates the E3 ligase activity and degradation only of cIAP-1 and cIAP-2, suggesting that XIAP ubiquitination may be regulated differently (240). Recently, a negative regulator of XIAP, ARTS, has been found to interacts with the E3 ligase Siah-1 to induce ubiquitination and degradation of XIAP (237). Here, I identify a positive regulator of XIAP, BRE, which stabilizes the cellular level of XIAP. Furthermore, this kind of stabilization may be exerted by removing or inhibiting the ubiquitination of XIAP. At first, I assumed that this type of ubiquitination was K48-linked, since K48-linked chains are well established as mediators of proteasomal degradation. However, according to the result, BRE removes or inhibits linear ubiquitination, but not K48- or K63-linked ubiquitination. This result corresponds with the recently reported finding that the linear type ubiquitin also works as a marker for proteasomal degradation by binding with ubiquitin-binding domain on the proteasome that recognizes K48-linked ubiquitin chains (241, 242). Thus, I propose that BRE promotes removal of linear ubiquitin chain of XIAP, or inhibition of the chain formation to prevent linear polyubiquitin-mediated proteasomal degradation of the protein. The mechanism for such interaction to occur between BRE and XIAP requires further investigation.

4.4 Possibility of BRE to attenuate apoptosis through affecting other NF-κB-activated anti-apoptotic proteins

Thus far, there are three well-characterized anti-apoptotic families of proteins including cFLIP, anti-apoptotic Bcl-2 family members, and inhibitors of apoptosis proteins (IAPs). In my experiment, the apoptotic susceptibility of the BRE-depleted cells to TNF-α alone suggests the absence of some of the anti-apoptotic proteins, which are up-regulated following NF-κB activation. Among the three anti-apoptotic families, cFLIP (243), IAPs (244-246), and three anti-apoptotic Bcl-2 family members Bcl-2 (247), Bcl-XL (248), and Bfl1/A1 (249, 250) are targets of NF-κB. We only tested the expression level of cFLIP, XIAP, cIAP-1, and c-IAP-2 in BRE-depleted cells, revealing only XIAP is down-regulated. However, possible involvement of anti-apoptotic member of Bcl-2 family proteins cannot be ruled out. These proteins decrease apoptosis mainly by preventing MOMP via neutralizing the activity of pro-apoptotic Bcl-2 members (multi-domain members and BH3 only members) (13, 251). The non-canonical activity of anti-apoptotic Bcl-2 family member is its ability to regulate cellular redox status to prevent excessive build-up of ROS (reactive oxygen species), which is detrimental to cells and tissues (251). The possibility of the involvement of promoting stability and/or function of anti-apoptotic Bcl-2 family member(s) in anti-apoptotic activity of BRE is discussed below.

(1) FKBP38 is a positive regulator of Bcl-2. FKBP38 interacts with the flexible loop domain of Bcl-2 directly, preventing Bcl-2 cleavage by caspases, such as caspase 3 and caspase 9 (252). Furthermore, deregulation of Bcl-2 by ubiquitination is also prevented by FKBP38 (253). FKBP38 is a FKBP family member. It has four functional domains, including a transmembrane motif (TM), a calcium/ calmodulin-binding motif (CaM), a tripartite tetratricopeptide repeat (TPR) domain, and a FK506-binding domain (FKBD) (254). The dual protective role of FKBP38 to Bcl-2 requires its TPR domain (255). No TPR domain, however, has been found in BRE by sequence homology.

(2) Rho is another positive regulator of anti-apoptotic Bcl-2 proteins. Rho inhibition reduced expression of anti-apoptotic Bcl-2 and Mcl-1 (256). Rho is a family of small (~21 kDa) signaling GTPase. GTPase are hydrolase enzymes that can bind and hydrolyze guanosine triphosphate (GTP) (257). The common feature of all GTPases is the highly conserved G domain. Three members of Rho family proteins have been studied in detail: Cdc42, Rac1, and RhoA (258). No characteristic G domain has been found in BRE by sequence homology.

(3) Beclin 1 is a possible positive regulator of the anti-apoptotic activity of Bcl-2. A proper interplay between Beclin 1 and Bcl-2 is responsible for the activity of Bcl-2 in apoptosis modulation (259, 260). Besides, Beclin 1 is responsible for the initiation of the formation of the autophagosome in autophagy, which is also related with Bcl-2 stabilization (259, 260).

There is no homology between BRE and Beclin 1. However, whether BRE is involved in autophagy needs further investigation.

(4) Pro-apoptotic BH3-only proteins, including Bad, Bim, Puma, Bid, Bik, Noxa, Hrk, and Bmf, are negative regulators of anti-apoptotic Bcl-2 proteins. Protein-protein interactions between them occur between the BH3 'ligand' domain in BH3-only proteins and a 'receptor' BH3-binding groove, formed by BH1-3 regions in the anti-apoptotic Bcl-2 proteins (261, 262). To date, whether BRE can inhibit the pro-apoptotic BH3-only proteins has not been reported.

(5) ROS and RNS can regulate Bcl-2 expression levels, thereby impacting its function (263). Nitric oxide (NO), one type of RNS, mediates S-nitrosylation of Bcl-2, prevents its ubiquitination and subsequent proteasomal degradation, leading to inhibition of apoptosis (263). NO is an important signaling molecule, produced endogenously from l-arginine in a reaction catalyzed by NO synthases. In contrast, super oxide anion (·O2-), one type of ROS, plays a pro-apoptotic role by causing down-regulation and degradation of Bcl-2 protein through the ubiquitin proteasomal pathway (263). ROS are byproducts of normal oxygen metabolism. However, it is not known whether BRE is involved in the generation or regulation of ROS and RNS.

4.5 BRE may function with other deubiquitinase to mediate deubiquitination of XIAP

Deubiquitinases (DUBs) can be divided into five families, UCHs, USPs, OTUs, Josephins, and JAMMs. JAMMs are zinc metalloproteases, whereas the other four families are Cys proteases (264). The reaction mechanism of Cys proteases is shown in Figure 4-1 (step 1-3) and Figure 4-2 (step 4-6) (264-266). During catalysis, a catalytic acyl intermediate is formed first, in which the carboxyl group is covalently bound to the catalytic Cys after the amino group has been cleaved (step 3, 4). The negatively charged transition state (step 2, 5) is stabilized by the nearby oxy-anion hole, which is formed by hydrogen-donating residues. Next, a water molecule hydrolyses the acyl-Cys intermediate to release the free DUB and ubiquitin (step 6). According to this mechanism, the catalytic Cys is pivotal. The catalytic Cys is formed by Cys and another one or two amino acid(s), forming a catalytic diad or triad. A nearby His side chain is necessary, which lowers the pKa of Cys. A third residue (usually Asp or Asn) is not always necessary. It can polarize and align the His. The mechanism of JAMMs is similar to Cys proteases. The difference is that JAMMs utilize a Zn^{2+} bond to polarize water (169). The catalytic core domain of DUB, which contains Cys or zinc ion, His, or a third residue (Asp or Asn), is conserved in DUB. The consensus sequences of the conserved catalytic core domains are shown in Figure 4-3 (174), none of which is present in BRE, indicating that BRE itself may not be a DUB. BRE is known to function with DUB, though. BRE is important in maintaining the structure and function of two complexes (BRCA1-A and

BRISC), which have deubiquitination activity. These two complexes are specific to K63-linked polyubiquitin chains due to the BRCC36, which is a JAMM type DUB (200, 201). However, in my study, BRE appears to negatively regulate the non-lysine-linked linear ubiquitination of XIAP, rather than the K63-linked ubiquitination. Thus, the promotion of DUB activity of BRCC36 by BRE may not relevant here.

Among all of the five subtypes of DUBs, JAMMs have a common specificity for K63 ubiquitin (264). The substrate of UCHs is relatively small protein (up to 20-30 amino acids) (174). Thus, I propose that the cooperative DUB of BRE could belong to USP, OTU, or Josephin. In vitro analysis shows that some members of USPs, such as IsoT, USP2, USP15, and CYLD can cleave linear ubiquitin chains (177). In TNF-α-induced NF-κB signaling pathway, both K63 and linear polyubiquitin chains can serve as recruitment platform for NEMO, which bridge NEMO with different proteins, thereby promoting IKK activation (147). Similarly, K11, K63, and linear polyubiquitin chains can serve as recruitment platform for RIP1, which bridge RIP1 with different proteins, resulting in activation of NF-κB (147). Recently, USP2 is found to be a positive regulator in this TNF-α-induced NF-κB signaling pathway, whereas its target and ubiquitin chains specificity in this pathway has not been determined yet (267). USP15 is a negative regulators of this pathway, whereas whether its targets involve NEMO and RIP1 needs further investigation (179). CYLD can remove the ubiquitin chains from NEMO (178) and RIP1 (179), thereby inactivating NF-κB activation. However, whether CYLD can remove the linear ubiquitin chains from NEMO and RIP1 has not been reported (179, 180). Two members of OTUs, A20 and TRABID, cannot hydrolyse linear chains in vitro. The ability for linear chains of other members of OTUs and Josephins has not been reported (177). DUBs are often found as part of large multi-protein complexes. The partners of DUB in the complex work to regulate the localization, substrate availability, and activity of DUB (268). BRE containing two ubiquitin-binding UEV domains (194) may strengthen the ability of DUB in a complex to recognize ubiquitin. Besides, BRE may function to sustain the integrity of the deubiquitinating complex, just like in the BRCA1-A and BRISC (202). Another possibility is that BRE may directly bridge DUB to XIAP.

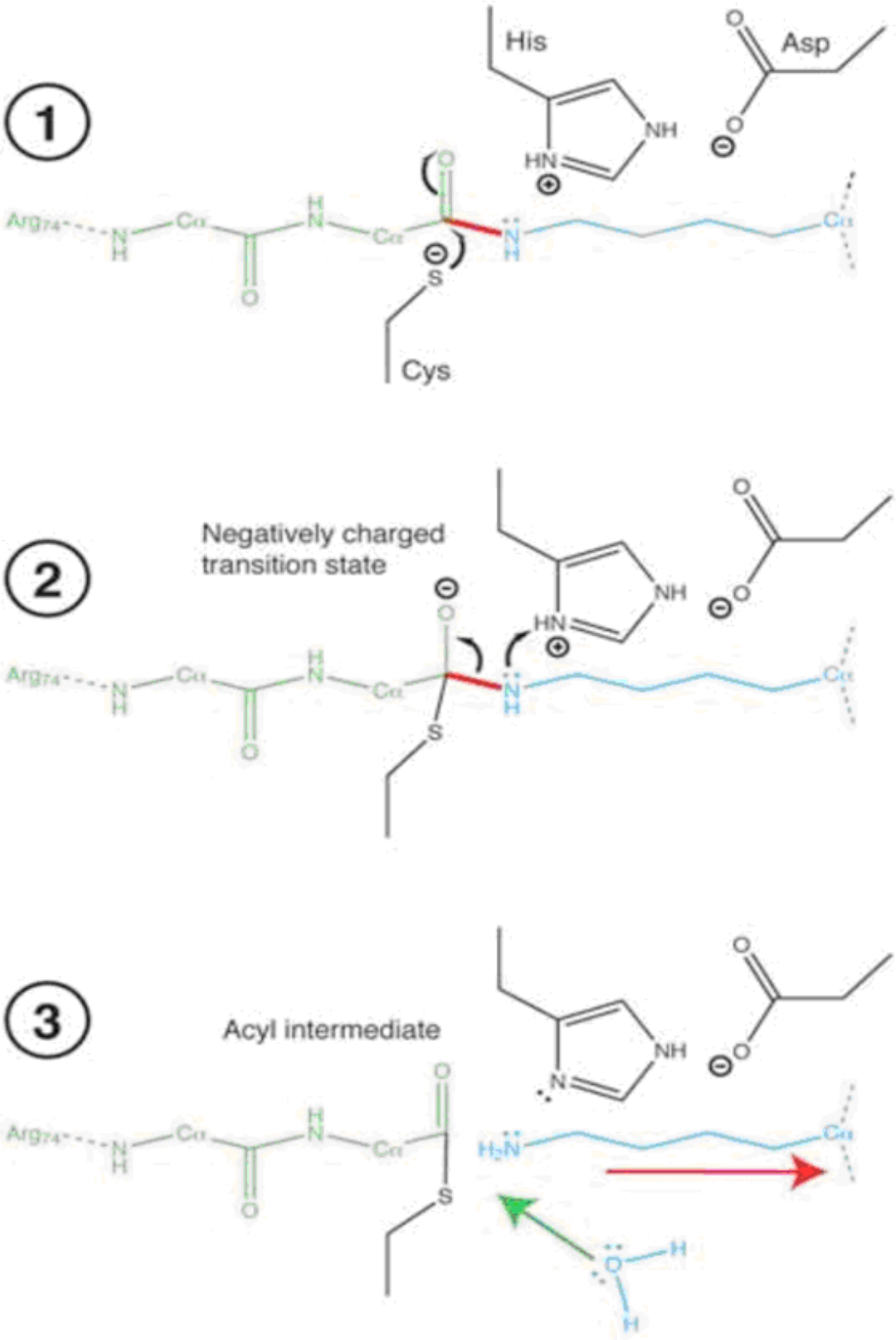

Figure 4-1. **Reaction mechanism for Cys deubiquitinases, step 1-3** (reproduced from reference (266))

C-terminus of ubiquitin is in green. Lys side chain of a linked proximal ubiquitin or substrate is in blue. The isopeptide bond is in red. Water molecule is in blue.

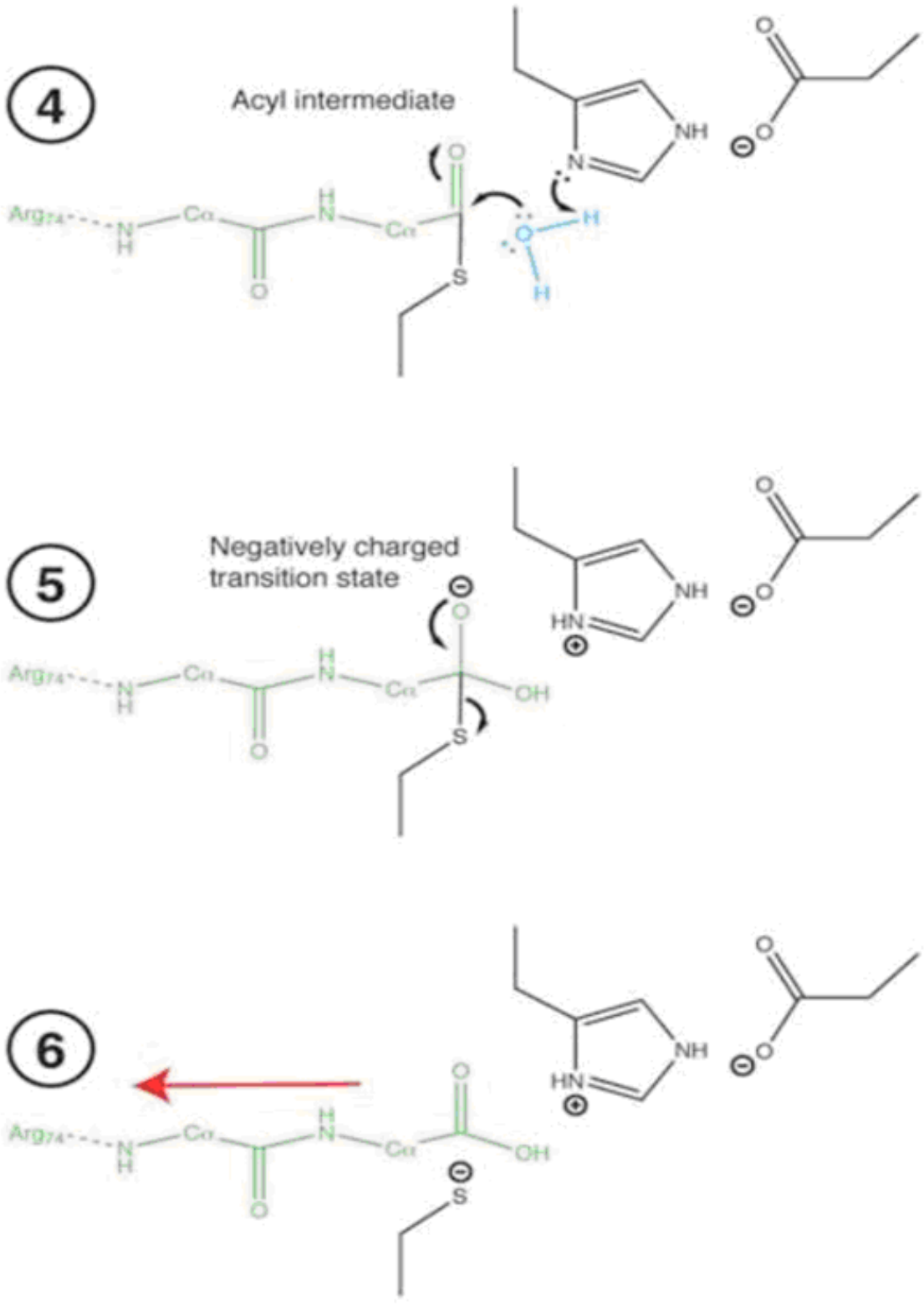

Figure 4-2. **Reaction mechanism for Cys deubiquitinases, step 4-6** (reproduced from reference (266))

C-terminus of ubiquitin is in green. Lys side chain of a linked proximal ubiquitin or substrate is in blue. The isopeptide bond is in red. Water molecule is in blue.

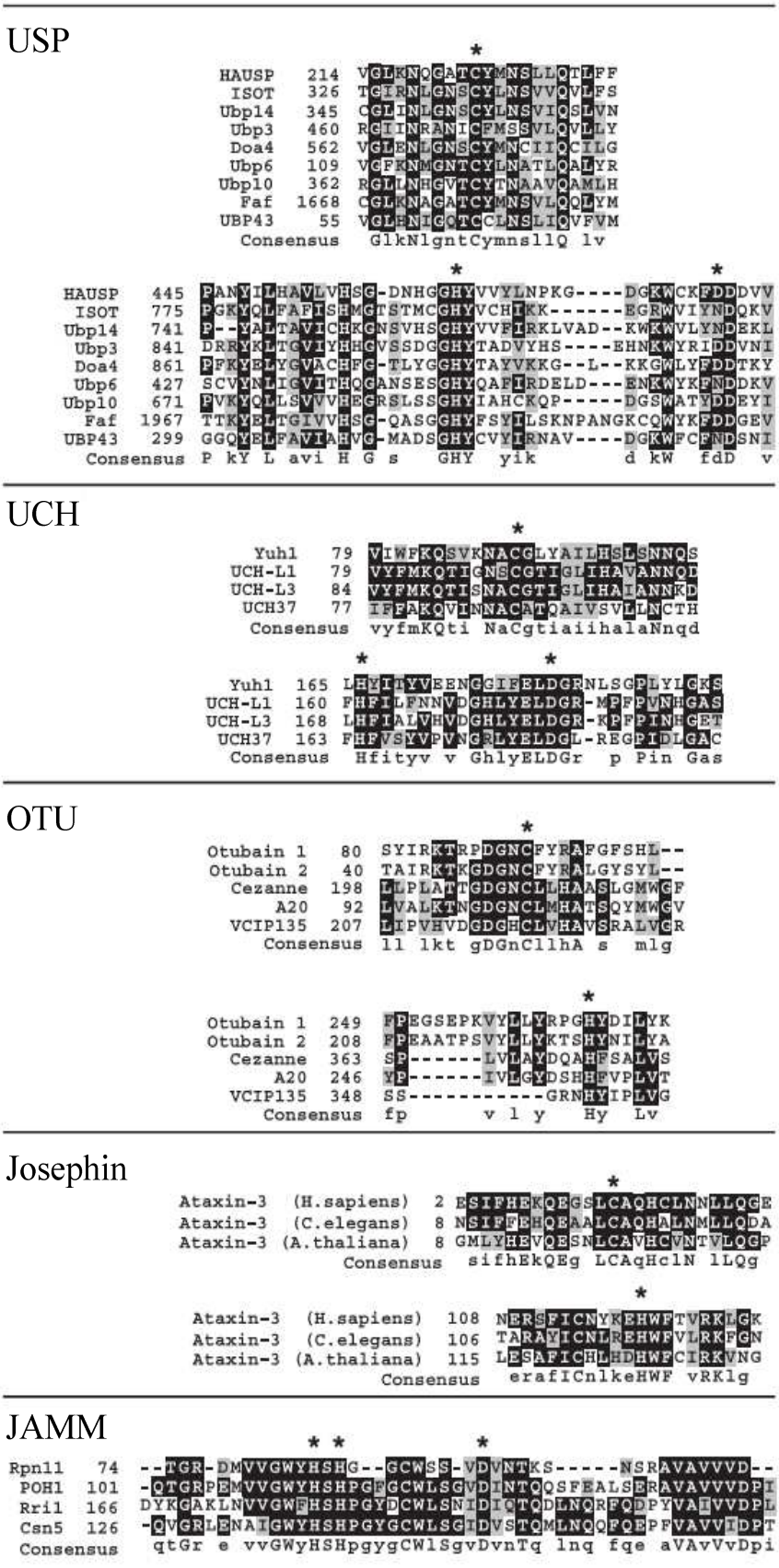

Figure 4-3. **Conserved catalytic core domain of deubiquitinases** (reproduced from reference (174))

4.6 Comparison of methodologies

Recently, a E3 ligase complex, LUBAC (linear ubiquitin chain assembly complex) is found to results in linear ubiquitination of RIP1 and NEMO and enables the NF-κB pathways to be activated (269-271). In general, three types of methods are used to demonstrate that the ubiquitin chain is really in head-to-tail conjugation:

(1) In vitro ubiquitination assays

Reaction mixtures contain E1, appropriate E2, appropriate E3 (LUBAC), and appropriate substrate (such as RIP1 or NEMO), are incubated with wide type ubiquitin, methylated ubiquitin, different lysine (K) only mutant, such as K48, K63, K6, K11, K27, K29, and K33 ubiquitin, and linear ubiquitin mutant, separately at 37℃ for indicated time in an ATP regeneration system. The ubiquitinated substrate is probed by anti-ubiquitin antibody or anti-substrate antibody (271). For LUBAC, only the methylated ubiquitin cannot be polymerized. The reason is that for linear ubiquitin chains, the isopeptide bond is formed between α-amino group of the N-terminal Met of one ubiquitin and the carboxyl group of the C-terminal Gly of another (264). Methylation of ubiquitin blocks all of the acceptor sites of ubiquitin including Lys and the amino group of the N-terminus, whereas all of the other ubiquitins still retain the amino group of N-terminus for linear ubiquitin extension (271).

(2) Mass spectrometry (MS) analysis

Two types of ubiquitinated substrate (in vivo or in vitro) are generated first. In vitro, ubiquitinated substrate is generated by the above-mentioned in vitro ubiquitination regeneration system. In vivo ubiquitinated substrate is anti-substrate immunoprecipitates from cells, such as HEK293T, co-expressing substrate and E3 (272). These in vivo and in vitro ubiquitinated substrate are analyzed using a method combining trypsin digestion and mass spectrometry (273, 274). For LUBAC, MS analysis shows that the peptides from ubiquitinated NEMO or ubiquitinated RIP1 are only linear linkage (271, 272).

(3) Specific anti-linear ubiquitin antibody analysis

Recently, a specific antibody against a peptide containing the boundary of head-to-tail-linked ubiquitin moieties has been prepared (272). In vivo or in vitro ubiquitinated substrates, as described in method (2), are probed by this specific anti-linear ubiquitin antibody to further confirm the type of the ubiquitin conjugated to substrate (272).

Furthermore, in vitro assays for DUB activity for linear ubiquitin chain have also been developed. It should be noted that in vivo assay method of such DUB activity is not yet available. The procedure of in vitro deubiquitination assay is similar to the above-mentioned in vitro ubiquitination regeneration assay. The main difference is that the reactants are appropriate DUB and different type of polyubiquitin chains. If DUB is specific to linear ubiquitin, this type of polyubiquitin chains will be degraded (177).

In my experiment, HEK293T cells were transfected with substrate (XIAP) and HA tagged linear ubiquitin, with or without BRE. The ubiquitinated substrate was probed by anti-XIAP or anti-ubiquitin antibodies. Comparing with the above-mentioned methods, my method has two shortcomings:

(1) Endogenous ubiquitin may conjugate together with the overexpressed linear ubiquitin.

(2) The overexpressed linear ubiquitin may not be the same as endogenous linear ubiquitin.

To directly analyze whether endogenous linear ubiquitination of XIAP can be affected by BRE, further experiments can be designed as follows: To transfect HEK293T cells with XIAP together with or without BRE, which is then followed by immunoprecipitation of ubiquitinated XIAP for immunoblotting using specific anti-linear ubiquitin antibody. Furthermore, the ubiquitinated XIAP can be analyzed using mass spectrometry. If BRE can remove or inhibit the endogenous linear ubiquitin chains of XIAP, the staining intensity of anti-linear ubiquitin antibody should be reduced with co-transfection of BRE. MS could also be used instead of the anti-linear ubiquitin antibody. Furthermore, to determine whether BRE or BRE-containing complex has linear Ub specific DUB activity, an in vitro deubiquitination assay, containing linear polyubiquitin chains with purified BRE or BRE over-expressing lysate, should be performed. If BRE alone has linear specific DUB activity, the linear polyubiquitin chains should be degraded when purified BRE is used. If BRE over-expressing lysate instead of purified BRE breaks down linear polyubiquitin chains, then BRE may function as a complex in this regard. Besides, BRE may inhibit the formation of linear ubiquitination of XIAP. Thus, an in vitro ubiquitination regeneration assay, containing E1, E2, E3, substrate (XIAP), linear ubiquitin with or without BRE, can be done to determine whether BRE can inhibit the linear ubiquitination formation of XIAP.

4.7 Lysine-linkage specificity of the ubiquitination of XIAP

Ubiquitination of XIAP is important for its stability. However, the exact lysine-linkage specificity of the ubiquitination of XIAP has not been examined clearly (232). Ubiquitination of XIAP can be catalyzed by itself or by some other RING finger-containing proteins. Some factors maintain cellular XIAP level by attenuating the ubiquitination and degradation process. These positive regulators include CDK4-binding protein $p34^{SEI-1}$ (275), PGI_2 (prostacyclin) , Notch (277), and Akt (278). On the other hand, some factors promote XIAP ubiquitination and proteasomal degradation. These negative factors include luteolin (279), triterpenoid electrophile Avicins (280), and Grim (89). Of note, none of these studies clarified the exact lysine-linkage specificity of the ubiquitinated of XIAP, only assuming that it was K48-linked. Recently, Nakhaei et al. reported that the lysine-linkage of Sendai virus infection-induced auto-ubiquitination of XIAP was K48-linked (281). As mentioned above, BRE promotes removal of linear ubiquitin chain of XIAP, or inhibition of the chain formation, to prevent

linear polyubiquitin-mediated proteasomal degradation of the protein. My data is not necessarily in contradiction with that of Nakhaei et al., since only K48- and K63-linked ubiquitination was analyzed in their study. Besides, auto-ubiquitination of XIAP induced by Sendai virus infection and other stimuli may result in different lysine-linkage specificities. It remains possible that XIAP may undergo linear-linked ubiquitination as proteasomal degradation marker for normal protein turnover under non-apoptotic condition, as the BRE-depleted cells in which reduction of XIAP occurs is not apoptotic.

4.8 Possibility of BRE to maintain XIAP level utilizing other mechanisms

I have proposed that the attenuation of proteasomal degradation of XIAP may be the mechanism by which BRE stabilizes this protein. Could BRE also utilize some other mechanisms to maintain cellular XIAP level? I have considered the following:

(1) Protein synthesis regulation

XIAP synthesis is controlled at the levels of transcription and translation (282). Transcription of XIAP is regulated by NF-κB (246). BRE may play a role in NF-κB activation. For example, after BRE overexpression, Map3K8 (mitogen-activated protein kinase 8) and TRAF6 (TNF receptor P70196 associated factor 6) are found to be up-regulated (283). Map3K8 is able to activate NF-κB by stimulating proteasome-mediated proteolysis of NF-κB1/p105 (284). TRAF6 is a adapter protein and signal transducer, which links members of the tumour necrosis factor receptor family to activation of NF-κB (285). Thus, it is possible for BRE to stabilize XIAP by regulating NF-κB. Whether this hypothesis is true requires further investigation. Apart from transcription, synthesis of XIAP is also regulated at the level of translation. Under normal condition, translation of XIAP is initiated using a 7-methylguanosine cap-dependent ribosome scanning mechanism, which is the translation mechanism for the majority of proteins in eukaryotic cells (286). Under conditions of cellular stress and apoptosis, cap-dependent translation is compromised (287, 288). However, translation of XIAP mRNA transcript still continues under such condition, relying on the cap-independent mechanism (289). This cap-independent translation of XIAP is mediated by a 162-nucleotides internal ribosome entry site (IRES) sequence, which is located in the 5'-untranslated region (UTR) of XIAP mRNA (289, 290). Proteins that modulate IRES function, are named as IRES trans-acting factors (ITAFs) (291). The ITAFs of XIAP include La autoantigen (289), hnRNP C1/C2 (292), and hnRNP A1 (293). Whether BRE is involved in the cap-dependent or cap-independent translation mechanism of XIAP has not been studied yet.

(2) Cell cycle-dependent protein expression

XIAP expression is not cell cycle-dependent (294). One antagonist of XIAP, XAF1, is

expressed in a cell cycle-dependent manner. It only expresses in G2/M phase (294). BRE-containing complex, BRCA1-A, plays a role in arresting the cell cycle to allow DNA repair to take place following DNA damage (200). p53 can induce growth arrest by holding the cell cycle at the G1/S phase on DNA damage recognition (295, 296). BRCA1-A might exert its cell cycle regulatory function by ubiquitinating p53 via its E3 ubiquitin ligase activity (200). After this ubiquitination process, p53 is activated to induce growth arrest (200). BRE is important for the cell cycle regulatory function of BRCA1-A. Following DNA damage, depletion of BRE and BRCC36 results in defects in G2/M checkpoint (200). Besides, BRE might maintain a basal level of cell growth by stabilizing p53 in a transcriptional way (283). Furthermore, BRE may regulate other cell cycle regulatory proteins, such as prohibitin, Mdm4, and Map3K8 (283). Thus, it is possible for BRE to maintain XIAP in a cell cycle-dependent way by attenuating its antagonist XAF1. Whether this hypothesis is true requires further investigation.

4.9 Interpretation of NEM-related data

Addition of NEM was found to abrogate the recognition of BRE by our anti-BRE antibody (Mab489-7) in cell lysate. However, the recognition of BRE by our anti-BRE antibody (Mab246) or the recognition of V5 tagged BRE by HRP-anti-V5 antibody remained intact in the same NEM-containing lysate. Therefore, NEM abolishes the binding between BRE and Mab489-7 without affecting BRE protein level. The anti-BRE (Mab489-7) and anti-BRE (Mab246) were generated using the human BRE protein fragment from 40 to 225 as immunogen (198). This peptide contains five cysteine residues, which NEM can irreversibly bind through formation of a strong thioester bond, resulting in changes of local structure. Mab489-7, but not Mab246, may bind to the NEM-sensitive epitope, which contains or is proximal to cysteine. As the amino acid sequence of V5 epitope, which is GKPIPNPLLGLDST, contains no cysteine. Thus, NEM does not interfere with the binding between V5 tagged BRE and HRP-anti-V5 antibody. Addition of NEM was found to reduce the immunoblotting staining signal by anti-XIAP and anti-FLAG antibodies. As the amino acid sequence of FLAG epitope, which is DYKDDDDK, contains no cysteine. Thus, XIAP level in the cell lysate with added NEM must also have been reduced. Taken together, addition to cell lysate of NEM, which binds to the cysteine residues of BRE, leads to the failure of anti-BRE (Mab489-7) to recognize the protein and decline of XIAP level in the same cell lysate. This provides in vitro evidence that BRE has a protective role for XIAP, and that this role is related to cysteine residues of BRE. It should be recognized that this inference requires further investigation.

4.10 Conclusion

Taken together, I have provided evidence that BRE exerts its anti-apoptotic function through

maintaining the cellular level of XIAP, a potent endogenous inhibitor of apoptosis. Promoting removal of linear ubiquitin chain of XIAP, or inhibition of the chain formation, to prevent linear polyubiquitin-mediated proteasomal degradation of XIAP may be the mechanism by which BRE stabilizes this protein.

Reference

1. Kerr JF, Wyllie AH, Currie AR. Apoptosis: A basic biological phenomenon with wide-ranging implications in tissue kinetics. *British journal of cancer* 1972;26(4):239-257.
2. Saikumar P, Dong Z, Mikhailov V, Denton M, Weinberg JM, Venkatachalam MA. Apoptosis: Definition, mechanisms, and relevance to disease. *The American journal of medicine* 1999;107(5):489-506.
3. Thompson CB. Apoptosis in the pathogenesis and treatment of disease. *Science (New York, NY* 1995;267(5203):1456-1462.
4. Cohen GM. Caspases: The executioners of apoptosis. *The Biochemical journal* 1997;326 (Pt 1):1-16.
5. Krammer PH, Arnold R, Lavrik IN. Life and death in peripheral t cells. *Nature reviews* 2007;7(7):532-542.
6. Fuentes-Prior P, Salvesen GS. The protein structures that shape caspase activity, specificity, activation and inhibition. *The Biochemical journal* 2004;384(Pt 2):201-232.
7. Vaux DL, Silke J. Iaps, rings and ubiquitylation. *Nat Rev Mol Cell Biol* 2005;6(4):287-297.
8. Moffitt KL, Martin SL, Walker B. From sentencing to execution--the processes of apoptosis. *The Journal of pharmacy and pharmacology*;62(5):547-562.
9. Suliman A, Lam A, Datta R, Srivastava RK. Intracellular mechanisms of trail: Apoptosis through mitochondrial-dependent and -independent pathways. *Oncogene* 2001;20(17):2122-2133.
10. Cory S, Adams JM. The bcl2 family: Regulators of the cellular life-or-death switch. *Nat Rev Cancer* 2002;2(9):647-656.
11. Scorrano L, Korsmeyer SJ. Mechanisms of cytochrome c release by proapoptotic bcl-2 family members. *Biochemical and biophysical research communications* 2003;304(3):437-444.
12. Ow YP, Green DR, Hao Z, Mak TW. Cytochrome c: Functions beyond respiration. *Nature reviews* 2008;9(7):532-542.
13. Youle RJ, Strasser A. The bcl-2 protein family: Opposing activities that mediate cell death. *Nature reviews* 2008;9(1):47-59.
14. Green DR. At the gates of death. *Cancer cell* 2006;9(5):328-330.
15. Eskes R, Desagher S, Antonsson B, Martinou JC. Bid induces the oligomerization and insertion of bax into the outer mitochondrial membrane. *Molecular and cellular biology* 2000;20(3):929-935.
16. Desagher S, Osen-Sand A, Nichols A, Eskes R, Montessuit S, Lauper S, Maundrell K, Antonsson B, Martinou JC. Bid-induced conformational change of bax is responsible for mitochondrial cytochrome c release during apoptosis. *The Journal of cell biology* 1999;144(5):891-901.
17. Balakrishnan G, Hu Y, Oyerinde OF, Su J, Groves JT, Spiro TG. A conformational switch to beta-sheet structure in cytochrome c leads to heme exposure. Implications for cardiolipin peroxidation and apoptosis. *Journal of the American Chemical Society* 2007;129(3):504-505.
18. Hengartner MO. The biochemistry of apoptosis. *Nature* 2000;407(6805):770-776.
19. Sen R, Baltimore D. Multiple nuclear factors interact with the immunoglobulin enhancer sequences. *Cell* 1986;46(5):705-716.
20. Gilmore TD. Introduction to nf-kappab: Players, pathways, perspectives. *Oncogene* 2006;25(51):6680-6684.
21. Nabel GJ, Verma IM. Proposed nf-kappa b/i kappa b family nomenclature. *Genes & development* 1993;7(11):2063.
22. http://en.wikipedia.org/wiki/File:NFKB_mechanism_of_action.png.
23. Brasier AR. The nf-kappab regulatory network. *Cardiovascular toxicology* 2006;6(2):111-130.
24. Perkins ND. Integrating cell-signalling pathways with nf-kappab and ikk function. *Nat Rev Mol Cell Biol* 2007;8(1):49-62.
25. Lobito AA, Gabriel TL, Medema JP, Kimberley FC. Disease causing mutations in the tnf and tnfr superfamilies: Focus on molecular mechanisms driving disease. *Trends in molecular medicine*;17(9):494-505.
26. Campbell KJ, Perkins ND. Regulation of nf-kappab function. *Biochemical Society symposium* 2006(73):165-180.
27. Micheau O, Tschopp J. Induction of tnf receptor i-mediated apoptosis via two sequential signaling complexes. *Cell* 2003;114(2):181-190.
28. Wang L, Du F, Wang X. Tnf-alpha induces two distinct caspase-8 activation pathways. *Cell* 2008;133(4):693-703.

29. Budd RC, Yeh WC, Tschopp J. Cflip regulation of lymphocyte activation and development. *Nature reviews* 2006;6(3):196-204.
30. Boatright KM, Deis C, Denault JB, Sutherlin DP, Salvesen GS. Activation of caspases-8 and -10 by flip(l). *The Biochemical journal* 2004;382(Pt 2):651-657.
31. Pop C, Oberst A, Drag M, Van Raam BJ, Riedl SJ, Green DR, Salvesen GS. Flip(l) induces caspase 8 activity in the absence of interdomain caspase 8 cleavage and alters substrate specificity. *The Biochemical journal*;433(3):447-457.
32. Hughes MA, Harper N, Butterworth M, Cain K, Cohen GM, MacFarlane M. Reconstitution of the death-inducing signaling complex reveals a substrate switch that determines cd95-mediated death or survival. *Molecular cell* 2009;35(3):265-279.
33. Micheau O, Thome M, Schneider P, Holler N, Tschopp J, Nicholson DW, Briand C, Grutter MG. The long form of flip is an activator of caspase-8 at the fas death-inducing signaling complex. *The Journal of biological chemistry* 2002;277(47):45162-45171.
34. Oberst A, Dillon CP, Weinlich R, McCormick LL, Fitzgerald P, Pop C, Hakem R, Salvesen GS, Green DR. Catalytic activity of the caspase-8-flip(l) complex inhibits ripk3-dependent necrosis. *Nature*;471(7338):363-367.
35. Chang L, Kamata H, Solinas G, Luo JL, Maeda S, Venuprasad K, Liu YC, Karin M. The e3 ubiquitin ligase itch couples jnk activation to tnfalpha-induced cell death by inducing c-flip(l) turnover. *Cell* 2006;124(3):601-613.
36. Riedl SJ, Shi Y. Molecular mechanisms of caspase regulation during apoptosis. *Nature reviews* 2004;5(11):897-907.
37. Birnbaum MJ, Clem RJ, Miller LK. An apoptosis-inhibiting gene from a nuclear polyhedrosis virus encoding a polypeptide with cys/his sequence motifs. *Journal of virology* 1994;68(4):2521-2528.
38. Hinds MG, Norton RS, Vaux DL, Day CL. Solution structure of a baculoviral inhibitor of apoptosis (iap) repeat. *Nature structural biology* 1999;6(7):648-651.
39. Sun C, Cai M, Gunasekera AH, Meadows RP, Wang H, Chen J, Zhang H, Wu W, Xu N, Ng SC, et al. Nmr structure and mutagenesis of the inhibitor-of-apoptosis protein xiap. *Nature* 1999;401(6755):818-822.
40. Lin SC, Huang Y, Lo YC, Lu M, Wu H. Crystal structure of the bir1 domain of xiap in two crystal forms. *Journal of molecular biology* 2007;372(4):847-854.
41. Liu Z, Sun C, Olejniczak ET, Meadows RP, Betz SF, Oost T, Herrmann J, Wu JC, Fesik SW. Structural basis for binding of smac/diablo to the xiap bir3 domain. *Nature* 2000;408(6815):1004-1008.
42. Srinivasula SM, Hegde R, Saleh A, Datta P, Shiozaki E, Chai J, Lee RA, Robbins PD, Fernandes-Alnemri T, Shi Y, et al. A conserved xiap-interaction motif in caspase-9 and smac/diablo regulates caspase activity and apoptosis. *Nature* 2001;410(6824):112-116.
43. Rothe M, Pan MG, Henzel WJ, Ayres TM, Goeddel DV. The tnfr2-traf signaling complex contains two novel proteins related to baculoviral inhibitor of apoptosis proteins. *Cell* 1995;83(7):1243-1252.
44. Uren AG, Pakusch M, Hawkins CJ, Puls KL, Vaux DL. Cloning and expression of apoptosis inhibitory protein homologs that function to inhibit apoptosis and/or bind tumor necrosis factor receptor-associated factors. *Proceedings of the National Academy of Sciences of the United States of America* 1996;93(10):4974-4978.
45. Lu M, Lin SC, Huang Y, Kang YJ, Rich R, Lo YC, Myszka D, Han J, Wu H. Xiap induces nf-kappab activation via the bir1/tab1 interaction and bir1 dimerization. *Molecular cell* 2007;26(5):689-702.
46. Yang Y, Fang S, Jensen JP, Weissman AM, Ashwell JD. Ubiquitin protein ligase activity of iaps and their degradation in proteasomes in response to apoptotic stimuli. *Science (New York, NY* 2000;288(5467):874-877.
47. Gyrd-Hansen M, Darding M, Miasari M, Santoro MM, Zender L, Xue W, Tenev T, da Fonseca PC, Zvelebil M, Bujnicki JM, et al. Iaps contain an evolutionarily conserved ubiquitin-binding domain that regulates nf-kappab as well as cell survival and oncogenesis. *Nature cell biology* 2008;10(11):1309-1317.
48. Blankenship JW, Varfolomeev E, Goncharov T, Fedorova AV, Kirkpatrick DS, Izrael-Tomasevic A, Phu L, Arnott D, Aghajan M, Zobel K, et al. Ubiquitin binding modulates iap antagonist-stimulated proteasomal degradation of c-iap1 and c-iap2(1). *The Biochemical journal* 2009;417(1):149-160.
49. Mehrotra S, Languino LR, Raskett CM, Mercurio AM, Dohi T, Altieri DC. Iap regulation of metastasis. *Cancer cell*;17(1):53-64.
50. Dogan T, Harms GS, Hekman M, Karreman C, Oberoi TK, Alnemri ES, Rapp UR,

Rajalingam K. X-linked and cellular iaps modulate the stability of c-raf kinase and cell motility. *Nature cell biology* 2008;10(12):1447-1455.
51. LaCasse EC, Mahoney DJ, Cheung HH, Plenchette S, Baird S, Korneluk RG. Iap-targeted therapies for cancer. *Oncogene* 2008;27(48):6252-6275.
52. Hunter AM, LaCasse EC, Korneluk RG. The inhibitors of apoptosis (iaps) as cancer targets. *Apoptosis* 2007;12(9):1543-1568.
53. Hwang C, Oetjen KA, Kosoff D, Wojno KJ, Albertelli MA, Dunn RL, Robins DM, Cooney KA, Duckett CS. X-linked inhibitor of apoptosis deficiency in the tramp mouse prostate cancer model. *Cell death and differentiation* 2008;15(5):831-840.
54. Harlin H, Reffey SB, Duckett CS, Lindsten T, Thompson CB. Characterization of xiap-deficient mice. *Molecular and cellular biology* 2001;21(10):3604-3608.
55. Liston P, Roy N, Tamai K, Lefebvre C, Baird S, Cherton-Horvat G, Farahani R, McLean M, Ikeda JE, MacKenzie A, et al. Suppression of apoptosis in mammalian cells by naip and a related family of iap genes. *Nature* 1996;379(6563):349-353.
56. Chamaillard M, Girardin SE, Viala J, Philpott DJ. Nods, nalps and naip: Intracellular regulators of bacterial-induced inflammation. *Cellular microbiology* 2003;5(9):581-592.
57. Verhagen AM, Coulson EJ, Vaux DL. Inhibitor of apoptosis proteins and their relatives: Iaps and other birps. *Genome biology* 2001;2(7):REVIEWS3009.
58. Dubrez-Daloz L, Dupoux A, Cartier J. Iaps: More than just inhibitors of apoptosis proteins. *Cell cycle (Georgetown, Tex* 2008;7(8):1036-1046.
59. Deveraux QL, Reed JC. Iap family proteins--suppressors of apoptosis. *Genes & development* 1999;13(3):239-252.
60. Deveraux QL, Takahashi R, Salvesen GS, Reed JC. X-linked iap is a direct inhibitor of cell-death proteases. *Nature* 1997;388(6639):300-304.
61. Trapp T, Korhonen L, Besselmann M, Martinez R, Mercer EA, Lindholm D. Transgenic mice overexpressing xiap in neurons show better outcome after transient cerebral ischemia. *Molecular and cellular neurosciences* 2003;23(2):302-313.
62. Deveraux QL, Roy N, Stennicke HR, Van Arsdale T, Zhou Q, Srinivasula SM, Alnemri ES, Salvesen GS, Reed JC. Iaps block apoptotic events induced by caspase-8 and cytochrome c by direct inhibition of distinct caspases. *The EMBO journal* 1998;17(8):2215-2223.
63. Conte D, Liston P, Wong JW, Wright KE, Korneluk RG. Thymocyte-targeted overexpression of xiap transgene disrupts t lymphoid apoptosis and maturation. *Proceedings of the National Academy of Sciences of the United States of America* 2001;98(9):5049-5054.
64. Takahashi R, Deveraux Q, Tamm I, Welsh K, Assa-Munt N, Salvesen GS, Reed JC. A single bir domain of xiap sufficient for inhibiting caspases. *The Journal of biological chemistry* 1998;273(14):7787-7790.
65. Wilkinson JC, Cepero E, Boise LH, Duckett CS. Upstream regulatory role for xiap in receptor-mediated apoptosis. *Molecular and cellular biology* 2004;24(16):7003-7014.
66. McManus DC, Lefebvre CA, Cherton-Horvat G, St-Jean M, Kandimalla ER, Agrawal S, Morris SJ, Durkin JP, Lacasse EC. Loss of xiap protein expression by rnai and antisense approaches sensitizes cancer cells to functionally diverse chemotherapeutics. *Oncogene* 2004;23(49):8105-8117.
67. Cummins JM, Kohli M, Rago C, Kinzler KW, Vogelstein B, Bunz F. X-linked inhibitor of apoptosis protein (xiap) is a nonredundant modulator of tumor necrosis factor-related apoptosis-inducing ligand (trail)-mediated apoptosis in human cancer cells. *Cancer research* 2004;64(9):3006-3008.
68. Sasaki H, Sheng Y, Kotsuji F, Tsang BK. Down-regulation of x-linked inhibitor of apoptosis protein induces apoptosis in chemoresistant human ovarian cancer cells. *Cancer research* 2000;60(20):5659-5666.
69. Chawla-Sarkar M, Bae SI, Reu FJ, Jacobs BS, Lindner DJ, Borden EC. Downregulation of bcl-2, flip or iaps (xiap and survivin) by sirnas sensitizes resistant melanoma cells to apo2l/trail-induced apoptosis. *Cell death and differentiation* 2004;11(8):915-923.
70. Eckelman BP, Salvesen GS, Scott FL. Human inhibitor of apoptosis proteins: Why xiap is the black sheep of the family. *EMBO reports* 2006;7(10):988-994.
71. Silke J, Ekert PG, Day CL, Hawkins CJ, Baca M, Chew J, Pakusch M, Verhagen AM, Vaux DL. Direct inhibition of caspase 3 is dispensable for the anti-apoptotic activity of xiap. *The EMBO journal* 2001;20(12):3114-3123.
72. Huang Y, Park YC, Rich RL, Segal D, Myszka DG, Wu H. Structural basis of caspase inhibition by xiap: Differential roles of the linker versus the bir domain. *Cell* 2001;104(5):781-790.
73. Suzuki Y, Nakabayashi Y, Takahashi R. Ubiquitin-protein ligase activity of x-linked inhibitor

of apoptosis protein promotes proteasomal degradation of caspase-3 and enhances its anti-apoptotic effect in fas-induced cell death. *Proceedings of the National Academy of Sciences of the United States of America* 2001;98(15):8662-8667.
74. Chai J, Shiozaki E, Srinivasula SM, Wu Q, Datta P, Alnemri ES, Shi Y. Structural basis of caspase-7 inhibition by xiap. *Cell* 2001;104(5):769-780.
75. Riedl SJ, Renatus M, Schwarzenbacher R, Zhou Q, Sun C, Fesik SW, Liddington RC, Salvesen GS. Structural basis for the inhibition of caspase-3 by xiap. *Cell* 2001;104(5):791-800.
76. Roy N, Deveraux QL, Takahashi R, Salvesen GS, Reed JC. The c-iap-1 and c-iap-2 proteins are direct inhibitors of specific caspases. *The EMBO journal* 1997;16(23):6914-6925.
77. Scott FL, Denault JB, Riedl SJ, Shin H, Renatus M, Salvesen GS. Xiap inhibits caspase-3 and -7 using two binding sites: Evolutionarily conserved mechanism of iaps. *The EMBO journal* 2005;24(3):645-655.
78. Shiozaki EN, Chai J, Rigotti DJ, Riedl SJ, Li P, Srinivasula SM, Alnemri ES, Fairman R, Shi Y. Mechanism of xiap-mediated inhibition of caspase-9. *Molecular cell* 2003;11(2):519-527.
79. Joazeiro CA, Weissman AM. Ring finger proteins: Mediators of ubiquitin ligase activity. *Cell* 2000;102(5):549-552.
80. Duckett CS, Li F, Wang Y, Tomaselli KJ, Thompson CB, Armstrong RC. Human iap-like protein regulates programmed cell death downstream of bcl-xl and cytochrome c. *Molecular and cellular biology* 1998;18(1):608-615.
81. Gyrd-Hansen M, Meier P. Iaps: From caspase inhibitors to modulators of nf-kappab, inflammation and cancer. *Nature reviews*;10(8):561-574.
82. Lotocki G, Alonso OF, Frydel B, Dietrich WD, Keane RW. Monoubiquitination and cellular distribution of xiap in neurons after traumatic brain injury. *J Cereb Blood Flow Metab* 2003;23(10):1129-1136.
83. Verhagen AM, Kratina TK, Hawkins CJ, Silke J, Ekert PG, Vaux DL. Identification of mammalian mitochondrial proteins that interact with iaps via n-terminal iap binding motifs. *Cell death and differentiation* 2007;14(2):348-357.
84. Wilkinson JC, Wilkinson AS, Galban S, Csomos RA, Duckett CS. Apoptosis-inducing factor is a target for ubiquitination through interaction with xiap. *Molecular and cellular biology* 2008;28(1):237-247.
85. Gottfried Y, Rotem A, Lotan R, Steller H, Larisch S. The mitochondrial arts protein promotes apoptosis through targeting xiap. *The EMBO journal* 2004;23(7):1627-1635.
86. Galban S, Hwang C, Rumble JM, Oetjen KA, Wright CW, Boudreault A, Durkin J, Gillard JW, Jaquith JB, Morris SJ, et al. Cytoprotective effects of iaps revealed by a small molecule antagonist. *The Biochemical journal* 2009;417(3):765-771.
87. Fu J, Jin Y, Arend LJ. Smac3, a novel smac/diablo splicing variant, attenuates the stability and apoptosis-inhibiting activity of x-linked inhibitor of apoptosis protein. *The Journal of biological chemistry* 2003;278(52):52660-52672.
88. Bertrand MJ, Milutinovic S, Dickson KM, Ho WC, Boudreault A, Durkin J, Gillard JW, Jaquith JB, Morris SJ, Barker PA. Ciap1 and ciap2 facilitate cancer cell survival by functioning as e3 ligases that promote rip1 ubiquitination. *Molecular cell* 2008;30(6):689-700.
89. Silke J, Kratina T, Ekert PG, Pakusch M, Vaux DL. Unlike diablo/smac, grim promotes global ubiquitination and specific degradation of x chromosome-linked inhibitor of apoptosis (xiap) and neither cause apoptosis. *The Journal of biological chemistry* 2004;279(6):4313-4321.
90. Silke J, Kratina T, Chu D, Ekert PG, Day CL, Pakusch M, Huang DC, Vaux DL. Determination of cell survival by ring-mediated regulation of inhibitor of apoptosis (iap) protein abundance. *Proceedings of the National Academy of Sciences of the United States of America* 2005;102(45):16182-16187.
91. Cheung HH, Plenchette S, Kern CJ, Mahoney DJ, Korneluk RG. The ring domain of ciap1 mediates the degradation of ring-bearing inhibitor of apoptosis proteins by distinct pathways. *Molecular biology of the cell* 2008;19(7):2729-2740.
92. Schile AJ, Garcia-Fernandez M, Steller H. Regulation of apoptosis by xiap ubiquitin-ligase activity. *Genes & development* 2008;22(16):2256-2266.
93. Vucic D, Deshayes K, Ackerly H, Pisabarro MT, Kadkhodayan S, Fairbrother WJ, Dixit VM. Smac negatively regulates the anti-apoptotic activity of melanoma inhibitor of apoptosis (ml-iap). *The Journal of biological chemistry* 2002;277(14):12275-12279.
94. MacFarlane M, Merrison W, Bratton SB, Cohen GM. Proteasome-mediated degradation of smac during apoptosis: Xiap promotes smac ubiquitination in vitro. *The Journal of biological chemistry* 2002;277(39):36611-36616.
95. Arora V, Cheung HH, Plenchette S, Micali OC, Liston P, Korneluk RG. Degradation of survivin by the x-linked inhibitor of apoptosis (xiap)-xaf1 complex. *The Journal of biological*

chemistry 2007;282(36):26202-26209.
96. Birkey Reffey S, Wurthner JU, Parks WT, Roberts AB, Duckett CS. X-linked inhibitor of apoptosis protein functions as a cofactor in transforming growth factor-beta signaling. *The Journal of biological chemistry* 2001;276(28):26542-26549.
97. Hofer-Warbinek R, Schmid JA, Stehlik C, Binder BR, Lipp J, de Martin R. Activation of nf-kappa b by xiap, the x chromosome-linked inhibitor of apoptosis, in endothelial cells involves tak1. *The Journal of biological chemistry* 2000;275(29):22064-22068.
98. Levkau B, Garton KJ, Ferri N, Kloke K, Nofer JR, Baba HA, Raines EW, Breithardt G. Xiap induces cell-cycle arrest and activates nuclear factor-kappab : New survival pathways disabled by caspase-mediated cleavage during apoptosis of human endothelial cells. *Circulation research* 2001;88(3):282-290.
99. Shim JH, Xiao C, Paschal AE, Bailey ST, Rao P, Hayden MS, Lee KY, Bussey C, Steckel M, Tanaka N, et al. Tak1, but not tab1 or tab2, plays an essential role in multiple signaling pathways in vivo. *Genes & development* 2005;19(22):2668-2681.
100. Kaur S, Wang F, Venkatraman M, Arsura M. X-linked inhibitor of apoptosis (xiap) inhibits c-jun n-terminal kinase 1 (jnk1) activation by transforming growth factor beta1 (tgf-beta1) through ubiquitin-mediated proteosomal degradation of the tgf-beta1-activated kinase 1 (tak1). *The Journal of biological chemistry* 2005;280(46):38599-38608.
101. Yamaguchi K, Nagai S, Ninomiya-Tsuji J, Nishita M, Tamai K, Irie K, Ueno N, Nishida E, Shibuya H, Matsumoto K. Xiap, a cellular member of the inhibitor of apoptosis protein family, links the receptors to tab1-tak1 in the bmp signaling pathway. *The EMBO journal* 1999;18(1):179-187.
102. Sanna MG, da Silva Correia J, Luo Y, Chuang B, Paulson LM, Nguyen B, Deveraux QL, Ulevitch RJ. Ilpip, a novel anti-apoptotic protein that enhances xiap-mediated activation of jnk1 and protection against apoptosis. *The Journal of biological chemistry* 2002;277(34):30454-30462.
103. O'Riordan MX, Bauler LD, Scott FL, Duckett CS. Inhibitor of apoptosis proteins in eukaryotic evolution and development: A model of thematic conservation. *Developmental cell* 2008;15(4):497-508.
104. Maine GN, Burstein E. Commd proteins and the control of the nf kappa b pathway. *Cell cycle (Georgetown, Tex* 2007;6(6):672-676.
105. van de Sluis B, Muller P, Duran K, Chen A, Groot AJ, Klomp LW, Liu PP, Wijmenga C. Increased activity of hypoxia-inducible factor 1 is associated with early embryonic lethality in commd1 null mice. *Molecular and cellular biology* 2007;27(11):4142-4156.
106. van De Sluis B, Rothuizen J, Pearson PL, van Oost BA, Wijmenga C. Identification of a new copper metabolism gene by positional cloning in a purebred dog population. *Human molecular genetics* 2002;11(2):165-173.
107. Burstein E, Ganesh L, Dick RD, van De Sluis B, Wilkinson JC, Klomp LW, Wijmenga C, Brewer GJ, Nabel GJ, Duckett CS. A novel role for xiap in copper homeostasis through regulation of murr1. *The EMBO journal* 2004;23(1):244-254.
108. Mufti AR, Burstein E, Csomos RA, Graf PC, Wilkinson JC, Dick RD, Challa M, Son JK, Bratton SB, Su GL, et al. Xiap is a copper binding protein deregulated in wilson's disease and other copper toxicosis disorders. *Molecular cell* 2006;21(6):775-785.
109. Bratton SB, Walker G, Srinivasula SM, Sun XM, Butterworth M, Alnemri ES, Cohen GM. Recruitment, activation and retention of caspases-9 and -3 by apaf-1 apoptosome and associated xiap complexes. *The EMBO journal* 2001;20(5):998-1009.
110. Du C, Fang M, Li Y, Li L, Wang X. Smac, a mitochondrial protein that promotes cytochrome c-dependent caspase activation by eliminating iap inhibition. *Cell* 2000;102(1):33-42.
111. Verhagen AM, Ekert PG, Pakusch M, Silke J, Connolly LM, Reid GE, Moritz RL, Simpson RJ, Vaux DL. Identification of diablo, a mammalian protein that promotes apoptosis by binding to and antagonizing iap proteins. *Cell* 2000;102(1):43-53.
112. Liston P, Fong WG, Kelly NL, Toji S, Miyazaki T, Conte D, Tamai K, Craig CG, McBurney MW, Korneluk RG. Identification of xaf1 as an antagonist of xiap anti-caspase activity. *Nature cell biology* 2001;3(2):128-133.
113. Fong WG, Liston P, Rajcan-Separovic E, St Jean M, Craig C, Korneluk RG. Expression and genetic analysis of xiap-associated factor 1 (xaf1) in cancer cell lines. *Genomics* 2000;70(1):113-122.
114. Yang L, Mashima T, Sato S, Mochizuki M, Sakamoto H, Yamori T, Oh-Hara T, Tsuruo T. Predominant suppression of apoptosome by inhibitor of apoptosis protein in non-small cell lung cancer h460 cells: Therapeutic effect of a novel polyarginine-conjugated smac peptide. *Cancer research* 2003;63(4):831-837.
115. Watson RW, Fitzpatrick JM. Targeting apoptosis in prostate cancer: Focus on caspases and

inhibitors of apoptosis proteins. *BJU international* 2005;96 Suppl 2:30-34.
116. Ma TL, Ni PH, Zhong J, Tan JH, Qiao MM, Jiang SH. Low expression of xiap-associated factor 1 in human colorectal cancers. *Chinese journal of digestive diseases* 2005;6(1):10-14.
117. Li J, Li ZN, Bao QL, Ge LP, Li XQ, Chen P. Evaluation of pleural fluid survivin and xiap for the diagnosis of malignant pleural effusion. *Tumour Biol*.
118. Worthey EA, Mayer AN, Syverson GD, Helbling D, Bonacci BB, Decker B, Serpe JM, Dasu T, Tschannen MR, Veith RL, et al. Making a definitive diagnosis: Successful clinical application of whole exome sequencing in a child with intractable inflammatory bowel disease. *Genet Med*;13(3):255-262.
119. Katzmann DJ, Odorizzi G, Emr SD. Receptor downregulation and multivesicular-body sorting. *Nature reviews* 2002;3(12):893-905.
120. Hicke L. Protein regulation by monoubiquitin. *Nature reviews* 2001;2(3):195-201.
121. Kerscher O, Felberbaum R, Hochstrasser M. Modification of proteins by ubiquitin and ubiquitin-like proteins. *Annual review of cell and developmental biology* 2006;22:159-180.
122. Haas AL, Rose IA. The mechanism of ubiquitin activating enzyme. A kinetic and equilibrium analysis. *The Journal of biological chemistry* 1982;257(17):10329-10337.
123. Haas AL, Warms JV, Hershko A, Rose IA. Ubiquitin-activating enzyme. Mechanism and role in protein-ubiquitin conjugation. *The Journal of biological chemistry* 1982;257(5):2543-2548.
124. Haas AL, Warms JV, Rose IA. Ubiquitin adenylate: Structure and role in ubiquitin activation. *Biochemistry* 1983;22(19):4388-4394.
125. Ciechanover A, Heller H, Katz-Etzion R, Hershko A. Activation of the heat-stable polypeptide of the atp-dependent proteolytic system. *Proceedings of the National Academy of Sciences of the United States of America* 1981;78(2):761-765.
126. Ciechanover A, Elias S, Heller H, Hershko A. "Covalent affinity" Purification of ubiquitin-activating enzyme. *The Journal of biological chemistry* 1982;257(5):2537-2542.
127. Haas AL, Bright PM. The resolution and characterization of putative ubiquitin carrier protein isozymes from rabbit reticulocytes. *The Journal of biological chemistry* 1988;263(26):13258-13267.
128. Haas AL, Bright PM, Jackson VE. Functional diversity among putative e2 isozymes in the mechanism of ubiquitin-histone ligation. *The Journal of biological chemistry* 1988;263(26):13268-13275.
129. Jin J, Li X, Gygi SP, Harper JW. Dual e1 activation systems for ubiquitin differentially regulate e2 enzyme charging. *Nature* 2007;447(7148):1135-1138.
130. Pelzer C, Kassner I, Matentzoglu K, Singh RK, Wollscheid HP, Scheffner M, Schmidtke G, Groettrup M. Ube1l2, a novel e1 enzyme specific for ubiquitin. *The Journal of biological chemistry* 2007;282(32):23010-23014.
131. Yuan W, Krug RM. Influenza b virus ns1 protein inhibits conjugation of the interferon (ifn)-induced ubiquitin-like isg15 protein. *The EMBO journal* 2001;20(3):362-371.
132. Zhao C, Denison C, Huibregtse JM, Gygi S, Krug RM. Human isg15 conjugation targets both ifn-induced and constitutively expressed proteins functioning in diverse cellular pathways. *Proceedings of the National Academy of Sciences of the United States of America* 2005;102(29):10200-10205.
133. Gong L, Yeh ET. Identification of the activating and conjugating enzymes of the nedd8 conjugation pathway. *The Journal of biological chemistry* 1999;274(17):12036-12042.
134. Desterro JM, Rodriguez MS, Kemp GD, Hay RT. Identification of the enzyme required for activation of the small ubiquitin-like protein sumo-1. *The Journal of biological chemistry* 1999;274(15):10618-10624.
135. Gong L, Li B, Millas S, Yeh ET. Molecular cloning and characterization of human aos1 and uba2, components of the sentrin-activating enzyme complex. *FEBS letters* 1999;448(1):185-189.
136. Furukawa K, Mizushima N, Noda T, Ohsumi Y. A protein conjugation system in yeast with homology to biosynthetic enzyme reaction of prokaryotes. *The Journal of biological chemistry* 2000;275(11):7462-7465.
137. Komatsu M, Chiba T, Tatsumi K, Iemura S, Tanida I, Okazaki N, Ueno T, Kominami E, Natsume T, Tanaka K. A novel protein-conjugating system for ufm1, a ubiquitin-fold modifier. *The EMBO journal* 2004;23(9):1977-1986.
138. Suzuki K, Ohsumi Y. Molecular machinery of autophagosome formation in yeast, saccharomyces cerevisiae. *FEBS letters* 2007;581(11):2156-2161.
139. Mizushima N, Noda T, Yoshimori T, Tanaka Y, Ishii T, George MD, Klionsky DJ, Ohsumi M, Ohsumi Y. A protein conjugation system essential for autophagy. *Nature* 1998;395(6700):395-398.
140. Chiu YH, Sun Q, Chen ZJ. E1-l2 activates both ubiquitin and fat10. *Molecular cell* 2007;27(6):1014-1023.

141. Hofmann RM, Pickart CM. In vitro assembly and recognition of lys-63 polyubiquitin chains. *The Journal of biological chemistry* 2001;276(30):27936-27943.
142. Burroughs AM, Jaffee M, Iyer LM, Aravind L. Anatomy of the e2 ligase fold: Implications for enzymology and evolution of ubiquitin/ub-like protein conjugation. *Journal of structural biology* 2008;162(2):205-218.
143. Zou W, Papov V, Malakhova O, Kim KI, Dao C, Li J, Zhang DE. Isg15 modification of ubiquitin e2 ubc13 disrupts its ability to form thioester bond with ubiquitin. *Biochemical and biophysical research communications* 2005;336(1):61-68.
144. Tatham MH, Geoffroy MC, Shen L, Plechanovova A, Hattersley N, Jaffray EG, Palvimo JJ, Hay RT. Rnf4 is a poly-sumo-specific e3 ubiquitin ligase required for arsenic-induced pml degradation. *Nature cell biology* 2008;10(5):538-546.
145. Michelle C, Vourc'h P, Mignon L, Andres CR. What was the set of ubiquitin and ubiquitin-like conjugating enzymes in the eukaryote common ancestor? *Journal of molecular evolution* 2009;68(6):616-628.
146. Winn PJ, Religa TL, Battey JN, Banerjee A, Wade RC. Determinants of functionality in the ubiquitin conjugating enzyme family. *Structure* 2004;12(9):1563-1574.
147. Schmukle AC, Walczak H. No one can whistle a symphony alone - how different ubiquitin linkages cooperate to orchestrate nf-kappab activity. *Journal of cell science*;125(Pt 3):549-559.
148. Ardley HC, Robinson PA. The role of ubiquitin-protein ligases in neurodegenerative disease. *Neuro-degenerative diseases* 2004;1(2-3):71-87.
149. Michael D, Oren M. The p53 and mdm2 families in cancer. *Current opinion in genetics & development* 2002;12(1):53-59.
150. Wasch R, Engelbert D. Anaphase-promoting complex-dependent proteolysis of cell cycle regulators and genomic instability of cancer cells. *Oncogene* 2005;24(1):1-10.
151. Robinson PA, Ardley HC. Ubiquitin-protein ligases--novel therapeutic targets? *Current protein & peptide science* 2004;5(3):163-176.
152. Scheffner M, Huibregtse JM, Vierstra RD, Howley PM. The hpv-16 e6 and e6-ap complex functions as a ubiquitin-protein ligase in the ubiquitination of p53. *Cell* 1993;75(3):495-505.
153. Bernassola F, Karin M, Ciechanover A, Melino G. The hect family of e3 ubiquitin ligases: Multiple players in cancer development. *Cancer cell* 2008;14(1):10-21.
154. Wang M, Pickart CM. Different hect domain ubiquitin ligases employ distinct mechanisms of polyubiquitin chain synthesis. *The EMBO journal* 2005;24(24):4324-4333.
155. Wang M, Cheng D, Peng J, Pickart CM. Molecular determinants of polyubiquitin linkage selection by an hect ubiquitin ligase. *The EMBO journal* 2006;25(8):1710-1719.
156. Rotin D, Kumar S. Physiological functions of the hect family of ubiquitin ligases. *Nature reviews* 2009;10(6):398-409.
157. Borden KL, Freemont PS. The ring finger domain: A recent example of a sequence-structure family. *Current opinion in structural biology* 1996;6(3):395-401.
158. Jackson PK, Eldridge AG, Freed E, Furstenthal L, Hsu JY, Kaiser BK, Reimann JD. The lore of the rings: Substrate recognition and catalysis by ubiquitin ligases. *Trends in cell biology* 2000;10(10):429-439.
159. Ardley HC, Robinson PA. E3 ubiquitin ligases. *Essays in biochemistry* 2005;41:15-30.
160. Cyr DM, Hohfeld J, Patterson C. Protein quality control: U-box-containing e3 ubiquitin ligases join the fold. *Trends in biochemical sciences* 2002;27(7):368-375.
161. Hatakeyama S, Nakayama KI. U-box proteins as a new family of ubiquitin ligases. *Biochemical and biophysical research communications* 2003;302(4):635-645.
162. Zwickl P. The 20s proteasome. *Current topics in microbiology and immunology* 2002;268:23-41.
163. Vierstra RD. The ubiquitin/26s proteasome pathway, the complex last chapter in the life of many plant proteins. *Trends in plant science* 2003;8(3):135-142.
164. Mykles DL. Intracellular proteinases of invertebrates: Calcium-dependent and proteasome/ubiquitin-dependent systems. *International review of cytology* 1998;184:157-289.
165. Glickman MH, Ciechanover A. The ubiquitin-proteasome proteolytic pathway: Destruction for the sake of construction. *Physiological reviews* 2002;82(2):373-428.
166. Voges D, Zwickl P, Baumeister W. The 26s proteasome: A molecular machine designed for controlled proteolysis. *Annual review of biochemistry* 1999;68:1015-1068.
167. Coux O, Tanaka K, Goldberg AL. Structure and functions of the 20s and 26s proteasomes. *Annual review of biochemistry* 1996;65:801-847.
168. Puente XS, Lopez-Otin C. A genomic analysis of rat proteases and protease inhibitors. *Genome research* 2004;14(4):609-622.
169. Ambroggio XI, Rees DC, Deshaies RJ. Jamm: A metalloprotease-like zinc site in the

proteasome and signalosome. *PLoS biology* 2004;2(1):E2.
170. Nijman SM, Luna-Vargas MP, Velds A, Brummelkamp TR, Dirac AM, Sixma TK, Bernards R. A genomic and functional inventory of deubiquitinating enzymes. *Cell* 2005;123(5):773-786.
171. Gregory JD. *J Am Chem Soc* 1955;77:3922-3923.
172. Nelson DLC, M. M. . Lehninger, principles of biochemistry. *Worth Publishing: New York ISBN 1-57259-153-6* 2000.
173. http://en.wikipedia.org/wiki/File:NEMmech.jpg.
174. Amerik AY, Hochstrasser M. Mechanism and function of deubiquitinating enzymes. *Biochimica et biophysica acta* 2004;1695(1-3):189-207.
175. Kee Y, Lyon N, Huibregtse JM. The rsp5 ubiquitin ligase is coupled to and antagonized by the ubp2 deubiquitinating enzyme. *The EMBO journal* 2005;24(13):2414-2424.
176. McCullough J, Clague MJ, Urbe S. Amsh is an endosome-associated ubiquitin isopeptidase. *The Journal of cell biology* 2004;166(4):487-492.
177. Komander D, Reyes-Turcu F, Licchesi JD, Odenwaelder P, Wilkinson KD, Barford D. Molecular discrimination of structurally equivalent lys 63-linked and linear polyubiquitin chains. *EMBO reports* 2009;10(5):466-473.
178. Massoumi R, Paus R. Cylindromatosis and the cyld gene: New lessons on the molecular principles of epithelial growth control. *Bioessays* 2007;29(12):1203-1214.
179. Harhaj EW, Dixit VM. Deubiquitinases in the regulation of nf-kappab signaling. *Cell research*;21(1):22-39.
180. Harhaj EW, Dixit VM. Regulation of nf-kappab by deubiquitinases. *Immunological reviews*;246(1):107-124.
181. Burnett B, Li F, Pittman RN. The polyglutamine neurodegenerative protein ataxin-3 binds polyubiquitylated proteins and has ubiquitin protease activity. *Human molecular genetics* 2003;12(23):3195-3205.
182. Scheel H, Tomiuk S, Hofmann K. Elucidation of ataxin-3 and ataxin-7 function by integrative bioinformatics. *Human molecular genetics* 2003;12(21):2845-2852.
183. Todi SV, Scaglione KM, Blount JR, Basrur V, Conlon KP, Pastore A, Elenitoba-Johnson K, Paulson HL. Activity and cellular functions of the deubiquitinating enzyme and polyglutamine disease protein ataxin-3 are regulated by ubiquitination at lysine 117. *The Journal of biological chemistry*;285(50):39303-39313.
184. Balakirev MY, Tcherniuk SO, Jaquinod M, Chroboczek J. Otubains: A new family of cysteine proteases in the ubiquitin pathway. *EMBO reports* 2003;4(5):517-522.
185. Evans PC, Smith TS, Lai MJ, Williams MG, Burke DF, Heyninck K, Kreike MM, Beyaert R, Blundell TL, Kilshaw PJ. A novel type of deubiquitinating enzyme. *The Journal of biological chemistry* 2003;278(25):23180-23186.
186. Wertz IE, O'Rourke KM, Zhou H, Eby M, Aravind L, Seshagiri S, Wu P, Wiesmann C, Baker R, Boone DL, et al. De-ubiquitination and ubiquitin ligase domains of a20 downregulate nf-kappab signalling. *Nature* 2004;430(7000):694-699.
187. Nanao MH, Tcherniuk SO, Chroboczek J, Dideberg O, Dessen A, Balakirev MY. Crystal structure of human otubain 2. *EMBO reports* 2004;5(8):783-788.
188. Cooper EM, Cutcliffe C, Kristiansen TZ, Pandey A, Pickart CM, Cohen RE. K63-specific deubiquitination by two jamm/mpn+ complexes: Brisc-associated brcc36 and proteasomal poh1. *The EMBO journal* 2009;28(6):621-631.
189. Chui YL LK, Chan JYH. Bre (brain and reproductive
organ-expressed(tnfrsf1a modulator)). *Atlas Genet
Cytogenet Oncol Haematol* 2011;15(3):255-258.
190. Ching AK, Li PS, Li Q, Chan BC, Chan JY, Lim PL, Pang JC, Chui YL. Expression of human bre in multiple isoforms. *Biochemical and biophysical research communications* 2001;288(3):535-545.
191. Ching AK, Li Q, Lim PL, Chan JY, Chui YL. Expression of a conserved mouse stress-modulating gene, bre: Comparison with the human ortholog. *DNA and cell biology* 2003;22(8):497-504.
192. Miao J, Panesar NS, Chan KT, Lai FM, Xia N, Wang Y, Johnson PJ, Chan JY. Differential expression of a stress-modulating gene, bre, in the adrenal gland, in adrenal neoplasia, and in abnormal adrenal tissues. *J Histochem Cytochem* 2001;49(4):491-500.
193. Dutt A, Beroukhim R. Single nucleotide polymorphism array analysis of cancer. *Current opinion in oncology* 2007;19(1):43-49.
194. Wang B, Hurov K, Hofmann K, Elledge SJ. Nba1, a new player in the brca1 a complex, is required for DNA damage resistance and checkpoint control. *Genes & development* 2009;23(6):729-739.

195. Hicke L, Schubert HL, Hill CP. Ubiquitin-binding domains. *Nature reviews* 2005;6(8):610-621.
196. Patterson-Fortin J, Shao G, Bretscher H, Messick TE, Greenberg RA. Differential regulation of jamm domain deubiquitinating enzyme activity within the rap80 complex. *The Journal of biological chemistry*;285(40):30971-30981.
197. Hu X, Kim JA, Castillo A, Huang M, Liu J, Wang B. Nba1/merit40 and bre interaction is required for the integrity of two distinct deubiquitinating enzyme brcc36-containing complexes. *The Journal of biological chemistry*;286(13):11734-11745.
198. Chan BC, Ching AK, To KF, Leung JC, Chen S, Li Q, Lai PB, Tang NL, Shaw PC, Chan JY, et al. Bre is an antiapoptotic protein in vivo and overexpressed in human hepatocellular carcinoma. *Oncogene* 2008;27(9):1208-1217.
199. Li Q, Ching AK, Chan BC, Chow SK, Lim PL, Ho TC, Ip WK, Wong CK, Lam CW, Lee KK, et al. A death receptor-associated anti-apoptotic protein, bre, inhibits mitochondrial apoptotic pathway. *The Journal of biological chemistry* 2004;279(50):52106-52116.
200. Dong Y, Hakimi MA, Chen X, Kumaraswamy E, Cooch NS, Godwin AK, Shiekhattar R. Regulation of brcc, a holoenzyme complex containing brca1 and brca2, by a signalosome-like subunit and its role in DNA repair. *Molecular cell* 2003;12(5):1087-1099.
201. Sobhian B, Shao G, Lilli DR, Culhane AC, Moreau LA, Xia B, Livingston DM, Greenberg RA. Rap80 targets brca1 to specific ubiquitin structures at DNA damage sites. *Science (New York, NY* 2007;316(5828):1198-1202.
202. Feng L, Huang J, Chen J. Merit40 facilitates brca1 localization and DNA damage repair. *Genes & development* 2009;23(6):719-728.
203. Shao G, Patterson-Fortin J, Messick TE, Feng D, Shanbhag N, Wang Y, Greenberg RA. Merit40 controls brca1-rap80 complex integrity and recruitment to DNA double-strand breaks. *Genes & development* 2009;23(6):740-754.
204. Kim H, Chen J, Yu X. Ubiquitin-binding protein rap80 mediates brca1-dependent DNA damage response. *Science (New York, NY* 2007;316(5828):1202-1205.
205. Wang B, Elledge SJ. Ubc13/rnf8 ubiquitin ligases control foci formation of the rap80/abraxas/brca1/brcc36 complex in response to DNA damage. *Proceedings of the National Academy of Sciences of the United States of America* 2007;104(52):20759-20763.
206. Kim H, Huang J, Chen J. Ccdc98 is a brca1-brct domain-binding protein involved in the DNA damage response. *Nature structural & molecular biology* 2007;14(8):710-715.
207. Liu Z, Wu J, Yu X. Ccdc98 targets brca1 to DNA damage sites. *Nature structural & molecular biology* 2007;14(8):716-720.
208. Huen MS, Grant R, Manke I, Minn K, Yu X, Yaffe MB, Chen J. Rnf8 transduces the DNA-damage signal via histone ubiquitylation and checkpoint protein assembly. *Cell* 2007;131(5):901-914.
209. Mailand N, Bekker-Jensen S, Faustrup H, Melander F, Bartek J, Lukas C, Lukas J. Rnf8 ubiquitylates histones at DNA double-strand breaks and promotes assembly of repair proteins. *Cell* 2007;131(5):887-900.
210. Feng L, Wang J, Chen J. The lys63-specific deubiquitinating enzyme brcc36 is regulated by two scaffold proteins localizing in different subcellular compartments. *The Journal of biological chemistry*;285(40):30982-30988.
211. Shao G, Lilli DR, Patterson-Fortin J, Coleman KA, Morrissey DE, Greenberg RA. The rap80-brcc36 de-ubiquitinating enzyme complex antagonizes rnf8-ubc13-dependent ubiquitination events at DNA double strand breaks. *Proceedings of the National Academy of Sciences of the United States of America* 2009;106(9):3166-3171.
212. Gu C, Castellino A, Chan JY, Chao MV. Bre: A modulator of tnf-alpha action. *Faseb J* 1998;12(12):1101-1108.
213. Scaffidi C, Fulda S, Srinivasan A, Friesen C, Li F, Tomaselli KJ, Debatin KM, Krammer PH, Peter ME. Two cd95 (apo-1/fas) signaling pathways. *The EMBO journal* 1998;17(6):1675-1687.
214. Engels IH, Stepczynska A, Stroh C, Lauber K, Berg C, Schwenzer R, Wajant H, Janicke RU, Porter AG, Belka C, et al. Caspase-8/flice functions as an executioner caspase in anticancer drug-induced apoptosis. *Oncogene* 2000;19(40):4563-4573.
215. Chan BC, Li Q, Chow SK, Ching AK, Liew CT, Lim PL, Lee KK, Chan JY, Chui YL. Bre enhances in vivo growth of tumor cells. *Biochemical and biophysical research communications* 2005;326(2):268-273.
216. Chui YL, Ching AK, Chen S, Yip FP, Rowlands DK, James AE, Lee KK, Chan JY. Bre over-expression promotes growth of hepatocellular carcinoma. *Biochemical and biophysical research communications*;391(3):1522-1525.
217. Balgobind BV, Zwaan CM, Reinhardt D, Arentsen-Peters TJ, Hollink IH, de Haas V, Kaspers

GJ, de Bont ES, Baruchel A, Stary J, et al. High bre expression in pediatric mll-rearranged aml is associated with favorable outcome. *Leukemia*;24(12):2048-2055.
218. Noordermeer SM, Sanders MA, Gilissen C, Tonnissen E, van der Heijden A, Dohner K, Bullinger L, Jansen JH, Valk PJ, van der Reijden BA. High bre expression predicts favorable outcome in adult acute myeloid leukemia, in particular among mll-af9-positive patients. *Blood*;118(20):5613-5621.
219. Cooper EM, Boeke JD, Cohen RE. Specificity of the brisc deubiquitinating enzyme is not due to selective binding to lys63-linked polyubiquitin. *The Journal of biological chemistry*;285(14):10344-10352.
220. Bernstein E, Caudy AA, Hammond SM, Hannon GJ. Role for a bidentate ribonuclease in the initiation step of rna interference. *Nature* 2001;409(6818):363-366.
221. Zhao Y, Srivastava D. A developmental view of microrna function. *Trends in biochemical sciences* 2007;32(4):189-197.
222. Bagasra O, Prilliman KR. Rna interference: The molecular immune system. *Journal of molecular histology* 2004;35(6):545-553.
223. Mittal V. Improving the efficiency of rna interference in mammals. *Nature reviews* 2004;5(5):355-365.
224. Rossi JJ. Expression strategies for short hairpin rna interference triggers. *Human gene therapy* 2008;19(4):313-317.
225. Xiang S, Fruehauf J, Li CJ. Short hairpin rna-expressing bacteria elicit rna interference in mammals. *Nature biotechnology* 2006;24(6):697-702.
226. Naviaux RK, Costanzi E, Haas M, Verma IM. The pcl vector system: Rapid production of helper-free, high-titer, recombinant retroviruses. *Journal of virology* 1996;70(8):5701-5705.
227. Mandelboim O, Vadai E, Fridkin M, Katz-Hillel A, Feldman M, Berke G, Eisenbach L. Regression of established murine carcinoma metastases following vaccination with tumour-associated antigen peptides. *Nature medicine* 1995;1(11):1179-1183.
228. Davis HE, Rosinski M, Morgan JR, Yarmush ML. Charged polymers modulate retrovirus transduction via membrane charge neutralization and virus aggregation. *Biophysical journal* 2004;86(2):1234-1242.
229. Shishodia S, Aggarwal BB. Nuclear factor-kappab activation: A question of life or death. *Journal of biochemistry and molecular biology* 2002;35(1):28-40.
230. Aggarwal BB. Signalling pathways of the tnf superfamily: A double-edged sword. *Nature reviews* 2003;3(9):745-756.
231. Yang YL, Li XM. The iap family: Endogenous caspase inhibitors with multiple biological activities. *Cell research* 2000;10(3):169-177.
232. Galban S, Duckett CS. Xiap as a ubiquitin ligase in cellular signaling. *Cell death and differentiation*;17(1):54-60.
233. Zeng W, Xu M, Liu S, Sun L, Chen ZJ. Key role of ubc5 and lysine-63 polyubiquitination in viral activation of irf3. *Molecular cell* 2009;36(2):315-325.
234. Xu M, Skaug B, Zeng W, Chen ZJ. A ubiquitin replacement strategy in human cells reveals distinct mechanisms of ikk activation by tnfalpha and il-1beta. *Molecular cell* 2009;36(2):302-314.
235. http://www.rndsystems.com/rnd_page_objectname_Ubiquitin.aspx.
236. Shin H, Okada K, Wilkinson JC, Solomon KM, Duckett CS, Reed JC, Salvesen GS. Identification of ubiquitination sites on the x-linked inhibitor of apoptosis protein. *The Biochemical journal* 2003;373(Pt 3):965-971.
237. Garrison JB, Correa RG, Gerlic M, Yip KW, Krieg A, Tamble CM, Shi R, Welsh K, Duggineni S, Huang Z, et al. Arts and siah collaborate in a pathway for xiap degradation. *Molecular cell*;41(1):107-116.
238. Ryu YS, Lee Y, Lee KW, Hwang CY, Maeng JS, Kim JH, Seo YS, You KH, Song B, Kwon KS. Trim32 protein sensitizes cells to tumor necrosis factor (tnfalpha)-induced apoptosis via its ring domain-dependent e3 ligase activity against x-linked inhibitor of apoptosis (xiap). *The Journal of biological chemistry*;286(29):25729-25738.
239. Vaux DL, Silke J. Mammalian mitochondrial iap binding proteins. *Biochemical and biophysical research communications* 2003;304(3):499-504.
240. Creagh EM, Murphy BM, Duriez PJ, Duckett CS, Martin SJ. Smac/diablo antagonizes ubiquitin ligase activity of inhibitor of apoptosis proteins. *The Journal of biological chemistry* 2004;279(26):26906-26914.
241. Xu P, Duong DM, Seyfried NT, Cheng D, Xie Y, Robert J, Rush J, Hochstrasser M, Finley D, Peng J. Quantitative proteomics reveals the function of unconventional ubiquitin chains in proteasomal degradation. *Cell* 2009;137(1):133-145.
242. Finley D. Recognition and processing of ubiquitin-protein conjugates by the proteasome.

Annual review of biochemistry 2009;78:477-513.
243. Kreuz S, Siegmund D, Scheurich P, Wajant H. Nf-kappab inducers upregulate cflip, a cycloheximide-sensitive inhibitor of death receptor signaling. *Molecular and cellular biology* 2001;21(12):3964-3973.
244. You M, Ku PT, Hrdlickova R, Bose HR, Jr. Ch-iap1, a member of the inhibitor-of-apoptosis protein family, is a mediator of the antiapoptotic activity of the v-rel oncoprotein. *Molecular and cellular biology* 1997;17(12):7328-7341.
245. Stehlik C, de Martin R, Binder BR, Lipp J. Cytokine induced expression of porcine inhibitor of apoptosis protein (iap) family member is regulated by nf-kappa b. *Biochemical and biophysical research communications* 1998;243(3):827-832.
246. Stehlik C, de Martin R, Kumabashiri I, Schmid JA, Binder BR, Lipp J. Nuclear factor (nf)-kappab-regulated x-chromosome-linked iap gene expression protects endothelial cells from tumor necrosis factor alpha-induced apoptosis. *The Journal of experimental medicine* 1998;188(1):211-216.
247. Catz SD, Johnson JL. Transcriptional regulation of bcl-2 by nuclear factor kappa b and its significance in prostate cancer. *Oncogene* 2001;20(50):7342-7351.
248. Lee RM, Gillet G, Burnside J, Thomas SJ, Neiman P. Role of nr13 in regulation of programmed cell death in the bursa of fabricius. *Genes & development* 1999;13(6):718-728.
249. Grumont RJ, Rourke IJ, Gerondakis S. Rel-dependent induction of a1 transcription is required to protect b cells from antigen receptor ligation-induced apoptosis. *Genes & development* 1999;13(4):400-411.
250. Zong WX, Edelstein LC, Chen C, Bash J, Gelinas C. The prosurvival bcl-2 homolog bfl-1/a1 is a direct transcriptional target of nf-kappab that blocks tnfalpha-induced apoptosis. *Genes & development* 1999;13(4):382-387.
251. Krishna S, Low IC, Pervaiz S. Regulation of mitochondrial metabolism: Yet another facet in the biology of the oncoprotein bcl-2. *The Biochemical journal*;435(3):545-551.
252. Choi BH, Feng L, Yoon HS. Fkbp38 protects bcl-2 from caspase-dependent degradation. *The Journal of biological chemistry*;285(13):9770-9779.
253. Nakagawa T, Shirane M, Iemura S, Natsume T, Nakayama KI. Anchoring of the 26s proteasome to the organellar membrane by fkbp38. *Genes Cells* 2007;12(6):709-719.
254. Kang CB, Hong Y, Dhe-Paganon S, Yoon HS. Fkbp family proteins: Immunophilins with versatile biological functions. *Neuro-Signals* 2008;16(4):318-325.
255. Choi BH, Yoon HS. Fkbp38-bcl-2 interaction: A novel link to chemoresistance. *Current opinion in pharmacology*;11(4):354-359.
256. Hippenstiel S, Schmeck B, N'Guessan PD, Seybold J, Krull M, Preissner K, Eichel-Streiber CV, Suttorp N. Rho protein inactivation induced apoptosis of cultured human endothelial cells. *American journal of physiology* 2002;283(4):L830-838.
257. Scheffzek K, Ahmadian MR. Gtpase activating proteins: Structural and functional insights 18 years after discovery. *Cell Mol Life Sci* 2005;62(24):3014-3038.
258. Boureux A, Vignal E, Faure S, Fort P. Evolution of the rho family of ras-like gtpases in eukaryotes. *Molecular biology and evolution* 2007;24(1):203-216.
259. Vazquez CL, Colombo MI. Beclin 1 modulates the anti-apoptotic activity of bcl-2: Insights from a pathogen infection system. *Autophagy*;6(1):177-178.
260. Lossi L, Gambino G, Salio C, Merighi A. Autophagy regulates the post-translational cleavage of bcl-2 and promotes neuronal survival. *TheScientificWorldJournal*;10:924-929.
261. Bajwa N, Liao C, Nikolovska-Coleska Z. Inhibitors of the anti-apoptotic bcl-2 proteins: A patent review. *Expert opinion on therapeutic patents*;22(1):37-55.
262. Portt L, Norman G, Clapp C, Greenwood M, Greenwood MT. Anti-apoptosis and cell survival: A review. *Biochimica et biophysica acta*;1813(1):238-259.
263. Azad N, Iyer A, Vallyathan V, Wang L, Castranova V, Stehlik C, Rojanasakul Y. Role of oxidative/nitrosative stress-mediated bcl-2 regulation in apoptosis and malignant transformation. *Annals of the New York Academy of Sciences*;1203:1-6.
264. Komander D, Clague MJ, Urbe S. Breaking the chains: Structure and function of the deubiquitinases. *Nature reviews* 2009;10(8):550-563.
265. Johnston SC, Riddle SM, Cohen RE, Hill CP. Structural basis for the specificity of ubiquitin c-terminal hydrolases. *The EMBO journal* 1999;18(14):3877-3887.
266. Storer AC, Menard R. Catalytic mechanism in papain family of cysteine peptidases. *Methods in enzymology* 1994;244:486-500.
267. Metzig M, Nickles D, Falschlehner C, Lehmann-Koch J, Straub BK, Roth W, Boutros M. An rnai screen identifies usp2 as a factor required for tnf-alpha-induced nf-kappab signaling. *International journal of cancer*;129(3):607-618.

268. Reyes-Turcu FE, Ventii KH, Wilkinson KD. Regulation and cellular roles of ubiquitin-specific deubiquitinating enzymes. *Annual review of biochemistry* 2009;78:363-397.
269. Gerlach B, Cordier SM, Schmukle AC, Emmerich CH, Rieser E, Haas TL, Webb AI, Rickard JA, Anderton H, Wong WW, et al. Linear ubiquitination prevents inflammation and regulates immune signalling. *Nature*;471(7340):591-596.
270. Walczak H, Iwai K, Dikic I. Generation and physiological roles of linear ubiquitin chains. *BMC biology*;10:23.
271. Kirisako T, Kamei K, Murata S, Kato M, Fukumoto H, Kanie M, Sano S, Tokunaga F, Tanaka K, Iwai K. A ubiquitin ligase complex assembles linear polyubiquitin chains. *The EMBO journal* 2006;25(20):4877-4887.
272. Tokunaga F, Sakata S, Saeki Y, Satomi Y, Kirisako T, Kamei K, Nakagawa T, Kato M, Murata S, Yamaoka S, et al. Involvement of linear polyubiquitylation of nemo in nf-kappab activation. *Nature cell biology* 2009;11(2):123-132.
273. Peng J, Schwartz D, Elias JE, Thoreen CC, Cheng D, Marsischky G, Roelofs J, Finley D, Gygi SP. A proteomics approach to understanding protein ubiquitination. *Nature biotechnology* 2003;21(8):921-926.
274. Saeki Y, Tayama Y, Toh-e A, Yokosawa H. Definitive evidence for ufd2-catalyzed elongation of the ubiquitin chain through lys48 linkage. *Biochemical and biophysical research communications* 2004;320(3):840-845.
275. Hong SW, Kim CJ, Park WS, Shin JS, Lee SD, Ko SG, Jung SI, Park IC, An SK, Lee WK, et al. P34sei-1 inhibits apoptosis through the stabilization of the x-linked inhibitor of apoptosis protein: P34sei-1 as a novel target for anti-breast cancer strategies. *Cancer research* 2009;69(3):741-746.
276. Liou JY, Matijevic-Aleksic N, Lee S, Wu KK. Prostacyclin inhibits endothelial cell xiap ubiquitination and degradation. *Journal of cellular physiology* 2007;212(3):840-848.
277. Liu WH, Hsiao HW, Tsou WI, Lai MZ. Notch inhibits apoptosis by direct interference with xiap ubiquitination and degradation. *The EMBO journal* 2007;26(6):1660-1669.
278. Dan HC, Sun M, Kaneko S, Feldman RI, Nicosia SV, Wang HG, Tsang BK, Cheng JQ. Akt phosphorylation and stabilization of x-linked inhibitor of apoptosis protein (xiap). *The Journal of biological chemistry* 2004;279(7):5405-5412.
279. Shi RX, Ong CN, Shen HM. Protein kinase c inhibition and x-linked inhibitor of apoptosis protein degradation contribute to the sensitization effect of luteolin on tumor necrosis factor-related apoptosis-inducing ligand-induced apoptosis in cancer cells. *Cancer research* 2005;65(17):7815-7823.
280. Gaikwad A, Poblenz A, Haridas V, Zhang C, Duvic M, Gutterman J. Triterpenoid electrophiles (avicins) suppress heat shock protein-70 and x-linked inhibitor of apoptosis proteins in malignant cells by activation of ubiquitin machinery: Implications for proapoptotic activity. *Clin Cancer Res* 2005;11(5):1953-1962.
281. Nakhaei P, Sun Q, Solis M, Mesplede T, Bonneil E, Paz S, Lin R, Hiscott J. Ikappab kinase epsilon-dependent phosphorylation and degradation of x-linked inhibitor of apoptosis sensitizes cells to virus-induced apoptosis. *Journal of virology*;86(2):726-737.
282. Phillipps HR, Hurst PR. Xiap: A potential determinant of ovarian follicular fate. *Reproduction (Cambridge, England)*.
283. Tang MK, Wang CM, Shan SW, Chui YL, Ching AK, Chow PH, Grotewold L, Chan JY, Lee KK. Comparative proteomic analysis reveals a function of the novel death receptor-associated protein bre in the regulation of prohibitin and p53 expression and proliferation. *Proteomics* 2006;6(8):2376-2385.
284. Kane LP, Mollenauer MN, Xu Z, Turck CW, Weiss A. Akt-dependent phosphorylation specifically regulates cot induction of nf-kappa b-dependent transcription. *Molecular and cellular biology* 2002;22(16):5962-5974.
285. Jensen LE, Whitehead AS. Ubiquitin activated tumor necrosis factor receptor associated factor-6 (traf6) is recycled via deubiquitination. *FEBS letters* 2003;553(1-2):190-194.
286. Kapp LD, Lorsch JR. The molecular mechanics of eukaryotic translation. *Annual review of biochemistry* 2004;73:657-704.
287. Harding HP, Zhang Y, Ron D. Protein translation and folding are coupled by an endoplasmic-reticulum-resident kinase. *Nature* 1999;397(6716):271-274.
288. Marissen WE, Lloyd RE. Eukaryotic translation initiation factor 4g is targeted for proteolytic cleavage by caspase 3 during inhibition of translation in apoptotic cells. *Molecular and cellular biology* 1998;18(12):7565-7574.
289. Holcik M, Korneluk RG. Functional characterization of the x-linked inhibitor of apoptosis (xiap) internal ribosome entry site element: Role of la autoantigen in xiap translation. *Molecular*

and cellular biology 2000;20(13):4648-4657.
290. Holcik M, Lefebvre C, Yeh C, Chow T, Korneluk RG. A new internal-ribosome-entry-site motif potentiates xiap-mediated cytoprotection. *Nature cell biology* 1999;1(3):190-192.
291. Spriggs KA, Bushell M, Mitchell SA, Willis AE. Internal ribosome entry segment-mediated translation during apoptosis: The role of ires-trans-acting factors. *Cell death and differentiation* 2005;12(6):585-591.
292. Holcik M, Gordon BW, Korneluk RG. The internal ribosome entry site-mediated translation of antiapoptotic protein xiap is modulated by the heterogeneous nuclear ribonucleoproteins c1 and c2. *Molecular and cellular biology* 2003;23(1):280-288.
293. Lewis SM, Veyrier A, Hosszu Ungureanu N, Bonnal S, Vagner S, Holcik M. Subcellular relocalization of a trans-acting factor regulates xiap ires-dependent translation. *Molecular biology of the cell* 2007;18(4):1302-1311.
294. Wang J, Gu Q, Li M, Zhang W, Yang M, Zou B, Chan S, Qiao L, Jiang B, Tu S, et al. Identification of xaf1 as a novel cell cycle regulator through modulating g(2)/m checkpoint and interaction with checkpoint kinase 1 in gastrointestinal cancer. *Carcinogenesis* 2009;30(9):1507-1516.
295. MacLachlan TK, Takimoto R, El-Deiry WS. Brca1 directs a selective p53-dependent transcriptional response towards growth arrest and DNA repair targets. *Molecular and cellular biology* 2002;22(12):4280-4292.
296. Fei P, El-Deiry WS. P53 and radiation responses. *Oncogene* 2003;22(37):5774-5783.

Supplementary result

To prove the hypothesis that BRE can maintain the cellular XIAP level. We tried to restore BRE via adenovirus transduction in the stable BRE-depleted cell line, C6, which is one of B07 cell lines. If the hypothesis is true, the cellular XIAP level should also be restored when BRE is restored. The adenovirus, which was named as adenovirus-BREV5, was generated by a recombinant of pAdTrack-CMV-BREV5 and pAdEasy®-1. It contained the gene of BRE tagged by V5 at the C-terminus. After adenovirus transduction, the expression level of ectopic V5 tagged BRE was very high. However, this adenovirus induced serious apoptosis in these BRE-depleted cells. Thus, XIAP failed to be restored due to this serious apoptosis.

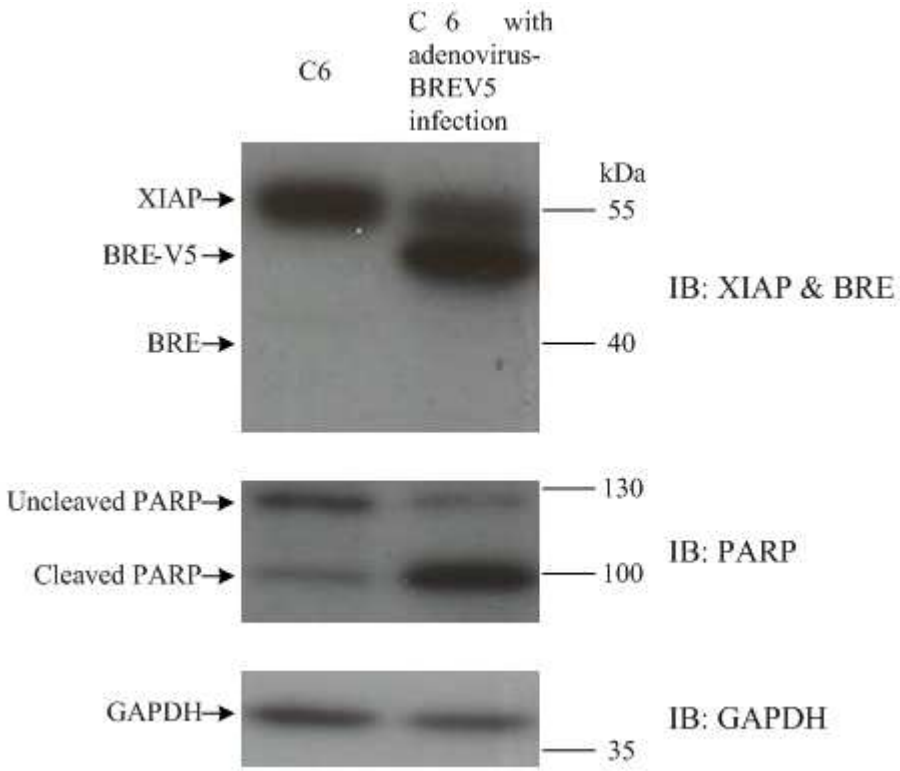

Figure 5-1. **Adenovirus induces apoptosis in BRE-depleted cells.**

Adenovirus-BREV5 was generated by transfection of a recombinant of pAdTrack-CMV-BREV5 and pAdEasy®-1 to the package cell line HEK293T. The ectopic BRE in adenovirus-BREV5 was tagged by V5 at the C-terminus. C6 is one of B07 cell lines, which are cell lines of D122 with stable BRE shRNA transfection. C6 was infected with adenovirus-BREV5 for 48 h. Apoptosis was indicated by the appearance of cleaved PARP. Protein loading was visualized by GAPDH. This experiment was performed once.